REACTIVE TRANSPORT OF URANIUM IN SUBSURFACE: MODELING BIOGEOCHEMICAL DYNAMICS AND IMPACT OF FIELD SCALE HETEROGENEITY

A THESIS SUBMITTED TO
THE GRADUATE SCHOOL OF NATURAL AND APPLIED SCIENCES
OF
MIDDLE EAST TECHNICAL UNIVERSITY

BY

SELİN GÖKÇE

IN PARTIAL FULFILLMENT OF THE REQUIREMENTS
FOR
THE DEGREE OF MASTER OF SCIENCE
IN
ENVIRONMENTAL ENGINEERING

NOVEMBER 2022

Approval of the thesis:

REACTIVE TRANSPORT OF URANIUM IN SUBSURFACE: MODELING BIOGEOCHEMICAL DYNAMICS AND IMPACT OF FIELD SCALE HETEROGENEITY

submitted by **SELİN GÖKÇE** in partial fulfillment of the requirements for the degree of **Master of Science in Environmental Engineering Department, Middle East Technical University** by,

Prof. Dr. Halil Kalıpçılar
Dean, Graduate School of **Natural and Applied Sciences** _____

Prof. Dr. Bülent İçgen
Head of Department, **Environmental Engineering** _____

Assist. Prof. Dr. Sema Sevinç Şengör
Supervisor, **Environmental Engineering Dept., METU** _____

Examining Committee Members:

Prof. Dr. Kahraman Ünlü
Environmental Engineering, METU _____

Assist. Prof. Dr. Sema Sevinç Şengör
Environmental Engineering, METU _____

Prof. Dr. Ülkü Yetiş
Environmental Engineering, METU _____

Prof. Dr. Tuba Hande Ergüder Bayramoğlu
Environmental Engineering, METU _____

Prof. Dr. Niğmet Uzal
Civil Engineering, AGU _____

Date: 30.11.2022

I hereby declare that all information in this document has been obtained and presented in accordance with academic rules and ethical conduct. I also declare that, as required by these rules and conduct, I have fully cited and referenced all materials and results that are not original to this work.

Name, Last Name: Selin Gökçe

Signature:

ABSTRACT

REACTIVE TRANSPORT OF URANIUM IN SUBSURFACE: MODELING BIOGEOCHEMICAL DYNAMICS AND IMPACT OF FIELD SCALE HETEROGENEITY

Gökçe, Selin

M.Sc., Department of Environmental Engineering

Supervisor: Asst. Prof. Dr. Sema Sevinç Şengör

November 2022, 103 Pages

The concept and role of aquifer heterogeneity have received considerable attention to understand the behavior of contaminant transport in subsurface environments. Although it has been proven that heterogeneity has significant control over quantithe fication of processes, the extent of this impact is yet to be studied. The main objective of this thesis is to investigate the impact of physical and chemical heterogeneity in understanding biogeochemical processes of contaminants, coupled with advective, dispersive transport in situ with mixing limitations. This study is particularly focused on an example of uranium behavior, where especially coupled bioreduction reactions with uranium reoxidation process in the presence of Fe (III) hydroxides are considered.

Model simulation results have shown that neglecting spatial heterogeneity might lead to an overestimation of uranium bioremediation in the subsurface environment, where physical heterogeneity has observed to have a greater impact than chemical

heterogeneity in the absence of adsorption reaction incorporations. On the other hand, when adsorption of uranium is included, the significance of chemical heterogeneity is more pronounced. Thus, when potential adsorption of contaminants is ignored in a chemically heterogeneous environment, the concentrations might be underestimated. The underestimation is seen to be more pronounced especially in the low hydraulic conductivity zones. The impact of the oxidation and reduction reactions are particularly enhanced in the zones with highest mixing, whereas the limited mixing within the low hydraulic conductivity zones remain with limited or no reaction potential. This mixing limitation impact is especially highly pronounced in chemically heterogeneous environments.

Keywords: Heterogeneity, Reoxidation, Biogeochemical Processes, Uranium, Reactive Transport Modeling

ÖZ

YERALTINDA URANYUM REAKTİF TAŞINIMI: BİYOJEOKİMYASAL SÜREÇLERİN VE ALANSAL HETEROJENİTE ETKİLERİNİN MODELLENMESİ

Gökçe, Selin
Yüksek Lisans, Çevre Mühendisliği Bölümü
Tez Yöneticisi: Dr. Öğr. Üyesi Sema Sevinç Şengör

Kasım 2022, 103 Sayfa

Akifer heterojenliğinin kavramı ve rolü, yer altı ortamlarında kirletici taşınımının davranışını anlamak için büyük ilgi görmüştür. Heterojenliğin bu süreçlerin nicelleştirilmesi üzerinde önemli bir kontrole sahip olduğu kanıtlanmış olsa da, bu etkinin boyutu henüz araştırılmamıştır. Bu tezin ana amacı, fiziksel ve kimyasal heterojenliğin, yer altı ortamındaki kirleticilerin biyojeokimyasal süreçlerini anlamada, ve taşınım ile birlikte etkisini araştırmaktır. Bu çalışmada, özellikle, Fe (III) hidroksitlerin varlığında uranyumun yeniden oksidasyon süreci ile beraber biyolojik indirgeme reaksiyonlarının dikkate alındığı, yeraltındaki uranyum davranışının bir örneğine odaklanılmaktadır.

Model simülasyon sonuçları, mekansal heterojenliğin ihmal edildiği durumlarda, yeraltı ortamındaki uranyumun biyoremediasyonunun fazla tahmin edilmesine yol açabileceğini göstermiştir. Ayrıca fiziksel heterojenliğin, adsorpsiyon reaksiyonu yokluğunda kimyasal heterojenliğe göre daha büyük bir etkiye sahip olduğu gözlemlenmiştir. Öte

yandan, uranyumun adsorpsiyonu dahil edildiğinde, kimyasal heterojenliğin önemi daha belirgindir. Bu nedenle, nispeten kimyasal olarak heterojen bir ortamda kirleticilerin potansiyel adsorpsiyonu göz ardı edildiğinde, kirletici konsantrasyonları hafife alınabilir. Eksik tahminin özellikle düşük hidrolik iletkenlik bölgelerinde daha belirgin olduğu görülmektedir. Oksidasyon ve indirgeme reaksiyonlarının etkisi, özellikle en yüksek karışımın olduğu bölgelerde artarken, düşük hidrolik iletkenlik bölgeleri içindeki sınırlı karışma, sınırlı veya hiç reaksiyon potansiyeli olmadan kalır. Bu sınırlı karışma etkisi, özellikle kimyasal olarak heterojen ortamlarda oldukça belirgindir.

Anahtar Kelimeler: Heterojenite, Reoksidasyon, Biojeokimyasal Tepkimeler, Uranyum, Reaktif Taşıma Modellemesi

To my beloved parents and brother

ACKNOWLEDGEMENT

I would like to earnestly acknowledge and give my deepest gratitude to my supervisor Asst. Prof. Dr. Sema Sevinç Şengör for providing sincere efforts and valuable time. I am thankful to my supervisor to give the opportunity to work with her and make thesis work possible and easy for me. During this thesis work, she has been an actual role model for me in terms of supervising, caring for me, and sharing her knowledge. She gave me motivation and inspiration which was very helpful for me to finish my thesis work.

I would like to express my deepest gratitude and many thanks to the dear examining committee members, Prof. Dr. Kahraman Ünlü, Prof. Dr. Ülkü Yetiş, Prof. Dr. Tuba Hande Ergüder Bayramoğlu and Prof. Dr. Niğmet Uzal for their contributions and suggestions.

I am grateful to Adnan Harun Doğan, Bahadır Kisbet, and Mert Basmacı for their worthful contributions and their support. I have been inspired by their intelligence, humility, and help.

I cannot begin to express my gratitude to my best friend Aysima Çalışan. She is the one that has supported me and laughed with me always all the time. I would like to my profound gratitude to her for being my inspiration and motivation through what have been difficult times for three years of graduate study.

Many thanks to my friends and my beloved roommates, for always sticking with me, showing their encouragement and patience.

This accomplishment would not have been possible without many people, but I am especially indebted to my family for giving me the strength to pursue my dreams. I'll never forget my family's positive belief in my success. I would like to dedicate this

study to my mother Nilgün Gökçe, father Sedat Gökçe, and brother Ali Gökmen Gökçe for their endless love, support, and understanding throughout my life.

TABLE OF CONTENTS

LIST OF TABLES

TABLES

LIST OF FIGURES

FIGURES

LIST OF ABBREVIATIONS

ABBREVIATIONS

K	Hydraulic Conductivity
SRB	Sulfate Reducing Bacteria
S	Sulfur
U.S. EPA	United States Environmental Protection Agency

CHAPTER 1

INTRODUCTION

1.1. Background

Groundwater is a very essential source of fresh water for sustaining life, where over 97% of freshwater exists in the world. Groundwater is used as the main source for drinking purposes, and to supply industries and farms for industrial and agricultural uses. It is obvious that groundwater should not be observed only as a drinking water source, but it has an important linkage to the hydrological cycle providing maintenance of surface water, so it should be protected as an environmental framework.

Groundwater can be named the “hidden source” because it is much more inaccessible than surface water in terms of pollution, prevention, and monitoring. This causes the characterization of groundwater pollution and understanding the impact of pollution to be more difficult. Thus, groundwater modeling can be used as a tool for a better understanding of the fate and transport of contaminants in groundwater. Although groundwater models may not be as detailed as real subsurface systems, they provide great insight into the mathematical representation of groundwater flow. However, the construction of groundwater modeling is not a straightforward process. Available and accurate measured data is very important to create a successful model. Groundwater modeling is the tool for understanding the system and predicting the behavior and response of the system. Majority of groundwater models within this context consists of various numerical modeling studies, developed to depict real aquifer system settings.

Heterogeneity which is the spatial variability of geological parameters of the subsurface is a key point impacting rates and patterns of subsurface flow. Starting from the 1960s,

the first studies on transport and spreading patterns of water in heterogeneous formations were conducted (Dagan, 1988). Until the 1990s, considerable attention has been devoted on the effect of heterogeneity in terms of physical characteristics of aquifer such as, pore size distributions, hydraulic conductivity, and porosity (Barber Ii A'b et al., 1992). The concept and role of aquifer heterogeneity has been increased with a greater interest to understand its impact on the behavior of contaminant or microbial species in groundwater (Harvey et al., 1993). In the late 1990s, many studies of direct interest were on the characterization of heterogeneity in terms of physically or chemically. According to the studies at that time, it has been revealed that understanding of the fate of hydrocarbons in a physically or chemically heterogeneous aquifer is crucial to explain the transport of substances in groundwater environments and to decide which bioremediation technologies would be best to use or if the natural attenuation of contaminants is proceeding well (Cozzarelli et al., 1999). Now, it is proved that the heterogeneity has an impact, but the extent of its impact is yet to be studied. Moreover, the concept of microbial heterogeneity has been raised, since microorganism attach and detach to the heterogeneously distributed iron solids in the subsurface, and this causes the heterogeneity in microbial species distribution as well. Data scarcity of aquifer heterogeneity within these frameworks is the main challenge for the prediction of groundwater flow and reactive contaminant transport in various natural subsurface settings. Due to the considerable cost of monitoring and lack of simple concepts, heterogeneity has not yet been fully incorporated into many field transport models up to now.

1.2. Scope and Objectives of the Study

The main scope of this study is to develop a simple and reliable 2D numerical biogeochemical reactive transport model to simulate the fate and transport of contaminants in heterogeneously distributed subsurface, integrating biotic and abiotic processes in a reducing environment. This study is particularly focused on an example of

uranium behavior in the subsurface, where especially coupled bioreduction reactions with uranium reoxidation process in the presence of Fe (III) hydroxides are considered. This work is intended to provide an insight into the role of physical and chemical heterogeneity in understanding biogeochemical processes of contaminants (e.g. uranium) in the subsurface environment, coupled with advective, dispersive transport in situ with mixing limitations. With this scope, several steps were completed to accomplish this goal, and they are listed below.

- Analysis of physical and chemical heterogeneity data in a hypothetical aquifer environment. This data is obtained from the literature (Scheibe et al., 2006).
- Determination of biogeochemical reaction database for uranium bioreduction with concomitant reoxidation in the presence of Fe(III)-(hydr)oxides in reducing environments. This data is compiled from the previous works of Spycher et al. (2011) and Sengor et al. (2015).
- Development of 2D groundwater flow and reactive transport model with the incorporation of biogeochemical reaction network using physical and chemical heterogeneity in the hypothetical aquifer environment. Model input parameters and determination of initial uranium and electron donor concentrations were compared with literature for consistency in real aquifer conditions.
- Conducting numerical model simulation experiments which include different scenarios: i.e. homogeneously and heterogeneously distributed physical (hydraulic conductivity) and chemical (Fe(III)hydroxide concentration) heterogeneity, with/without reoxidation & with/without surface complexation processes.
- Conducting the model simulation runs to determine the impact of heterogeneity within different scenarios.
- Comparison of the simulated scenarios to predict the impacts of physical and chemical heterogeneity, as well as the impacts of incorporating surface

complexation process modeling in the presence and absence of uranium reoxidation processes on subsurface flow and reactive contaminant transport.

This study provides an insight about the impacts of physical and chemical heterogeneity on overall uranium biogeochemical dynamics. Bioreduction of soluble uranium to uraninite mineral (UO_2) is currently being considered as a treatment strategy for uranium contaminated sites. It is also known that, however, uraninite (UO_2) can be reoxidized back to soluble uranium in the presence of different oxidizing agents. Due to the prevalence of different minerals (hematite, goethite etc.) in the subsurface and the fact that the reoxidation of UO_2, in this case, has been demonstrated to occur even under sulfate-reducing circumstances, reoxidation of UO_2 by Fe(III)(hydr)oxides has garnered particular interest. The presented numerical model in this study is aimed to determine the impact of heterogeneity in predicting the fate and reactive transport of uranium in subsurface by using numerical modeling. The ultimate findings of the study can set light to the determination of bioremediation strategies for contaminants within heterogeneously distributed sites with mixing-induced limitations.

CHAPTER 2

LITERATURE SURVEY

2.1. Concept of Heterogeneity

Over the years, disposal of hazardous substances has created groundwater contamination. Continued discharge of contaminants to the groundwater may threaten the groundwater supplies (EPA, 2022). Because of the heterogeneous nature of geological formations, groundwater subsurface has heterogeneous characteristics accordingly. The complex spatial variability causes uncertainty in groundwater flow and contaminant transport. Much has been written to state that heterogeneity affects hydrogeological prediction and assessment in terms of contaminant transport (Ma et al., 2020; Mailloux et al., 2003; Zhang et al., 2019). Therefore, characterization of subsurface hydrogeology has become a significant priority in terms of groundwater remediation strategies. While the past studies have shown that the role of aquifer heterogeneity in terms of contaminant movement in groundwater was not much known, aquifer heterogeneity since then has been an emerging interest in groundwater studies (Cozzarelli et al., 1999; L. Li et al., 2010; Zhang et al., 2019).

Aquifer heterogeneity is the variability of the spatial distribution of hydraulic, geochemical, and transport characteristics in the subsurface (Cozzarelli et al., 1999; Cunningham & Fadel, 2007; Fakhreddine et al., 2016). It is known that all aquifers have heterogeneous characteristics and the heterogeneity changes with the scale, ranging from pore to macro scale within the aquifer environments (Maliva, 2016). For example, the spatial distribution of contaminants, hydraulic conductivity, porosity, and specific storage in the subsurface are associated with aquifer heterogeneity (Jang et al., 2017).

Aquifer heterogeneity strongly affects the transport of contaminants in the subsurface in terms of reaction rates and directions in the field (Maliva, 2016). It implies being a key challenge in determining the flow and transport of contaminants in the subsurface. Predicting the effect of aquifer heterogeneity on groundwater has a critical role in understanding groundwater flow and contaminant transport with different subsurface scenarios (Berg & Illman, 2011; Chrysikopoulos et al., 1990; Fakhreddine et al., 2016; Jang et al., 2017; Uçankuş & Ünlü, 2008).

Aquifer heterogeneity is also very challenging in bioremediation applications at the field scale because of having uncertainty and complexity of contaminated sites (L. Li et al., 2011; Liu et al., 2009; F. Zhang et al., 2010). The description of heterogeneity has significant importance for better contaminant behavior delineation in the subsurface. On the other hand, the determination of aquifer heterogeneity is very demanding in terms of unpredictable distributions. Groundwater is invisible because it is highly demanding to determine the heterogeneity and anisotropy of groundwater, and the distribution of point or non-point source pollution to the groundwater environment (Wang et al., 2019). Groundwater media has characteristics which are significantly variable, and they are caused by a combination of geological composition and biogeochemical reactions (Edwards, 2016; Jang et al., 2017; Michael & Khan, 2016).

To predict the fate and transport of contaminants in the subsurface, groundwater modeling is an emerging interest to create representative scenarios. Numerical modeling has become a very essential tool for the determination of groundwater quality and quantity. However, qualified, and sufficient data are necessary for a better understanding of groundwater flow and transport (Maliva, 2016). Uncertainty in the aquifer and insufficient data information may create difficulty in the accurate prediction of subsurface flow and transport (D. Li et al., 2011). In order to elucidate the effects of heterogeneity, numerical modeling and stochastic methods have been studied to date

(Miralles-Wilhelm, 2000; M. Mohamed et al., 2010; Roden & Scheibe, 2005; Y. Zhang et al., 2019).

According to Sarris et al., (2019), heterogeneity can limit the potential transport and biogeochemical processes. Variability in subsurface complicates the study of fate and transport of contaminants, knowing that spatially varied scale allows to obtain more accurate determination. This would have significant implications in using groundwater modeling tools for groundwater remediation applications (Wang et al., 2019). The characteristics of the subsurface contain a degree of porosity, strength, cohesion, geochemistry, density, and these parameters influence the other variables. For instance, the variable distribution of hydraulic conductivity creates a large extent of groundwater flow patterns, which in turn relatively affects the fate and transport of chemicals in subsurface. Subsurface compositions have different physical and chemical complexities which are spatially variable (Cunningham & Fadel, 2007; Jang et al., 2016). Moreover, the concept of microbial heterogeneity has also an emerging interest because the microbial species may attach and detach the heterogeneously distributed solid grain, so this leads to microbial heterogeneity (Scheibe et al., 2006). All these types of heterogeneity are summarized below.

2.1.1. Physical Heterogeneity

Physical heterogeneity is the spatial variation of physical properties of the subsurface, which is spatially distributed characteristics of groundwater such as hydraulic conductivity, particle size distribution and porosity (Aksoy et al., 2004; Haberer et al., 2015; Harvey et al., 1993). The determination of physical properties of aquifer is critical for accurate delineation of contaminant transport, selection of remediation strategy and successful groundwater resources management. Thus, spatially variable distributed physical heterogeneity has significant control towards the transport of contaminant

plume, and it has significant importance in terms of understanding the fate of solutes in the groundwater (Edwards, 2016; Englert et al., 2009; Fakhreddine et al., 2016).

Over the past decades, physical heterogeneity has been associated with the spatial variation in both hydraulic conductivity, particle-size distribution, specific storage and porosity. Spatial variability on physical characteristics of subsurface has long been known to impact fate and transport processes (Dagan, 1990.; L. Li et al., 2010). Physical heterogeneity has also considered as a predominant factor controlling bacteria attachment (Mailloux et al., 2003). Moreover, physical heterogeneity is associated with the interstitial fluxes in subsurface, which influences the distribution of organic matter and nutrient. It is therefore obvious that there is a strong relationship between microbial diversity and hydraulic conductivity. Microbial diversity can be attributed to hydraulic heterogeneities (Atchley et al., 2014; Griebler & Lueders, 2009).

Physical heterogeneity has also a significant impact on bioremediation processes, which need the presence of co-occurrence of several reacting agents such as, electron donor, electron acceptor and biomass. The complex interactions between concurrent hydrological, geochemical, and biological processes that take place in the field as well as the effects of heterogeneities on these processes have a significant impact on the level of co-occurrence of these reacting agents. Atchley et al., (2014) also states that physical heterogeneity is related to the movement of conservative solutes in subsurface. For example, it can be presumed that the heterogeneity in hydraulic conductivity would control the fate and transport of an injected electron donor. Therefore, the degree of interactions between reacting agents and the spatial distribution of reaction products are determined by the physical and geochemical heterogeneities. Despite the significance of porous medium heterogeneities in regulating reactive transport processes during bioremediation, comprehensive high-resolution characterization of field sites is difficult, expensive, if not impossible. As a result, the difficulty of estimating the spatial distribution of physical and geochemical properties from sparse data is encountered, a

task that is inevitably complicated by uncertainty and non-uniqueness (L. Li et al., 2010).

L. Li et al., (2010) summarizes that while physical heterogeneity effects on the flow and transport processes have been relatively known, the impacts of geochemical heterogeneities have been recognized more recently. E. Jang et al., (2017) also emphasizes that the major controlling factor of redox reactions is physical heterogeneity, indicating that hydraulic conductivity affects the chemical species and their transformation processes. In many studies, the relationship between the physical heterogeneity within the porous media, and their impacts on microbial attachment is described. Mailloux et al., (2003) show that the predominant factor of microbial attachment is a porous medium (grain size) of physical heterogeneity. According to the Dong et al., (2002) as cited in Mailloux et al., (2003), determining the correlation between microbial transport and physical heterogeneity is possible with high-resolution data and extensive site characterization in field scale. Physical heterogeneity is associated with its short-term impacts on redox reactions in the subsurface. On the other hand, chemical heterogeneity is more substantial regarding its long-term impacts. Both physical and chemical heterogeneities affect the geochemical and transport processes (E. Jang et al., 2017).

2.1.2. Chemical Heterogeneity

Groundwater exhibits spatial distribution in terms of both physical and chemical heterogeneity. While the physical heterogeneity has been known for a long time in terms of its impact on subsurface flow and transport, the influence of chemical heterogeneity has been recognized more recently at laboratory and field scale studies (Aksoy et al., 2004.; L. Li et al., 2010; M. Mohamed et al., 2010; Tompson et al., 1996). Subsurface flow and behavior of chemical species migration in subsurface have significant importance in terms of the management of environmental contamination problems (J. Y.

Chen et al., 2001; Tompson et al., 1996). Chemical heterogeneity is the spatial variability of geochemical properties of subsurface, and many studies shows the relationship between the chemical heterogeneity and electron acceptor/electron donor (Jang et al., 2017c; L. Li et al., 2010; M. Mohamed et al., 2010). As mentioned in the study by Cunningham et al., (2007), determination of the biogeochemical heterogeneity is very critical when natural attenuation is selected as the more favorable bioremediation strategy in the field, as this may lead to spatial variability in the results.

It is known that the concentrations of electron donor and acceptor are important parameters for redox processes. Recent studies show that the physical and chemical heterogeneities are important factors in controlling the redox processes within the subsurface environment, whereas the chemical heterogeneity has a minor role (Jang et al., 2017). E. Jang et al., (2017) also demonstrates the impacts of physical and chemical heterogeneity on redox processes, and it has been determined that physical heterogeneity has a major component affecting nitrate reduction. According to the Jang et al., (2017) study, the influence of nitrate reduction capacity is correlated with chemical aquifer heterogeneity, but its impact is rather observed in the long term. On the other hand, the result of this study shows that physical heterogeneity has an impact on groundwater transport in short term. This study demonstrates that the limiting factors of both physical and chemical heterogeneity are the amounts of electron donor and the low permeability areas in homogeneous flow, respectively. When determining the impact of physical heterogeneity in a short term, ignoring chemical heterogeneity causes underestimation of results. In this study, the correlation between physical and chemical heterogeneity is presented (J. Y. Chen et al., 2001). Chemical heterogeneity in aquifer affects the charge distribution of subsurface species and particle mobility (Micić et al., 2020). Moreover, Aksoy et al., (2004) demonstrates the chemical heterogeneity impact on subsurface in terms of economic aspects. Thus, consideration of chemical heterogeneity is also emphasized in terms of the remediation costs and characterization cost of the chemical heterogeneity in this study.

In the last decades, numerous studies have demonstrated the geochemical controls of radionuclide mobilization. (Fakhreddine et al., 2016) indicates the impacts of geochemical characterization of the subsurface environment in terms of remediating an arsenic contaminated site. In this study, coupling of physical and chemical heterogeneity is stated to be vital for ensuring the groundwater management and maintaining the reliability of the groundwater transport model. Scheibe et al., (2006) reports on numerical simulations which provide to have an insight on the role of physical and chemical heterogeneity on biogeochemical processes in subsurface. According to (Cunningham & Fadel, 2007), the correlation between physical and chemical heterogeneity are poorly understood, and more data is needed to expand the knowledge about this correlation. Therefore, to manage remediation applications in the subsurface settings, the relationship between physical and chemical heterogeneity may be critical.

Spatial variability of physical and chemical heterogeneities has been identified in some studies. Scheibe et al., (2006) developed a 2D transport model including the physical and chemical heterogeneity and biogeochemical reactions, where their heterogeneity data is obtained by using geostatistical methods. L. Li et al., (2010) indicates that the chemical heterogeneities of minerals influence the biomass and mineral precipitates in the porous medium based on wide range of geochemical properties. It is indicated that ignoring the heterogeneity can lead to overestimation of the remediation efforts.

2.1.3. Microbial Heterogeneity

Understanding microbial activity and their metabolic potential has significant importance concerning new and effective bioremediation strategies. Microorganism having a phylogenetically diverse respiratory pathways are indicated to stimulate the bioremediation of the contaminant in concern accordingly, such as various studies which are reported on the bioreduction of uranium (Akob et al., 2007). These different microbial species are widely distributed, and many researches show that their

metabolism is limited with respect to the presence of carbon, pH and cocontaminant, such as nitrate and aluminum (Finneran et al., 2002; Istok et al., 2004a; Vrionis et al., 2005; Williams et al., 2013). Subsurface conditions influence the spatial heterogeneity in subsurface in terms of microbial population and diversity (Akob et al., 2007).

Groundwater has physical and chemical differences in different dimensions, which are major factors for microbial ecosystems. There is an important relationship between microbial diversity and physical/chemical heterogeneity (Griebler & Lueders, 2009; Zhou et al., 2012). Spatial variability of hydrological characteristics in groundwater has a significant factor in terms of shaping groundwater microbial habitats (Yan et al., 2020). To date, very limited studies have examined the relationship between hydrology and microbial population and distribution in groundwater (Maamar et al., 2015). Microbial or biological heterogeneity is described as heterogeneous distribution of microbial biomass, species, and activity. In spite of limited knowledge about these factors in terms of heterogeneity, it is assumed that spatial variability in biological reactions have a significant impact on transport of contaminants in the groundwater environment (M. M. A. Mohamed et al., 2006).

Aquifers are occupied by a wide range of microorganisms, which play an important role for biogeochemical processes and fate of the contaminant of concern. Microorganisms' life in subsurface depends on the oxidation and reduction reactions of inorganic chemicals because groundwater has low amount of carbon to meet the living organisms' needs. Thus, maintenance of microbial population is provided with the attainment of suitable geochemical conditions, especially the availability of electron donor and acceptor (Flynn et al., 2015; Maamar et al., 2015). Hence the types of electron acceptor and electron donor within the groundwater structure are the main driving force for enabling bacterial community (Akob et al., 2007; Flynn et al., 2015; Nyyssönen et al., 2014; Sitte et al., 2010). The microbial community adheres to groundwater residence

time and the amount of energy, as well as nutrients which are originated from the subsurface (Maamar et al., 2015).

Murphy et al., (2000) describes that there is a correlation between physical heterogeneity and microbial attachment, and that the physical heterogeneity is a major factor for microbial attachment (Harvey et al., 1993). Mailloux et al., (2003) conducted several experiments showing the impact of microbial and aquifer heterogeneity on the transport of bacterial population. Mailloux et al., (2003)'s study includes field-scale transport modeling studies depending on the results of their experiments, where microbial heterogeneity is observed to play an important role regarding subsurface transport, which is in turn affected by the physical heterogeneity of the porous medium. According to Campbell Rehmann and Welty (1999), the attachment of bacteria is affected by subsurface heterogeneity, such as flow velocity. Groundwater flow velocity, groundwater flow direction, and attachment of injected bacteria are all affected by the heterogeneity of the subsurface. The types of permeability impact the flow velocity. High permeability leads to high flow, whereas low permeability causes low velocity. Bacterial attachment rate is inversely proportional with velocity (Mailloux et al., 2003; Y. Zhang et al., 2019).

Cunningham & Fadel (2007) provides an insight into the positive correlation between hydraulic conductivity of physical heterogeneity and microbial population, which is observed to be a primary factor for biodegradation. Due to the spatial heterogeneity in microbial distribution and composition, bioremediation implementation might be complex and need to be incorporated in the numerical models accordingly.

Redox sensitive metals might be reduced as a result of microbially mediated reactions, and this provides the bioremediation of metal contaminated subsurface. Sulfate reducing bacteria (SRB) are essential component of the microbial population regarding metal reduction in different environments. Metal reducing microorganisms capable of reducing

uranium to uraninite, and especially SRB has significant importance in removing uranium in subsurface. (Chang et al., 2001) demonstrates that the determination of microbial diversity in subsurface is crucial concerning the bioremediation potential of a site.

2.2.An Example of Uranium

Radionuclide contamination is a considerable important problem causing the contamination of different environments such as soils, water, and sediments. Numerous U.S. Department of Energy (DOE) sites have groundwater contamination problem caused by unacceptable levels of different radionuclides (e.g. Tc, U) (Roh et al., 2000). In Turkey, radionuclide contamination which is the major enhancement of both of coal-burning plant and thermal plant adversely affect the quality of groundwater (Baba & Tayfur, 2011). Uranium is the most common radionuclide found as a pervasive element in the environment that creates a legacy of soil and groundwater contamination, and risks for the human health (Hee et al., 2007; Waseem et al., 2015; You et al., 2021).

Due to geochemical reactions and geological formations, uranium occurs naturally in rocks, sediments, and soils (Ma et al., 2020; Nolan & Weber, 2015). Uranium contamination is also caused by human activities, which are mining & milling activities, nuclear facility operations, and phosphate fertilizer processes. Moreover, human activities may change the geological distribution of uranium, which is why uranium is released into the environment disproportionately (Ma et al., 2020). U-contaminated groundwater poses a significant threat to human health and the ecosystem (Sengor et al., 2016).

Uranium can be oxidized in air, which is found as a uranyl ion (UO_2^{+2}) (J. P. Chen & Yiacoumi, 2002). The oxidized form of uranium (U(VI)) is more mobile, toxic, and soluble as compared to the other forms of uranium. (Cheng et al., 2021.; Hyun et al., 2014; Yabusaki et al., 2015). Uranium can also be in different valence states such as

trivalent, tetravalent and pentavalent, which are less common when compared with the uranyl ion. These forms of uranium can only be present under specific chemical conditions. For example, a tetravalent form of uranium (U(IV)) is found in wet and low redox conditions (Yabusaki et al., 2015).

Uranium has become an important environmental problem in terms of having high level of solubility, mobility, and toxicity (Renshaw et al., 2005; Şengör et al., 2016; Tokunaga et al., 2008; Wilkins et al., 2006). Engineered removal and remediation strategies have been developed in many uranium contaminated sites, such as chemical pump and treat methods and in situ biostimulation experiments (Tokunaga et al., 2008; Wilkins et al., 2006; Yabusaki et al., 2008). Although pump-and-treat method has been used in different contaminated sites around the world, it is a very expensive traditional strategy that may give inadequate results (Aksoy et al., 2004; Boonchayaanant et al., 2009; Williams et al., 2013). Although there are different remediation technologies for uranium, microbially mediated remediation technologies are a promising approach due to being cost-effective and durable; and thus they have shown considerable interest among other remediation strategies. According to Yabusaki et al., (2011) there are three significant benefits of microbially mediated U(VI) reduction: 1) uranium can be immobilized easily by surface exposure, 2) electron donors to be provided are commonly inexpensive, and 3) the microbial species of interest are already present in the natural subsurface environment (Yabusaki et al., 2011).

Aerobic and anaerobic microorganisms are widespread in soil and subsurface environments. Uranium might be interacting with these species via different mechanisms, including bioreduction, biomineralization, and bioaccumulation. Bioreduction of uranium is the most extensively demonstrated mechanism for the removal of uranium from the groundwater because of its low cost and effectiveness (Anderson et al., 2003; Gihring et al., 2011; Wufuer et al., 2017; Yabusaki et al., 2015). Bioreduction of uranium can be considered as the hexavalent uranium (U(VI)) to be

transformed into tetravalent uranium (U(IV)) form, which is less mobile, less toxic, and insoluble; in the presence of electrons with the response of certain microorganisms under reducing conditions (Gu et al., 2005; Renshaw et al., 2005; Şengör et al., 2015; Wufuer et al., 2017). So in other words, this process promotes the precipitation of soluble uranium in U(VI) form to the insoluble U(IV) form, which is the uraninite (UO_2) mineral. Most of the microbial species of prokaryotes can transform U(VI) to U(IV) (Suzuki et al., 2003). Metal-reducing bacteria, which are the most common species, especially iron reducing and sulfate-reducing bacteria, enhance to stimulate the reduction of U(VI) to U(IV) in the presence of suitable electron donor such as acetate, lactate, and glucose (Anderson et al., 2003; Hyun et al., 2014; Senko et al., 2002; Vrionis et al., 2005; Wufuer et al., 2017; Yabusaki et al., 2015). However, it should be noted that Sani et al., (2004) have indicated that when the electron donor (e.g. lactate, acetate, ethanol, etc.) is entirely consumed, uraninite may be reoxidized in the presence of oxidizing agents, and is converted to uranium again. Thus, it impedes the cleanup efforts in uranium-contaminated sites.

Furthermore, there are some significant considerations for implementing microbially mediated uranium reduction. Microbial species, which already exist in an aquifer, can utilize electron donors, but the consumption of electron donors can be important in terms of remediation design (Wu et al., 2006; Yabusaki et al., 2011). To maintain effective remediation, an understanding of microbe-radionuclide interactions and site characteristics are very crucial. Groundwater modeling is a useful tool for providing site-specific information about contaminant transport and evaluating remediation performance. Although modeling is a more effective way to monitor the behavior of contaminants in the subsurface, there are some challenges to the development of effective and reliable modeling scenarios (Cunningham et al., 2007).

2.3.Biogeochemical Processes of Uranium

Microbial agents have been used to catalyze remediation of the radionuclide contaminated sites. Recent studies show that microbial activity has the potential to biodegrade radionuclides to toxic and immobile forms (Lovely et al., 2002; Gadd et al., 2002). Microbial activity stimulates the bioremediation of radionuclide contamination. Microbial relationship between radioactive elements and indigenous microorganisms has been reported extensively for a long time (Lovley et al., 1993; Luo et al., 2007; Newsome et al., 2014 ; Wilkins et al., 2006). The bioavailability balance varies with microorganism-radionuclide interaction and biogeochemical condition (Gadd et al., 2002). Typically, microorganisms are able to use organic substrates such as lactate, ethanol, and acetate in the environment in order to stimulate bioreduction processes of radionuclide, which helps to remediate the contaminant of concern (Singh et al., 2014). Bioremediation of uranium is one promising approach in order to remove uranium contamination in subsurface (F. Zhang et al., 2010) . These processes are mediated by iron reducing bacteria (*Geobacter* sp. and *Shewanella* sp.), sulfate reducing bacteria (*Desulfotomaculum* sp. and *Desulfovibrio* sp.) and other microorganisms (*Clostridium* sp.)(Senko et al., 2002; W. M. Wu et al., 2007). Many laboratory experiments have been conducted for more than 20 years showing that dissimilatory metal reducing bacteria growing in the presence of electron donor could be used as a remediation method to stabilize uranium (U(VI)) in terms of transforming it into uraninite U(IV) mineral. However, when the organic substrates in the environment are consumed, microorganism tends to use other electron acceptors with respect to thermodynamic favorability corresponding to the electron redox tower in reducing conditions which impede the clean-up efforts (Sengor et al., 2013; Spycher et al., 2011). Metal reducing bacteria utilize oxidized metallic elements such as Fe (III), U (VI) as a terminal electron acceptor for metabolic activities (Lovley et al., 1993; Williams et al., 2013). Microorganisms obtain energy for their metabolic activities by using electron acceptor with respect to the redox tower, as shown in Figure 2.1. The electron redox tower depicts the order of

electron acceptor being used by indigenous microorganisms according to their thermodynamic favorability (Weber et al., 2006).

As seen in the Figure 2.1., oxygen is the terminal electron acceptor, and provides bacteria more energy with oxygen reduction than others. Microorganisms utilize electron acceptors regarding the order of redox tower, and biodegradation processes occur. Radionuclide mobility and toxicity alter with the biodegradation processes, and most recent studies have focused on the microbial activity on radionuclides, that is radionuclide biodegradation (Newsome et al., 2014b; Renshaw et al., 2005; Weber et al., 2006).

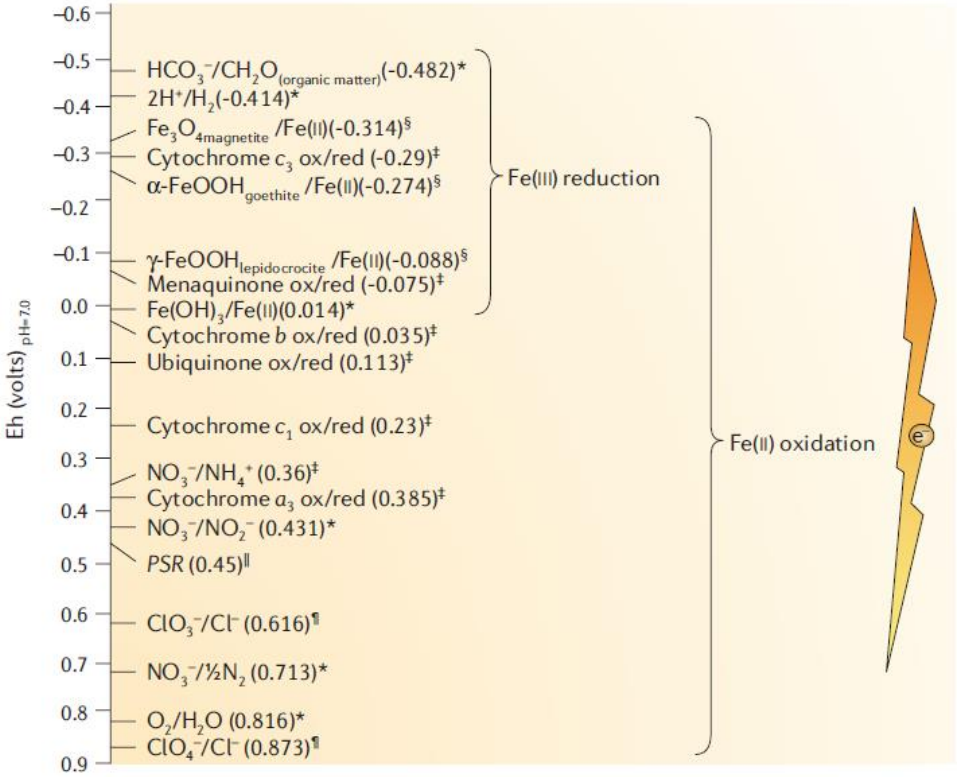

Figure 2.1. A redox tower (from Weber et al., 2006)

2.4.Reoxidation of Uranium

As mentioned above, microbially mediated reduction and oxidation processes for soluble U(VI) to U(IV) is an important concern for field scale uranium bioremediation processes. After bioreduction of U(VI), reoxidation of biologically reduced U(IV) is observed in lab and field scale experiments (Boonchayaanant et al., 2009). Research indicates that the mineral form of uranium (UO_2) is very susceptible to reoxidation in reducing conditions, causing challenges in terms of the long-term stability of uraninite in treated sites (Boonchayaanant et al., 2009; Komlos et al., 2008; Singh et al., 2014; Spycher et al., 2011). Reoxidation of uraninite can occur in the groundwater environment in case of introducing oxidizing agents such as O_2, NO_3^- , NO_2^- into the medium. Metal reducing bacteria can utilize the Fe (III) and Mn (IV) which are abundant in the subsurface as an electron donor to reoxidize uraninite to uranium under reducing conditions. Thus, it is very crucial to identify and specify the reaction mechanism including the reoxidation of biogenic uranium (U(IV)). Research indicates that the mineral form of uranium (UO_2) is very susceptible to reoxidation causing challenges in terms of the long-term stability of uraninite in treated sites (Komlos et al., 2008; Spycher et al., 2011). U(VI) can also be adsorbed onto Fe(III)hydroxides or form insoluble complexes with PO_4^{-3}, which could prevent the reduction process (Komlos et al., 2008).

Biological reduction of uranium in groundwater has been proposed by the scholars in the late 1980s and early 1990s. With in situ bioremediation both soluble and sorbed U(VI) can be reduced and immobilized by bacteria. In the presence of carbon, nitrogen, and phosphorus sources, these bacteria will be stimulated in the following order: denitrifying bacteria, metal-reducing bacteria, and finally sulfate-reducing bacteria (Abdelouas et al., 2000).

Microbial respiration can cause an increase in the bicarbonate concentration and formation of very stable uranyl carbonate complexes which increases the thermodynamic possibility of U(IV) oxidation. It has been suggested that, the reason behind this phenomenon is that the terminal electron acceptors (TEAs) for U reoxidation, Fe-(III) and perhaps Mn(IV) were able to persist due to kinetic restrictions, including reduced mass transfer. These findings demonstrate that in sediments and groundwaters with neutral to alkaline pH, where uranyl carbonates are most stable, in-situ U remediation via organic carbon-based reductive precipitation can be troublesome (Wan et al., 2005).

In another study conducted by Sani et al. (2004) in a laboratory environment, U(VI) wasn dissolved in a lactate containing medium and was treated with Fe(III) hydroxides such as hematite, ferrihydrite and goethite. The U(VI)-mineral suspensions were equilibrated before sulfate-reducing bacteria were added. Significant G20 (*Desulfovibrio Desulfuricans*) growth was observed after the suspensions containing the sulfate-limited medium were injected, and sulfate and U(VI) were simultaneously reduced within the solution. However, in the lactate-limited medium, part of the uranium was resolubilized when the lactate was depleted in the hematite treatments and, to a lesser amount, in the goethite treatments. So long as a suitable electron donor is present, their results imply that SRB facilitate reduction of soluble U(VI) to an insoluble U(IV) oxide. Incomplete reduction of the surfaces of crystalline Fe(III)- (hydr)oxides may cause partial reoxidation of the U(IV) to soluble U(VI) species when the electron donor is depleted (Sani et al., 2004).

In a case study in Old Rifle, Colorado, conducted by Campbell and other scholars (2011), it has been observed that the presence of biomass retarded the oxidation rates and diffusion of U(IV), which is a desirable outcome. These findings suggest that groundwater geochemistry, permeability, and the presence of bacterial cells and cell

exudates all have a significant impact on the protracted stability of U(IV) species in aquifers (Campbell et al., 2015).

On the other hand, Fe(III) hydroxides play a crucial role in the reoxidation of microbially reduced UO_2, making it sensitive to this process. In a study carried out by Stewart et al. (2012) the effect of chelators were discussed in the reoxidation process with Fe(III) and Fe(II) hydroxides such as ferrihydrite, goethite and hematite in a bicarbonate solution which helps the reoxidation process of UO_2. These findings suggest that U(IV) may be mobilized significantly by chelators present in U(VI)-contaminated areas, which may have an impact on bioremediation efforts (Stewart et al., 2012).

According to Spycher et al. (2011), it is anticipated that the concentration of U(VI) would increase typically with the reoxidation of UO_2 by minerals such as goethite, hematite and ferrihydrite, with the thermodynamically decreasing stability of these minerals. However, this may not always be the case, where in some circumstances the concentration of U(VI) would be higher in hematite solutions than in ferrihydrite and goethite solutions, suggesting increase in stability of the U(VI) concentration. One possible explanation according to their study is that the surface area of hematite, goethite and ferrihydrite increase respectively which could result in different adsorption rates, thus resulting in different reoxidation rates of UO_2 (Spycher et al., 2011).

Remediating uranium-contaminated groundwater is rendered to be difficult by the reoxidation and mobilization of previously reduced and immobilized uranium by dissolved phase oxidants. In a study conducted by Paradis and others (2016) in situ, ten test wells were injected with various amounts of nitrate, nitrite, sulfate, U(VI) and ethanol in order to study the effect of these compounds in the reoxidation and mobilization process of U(IV). According to the findings of their field study, preferential oxidation of reduced sulfur-bearing species can significantly limit the reoxidation of uranium under nitrate-reducing conditions (Paradis et al., 2016).

CHAPTER 3

MATERIALS AND METHODS

3.1.Modeling Approach and Description of the Study Site

In this study, the impact of physical and chemical heterogeneity on the transport and mobility of subsurface contaminants under multicomponent biogeochemical dynamics is presented by a 2D reactive transport model, using the previous works of Spycher et al., (2011) and Sengor et al., (2015) for uranium bioreduction and concomitant reoxidation as an example. Spycher et al., (2011) presented biogeochemical simulations of batch laboratory experiments conducted by Sani et al., (2004), capturing key biogeochemical reaction processes for reduction of soluble U(VI) to insoluble U(IV) by means of uraninite precipitation by sulfate-reducing bacteria; and the reoxidation of uraninite by Fe(III)-(hydr)oxides back to soluble U(VI) when electron acceptors are consumed in the medium. Sengor et al., (2015) later demonstrated 1D and 2D reactive transport models of the uranium bioreduction and reoxidation experiments in homogeneous environments, mainly to assess and compare different reactive transport simulator performances for complex reaction kinetics coupled with physical transport. However, spatial variability of aquifer characteristics would have significant impact on in-situ remediation activities, rendering numerical model predictions to be highly sensitive for accurate assessment of bioremediation effectiveness. As physical and chemical characteristics of natural aquifer systems, particularly reactive Fe-(hydr)oxide surfaces and hydraulic conductivity are mostly heterogeneously distributed, and these can exert significant controls on transport and bioremediation process dynamics with mixing limitations. This study presents a mixing-controlled reactive transport model coupled with complex biogeochemical reaction dynamics by means of extending the previously studied reaction network to a

heterogeneous granular aquifer environment. The model site is based on a hypothetical aquifer site located in eastern Virginia, which is known as South Oyster site as mentioned in Scheibe et al., (2006) . This field site, although is not actually been contaminated with uranium, has been used for research on subsurface bioremediation and microbial transport, since an extensive characterization data of the aquifer matrix has been available. Scheibe et al., (2006) have generated highly resolved 2D and 3D simulations of heterogeneous property distributions for the South Oyster site using geostatistical methods, where a highly resolved 2D realization of hydraulic conductivity and corresponding realization of Fe(III) have been selected to be used in this work to incorporate physical and chemical heterogeneity, respectively. Therefore, the model developed here incorporates the highly resolved field-scale property distributions to investigate heterogeneity impact on biogeochemical dynamics under hypothetical but realistic aquifer conditions, in accordance with Scheibe et al., (2006) .

This model domain has a length of 11.9 m and a thickness of 5.4 m. The 2D numerical model of groundwater flow and transport is defined with a uniform grid discretization of 0.1 m. Thus, the model is represented as 119 x 54 cells with a total of 6426 cells. The model domain is represented in Figure 3.1. Green line shows the location of lactate injection which is 6m away from the upgradient boundary, and blue line represents the location where cross sectional data at x=9m have been used to investigate the impact of heterogeneity along the cross section. The flow of groundwater was assumed as steady state. With the injection of lactate, which is from the green line at Figure 3.1., bioreduction processes are promoted, and the results pertaining to biogeochemical dynamics in the system are obtained for different scenario cases. Hydraulic head difference was assigned as 0.3 m gradient with constant head boundaries at both ends of the model domain, as mentioned in Scheibe et al., (2006). Porosity was assigned as 0.34 as spatially uniform along the model site. The value of longitudinal and transverse dispersivity were assumed as 1.0 and 0.1 m respectively (Scheibe et al., 2006).

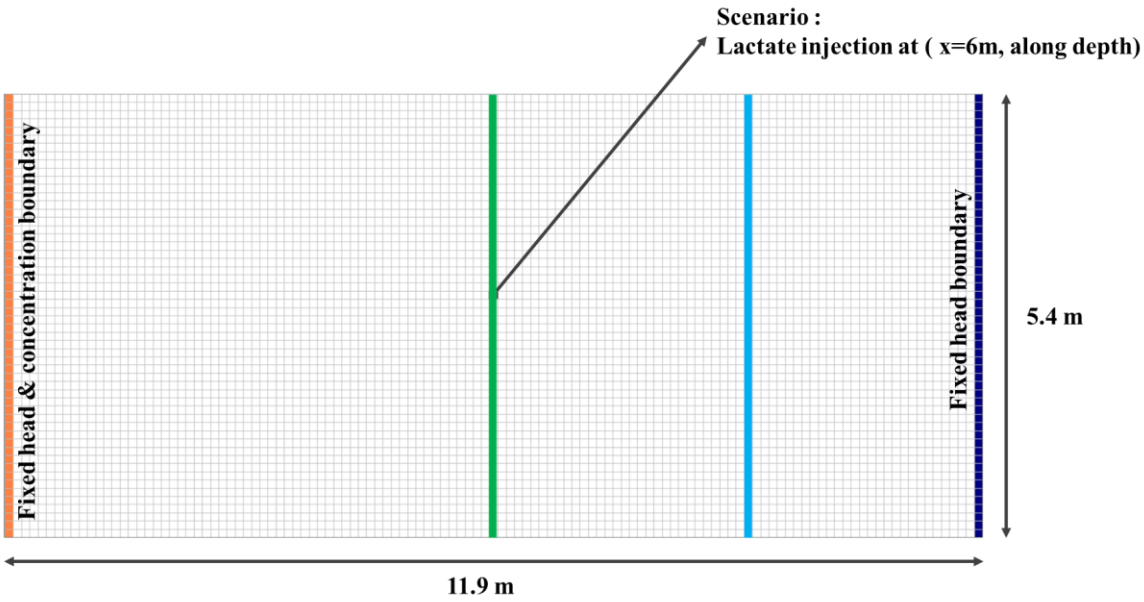

Figure 3.1. Model domain and boundary conditions for used in the numerical model

In order to investigate the impact of physical and chemical heterogeneity in uranium immobilization and solubilization dynamics considering the biogeochemical reaction kinetics at the model site, numerical model simulations have been set-up with decreasing levels of heterogeneity in three cases as follows:

1. Reactive transport simulations are carried out with both physical and chemical heterogeneity (i.e., heterogeneous K and heterogeneous Fe case),
2. Reactive transport simulations are carried out with physical but no chemical heterogeneity (i.e., heterogeneous K and homogeneous Fe case),
3. Reactive transport simulations are carried out with no physical or chemical heterogeneity (i.e., homogeneous K and homogeneous Fe case).

In the first part of the model runs which is detailed in Chapter 4.1., the numerical model simulations are run with no surface adsorption of uranium or any other species onto the aquifer solids. In the second part, adsorption of uranium onto Fe(III)- (hydr)oxide

surfaces are implemented by surface complexation reactions (Chapter 4.2.). All model simulations have also been carried out with- and without the U(IV) reoxidation reaction by Fe(III)-(hydr)oxide minerals, in order to elucidate the impact of U(IV) reoxidation specifically on the overall biogeochemical dynamics, and the reoxidation effects are detailed in Chapter 4.3. As mentioned previously, as the mere goal of this study is to investigate the impact of physical and chemical heterogeneity on the overall biogeochemical network for subsurface contaminant transport (uranium is used as an example) with strong reactivity on Fe(III)-(hydr)oxide surfaces under realistic in-situ subsurface environmental conditions, any calibration of model parameters to fit any specific field data is not considered here. Therefore, a hypothetical uranium contamination is considered using the South Oyster site under realistic model conditions as described by Scheibe et al. (2006). The length of the model time steps is determined as 0.01 d, where this value is calculated by taking into consideration of Peclet and Courant number criteria. The reactive transport modeling simulations are conducted using PHT3D code (Prommer et al., 2003), whereas the MODFLOW 2005 (Harbaugh et al., 2005) is used as the groundwater flow model to calculate the velocity fields. Concentration of key species and reaction rates of biogeochemical processes have been monitored in model simulations. Initial and boundary conditions, as well as the biogeochemical reaction network is described in detail in below sections.

3.1.Groundwater Model Inputs and Transport Model Setup

The initial water composition used in the modeling study here depends on the previous work by Sengor et al., (2015), which used the initial conditions based on the original laboratory batch experiments conducted by Sani et al., (2004). However, especially the initial uranium and electron donor (lactate) concentrations are compared with the literature, to make sure representative values have been used for real uranium-contaminated field conditions. The initial water composition is summarized in Table 3.1.

A summary of concentration values for uranium and electron donors reported in different studies for various uranium contaminated field sites is shown in Table 3.2.

Table 3.1. Initial water composition used for the model study (from Sengor et al., 2015)

Chemical species	**Concentration (mol/L_{water})**
Lactate	3e-7[(a)]
Acetate	1e-23
Sulfate	0.02
S (-II)	1e-8
Fe(II)	1e-23
Fe (III)	1e-11
U(VI)	1e-6
Ca	0.00042
Mg	0.004
C(IV)	1.7e-7
U(IV)	1e-23
Na	0.06
Cl	8.2e-4
Pip	0.03[(b)]
pH	7.2

(a) 3e-10 M is specified at the first three colums, and the others is specified as 3e-7 M
(b) "Pip" is represent the PIPES [piperazine-N,N-bis(2-ethanrsulfonic acid)] which is specified as 0.03 M to keep the buffer capacity of the medium
- Pip-+H+=HPip log_7.2 (The speciation reaction)

Table 3.2. Summary of concentration values for uranium and electron donors (used for bioremediation activities for uranium removal) compiled from various literature sources for uranium contaminated field sites

Uranium Concentration	Electron Donor	Electron Donor Concentration	Reference
1 μM	Lactate	0.03 M	This study based on Sengor et al.,(2015)
0.4-1.4 μM	Acetate/Bromide	0.001-0.003M 0.0001-0.0003M	Anderson et al.,(2003)
0.68 μM	Acetate /Bromide	0.05M/0.02M	Bao et al., (2014)
0.65-0.95 μM	Acetate/ Potassium Bromide	0.005 M/ 0.002 M	Bopp et al., (2010)
0-5.8 μM	Ethanol/Glucose /Acetate	0.02-0.2 M	Istok et al., (2004)
0.85 μM	Acetate	0.005	Li et al., (2011)
30 μM	Acetate	0.02 M	Scheibe et al., (2006)
1.06- 1.51 μM	Acetate/Bromide	0.001-0.003M 0.0001-0.0003M	Vrinois et al., (2005)
0.1-0.05 μM	Acetate	0.005-0.03 M	Williams et al., (2011)
1 μM	Acetate	0.005 M	Yabusaki et al., (2011)
2.24 μM	Acetate	0.00387 M	Yabusaki et al., (2015)

According to the U.S. Environmental Protection Agency (EPA), maximum threshold of uranium concentration in drinking water is 0.126 μM. However, concentration values range widely for various contaminated sites as reported from various sources in literature (Table 3.2.). 1μM concentration value as used in Sengor et al., (2015) has been observed to be representative, compared to other reported real field site studies and EPA reports. Thus, the model domain in this study is assumed to be contaminated with uranium at a uniform concentration of 1μM, where a continuous influx of 1μM U(VI) was assumed to be coming from the upstream boundary with a defined specified concentration boundary at the upstream end. Reactive transport simulations, including

the runs with surface complexation of U(VI) onto Fe(III)hydroxide surfaces (Sections 4.1 and 4.2.1) are carried out using uniform initial water composition (Table 3.1.) at t=0. However, in Section 4.2.2. reactive transport simulations including surface complexation of U(VI) are also carried out using initial water composition after 25 yr of U(VI) loading period with surface complexation at t=0, which is more representative of natural field conditions when considering the influence of surface complexation. In this case, model site is first loaded with uranium from an upgradient source at a uniform concentration of $1x10^{-6}$ μmol/L for 25 years, where quasi-equilibrium state for aqueous and sorbed U(VI) distributions are obtained. Then the quasi-equilibrium distribution of uranium concentration is used as the initial condition for transient flow runs. In these runs only equilibrium surface complexation reaction of U(VI) onto hematite surfaces is included, whereas all other reaction network is ignored.

The electron donor concentration values on the other hand, were observed to be relatively similar in other previous works reported in literature that studied in-situ uranium bioremediation activities, where the electron donor was applied to reduce uranium biologically to insoluble U(IV) forms (Table 3.2.). Comparing with literature values, the concentration of electron donor is specified as 0.03M lactate in this study, as was used in Sengor et al., (2015) and in conjunction with other uranium contaminated studies specified in literature. Lactate as the electron donor is injected in the relatively middle position of the field uniformly all throughout the depth (x=6m) at a rate of 0.02 m^3/day for the first 8 days of simulation period for all runs. The composition of inflowing water at the injection well is listed Table 3.3.

Table 3.3. Composition of inflowing water at the injection well (from Sengor et al., 2015)

Chemical species	**Concentration (mol/L_{water})**

Chemical species	**Concentration (mol/L_{water})**
Lactate	0.03[(a)]
Acetate	1e-23
Sulfate	0.02
S (-II)	1e-23
Fe(II)	1e-23
Fe (III)	1.3e-12
U(VI)	1e-23
Ca	0.00042
Mg	0.004
C(IV)	1.187e-04[(b)]
U(IV)	1e-23
Na	0.07914[(c)]
Cl	8.2e-4
Pip	0.03
pH	7.2

(a) 0.03 M lactate is injected for the first 8 days.
(b) C(IV) is specified as 1.187e-04 M for the first 8 days and to satisfy the charge balance it is specified as 1.134e-04 M for the rest of the model simulation.
(c) Na is specified as 0.07914 M for the first 8 days and to satisfy the charge balance it is specified as 0.04891 M for the rest of the model simulation.

The hydraulic conductivity and Fe(III) hydroxide data, which is used to demonstrate the impacts of physical and chemical heterogeneity in this study are obtained from Scheibe et al., (2006). The data generated by Scheibe et al., (2006) have been obtained by using different geostatistical methods to generate 2D and 3D simulations of heterogeneous property distributions. As discussed in detail by Scheibe et al., (2006), Fe(III) hydroxide distributions and corresponding hydraulic conductivity distributions have been simulated to examine the impact of heterogeneity for the hypothetical aquifer at the South Oyster site, including realistic aquifer properties. Hydraulic conductivity and Fe(III) hydroxide data depend on experimental correlations which resulted from geophysical and well

observations. The summary of statistics which have been used to create the data are detailed in Table 3.4. given below for different type of facies (Scheibe et al., 2006).

Table 3.4. The summary of statistics which are used in determination of heterogeneity data (from Scheibe et al., 2006)

	Mud			Sand		
	GPR radar attenuation	**Hydraulic Conductivity (cm/s)**	**Total Fe(III) (µmol/cm^3)**	**GPR radar attenuation**	**Hydraulic Conductivity (cm/s)**	**Total Fe(III) (µmol/cm^3)**
Mean	0.7468	0.00166664	7.173	0.4874	0.00719868	29.929
Standard error	0.0839	0.00163977	2.54	0.0133	0.00108659	3.669
Median	0.6387	0.00000073	3.172	0.4854	0.00278864	17.367
Standard deviation	0.3024	0.00751436	11.639	0.1089	0.0093472	31.561
Kurtosis	2.2076	20.99638794	6.017	0.7461	3.52747212	1.511
Skewness	1.6241	4.58201351	2.516	0.3238	1.84045242	1.118
Range	1.0749	0.03446071	44.355	0.6124	0.04573921	150.36
Minimum	0.4193	0.00000007	0.025	0.2297	0.00000007	0.025
Maximum	1.4943	0.03446078	44.38	0.8421	0.04573928	150.385
Count	13	21	21	67	74	74
Confidence level of mean (95.0%)	0.1828	0.00342049	5.298	0.0266	0.00216557	7.312

As mentioned above, hydraulic conductivity is associated with the physical heterogeneity, and Fe(III) hydroxide distribution represents the chemical heterogeneity for this study. For homogeneous hydraulic conductivity case, a uniform horizontal hydraulic conductivity value of 0.432 m/d was assigned for all cells throughout the domain (based on the previous work specified by (Sengor et al., 2015). For the physical heterogeneous cases, horizontal hydraulic conductivity values were assigned based on the physical heterogeneity data obtained from Scheibe et al., (2006) as shown in Figure

3.2. Vertical hydraulic conductivity values were assumed as the 1:10 ratio of horizontal hydraulic conductivity (based on Scheibe et al., (2006)) for all homogeneous and heterogeneous scenarios.

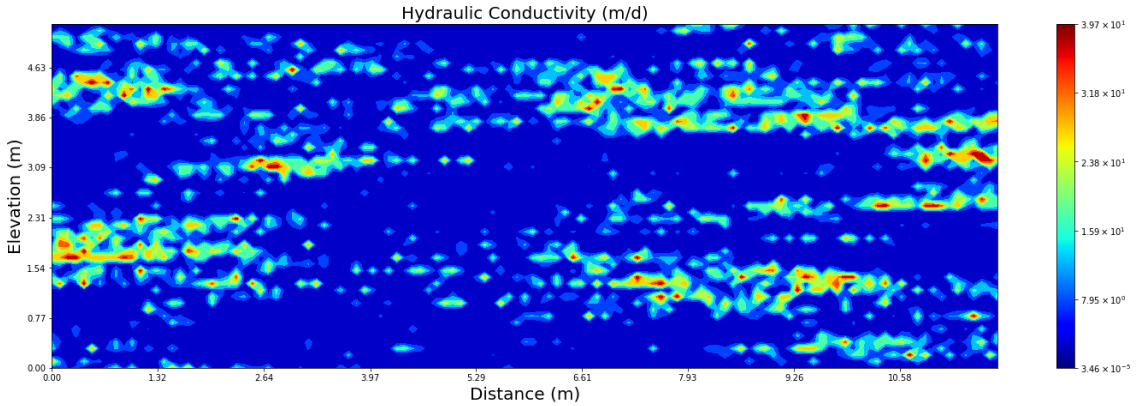

Figure 3.2. Heterogeneously distributed hydraulic conductivity (from Scheibe et al., (2006))

In this present study, Fe(III) hydroxide distribution was used to demonstrate the effect of chemical heterogeneity. Fe(III) hydroxide distribution data yielded by Scheibe et al., (2006), as shown in Figure 3.3., was used to demonstrate the effect of chemical heterogeneity for uranium bioreduction and reoxidation processes for heterogeneous Fe(III) based scenarios. For homogeneous Fe(III) based cases, a uniform value of 7.25 x 10^{-3} moles/L_{water} of initial hematite solid concentration (based on Sengor et al., (2015)) was assigned for all cells.

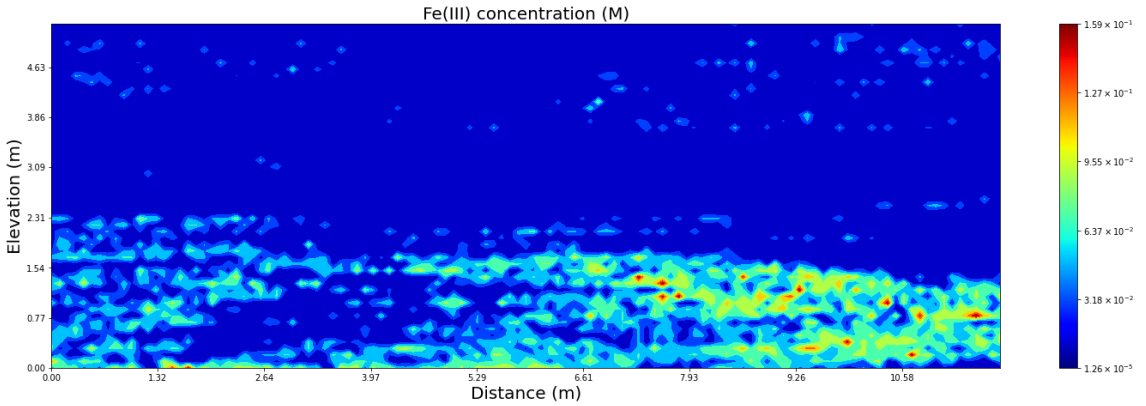

Figure 3.3. Distribution of Fe(III) hydroxide concentration (from Scheibe et al., (2006))

Biogeochemical reactions database is composed of biotic and abiotic reactions. Simplified conceptual model of reaction network is illustrated in Figure 3.4. The reaction benchmark is further discussed in detail in biogeochemical reaction networks part below.

3.2.Groundwater Biogeochemical Reaction Networks

Biogeochemical reaction database is composed of biotic and abiotic reactions compiled using the biogeochemical reaction network outlined by Spycher et al., (2011) and Sengor et al., (2015), consisting of equilibrium and kinetically controlled reactions. Kinetically controlled reactions included sulfate bioreduction by lactate, Fe(III) bioreduction by lactate, U(IV) bioreduction, U(IV) reoxidation by Fe(III), sulfide reoxidation by Fe(III) and precipitation/dissolution of sulfur. Kinetically controlled reactions and their corresponding reaction rates are listed in Table 3.6 and Table 3.7 respectively.

The kinetic reactions and their associated kinetic rate laws are described in detail below:

Reaction 1: Sulfate bioreduction (lactate degradation - biotic):

$$2\ C_3H_5O_3^- + SO_4^{-2} \rightarrow 2\ CH_3COO^- + 2\ CO_3^{-2} + HS^- + 3\ H^+ \quad (1)$$

$$\log(K_{25C}) = 2.252$$

Reaction 2: Fe(III) bioreduction ((lactate degradation - biotic):

$$C_3H_5O_3^- + 4\ Fe^{+3} + 2\ H_2O \rightarrow CH_3COO^- + CO_3^{-2} + 4\ Fe^{+2} + 6\ H^+ \quad (2)$$

$$\log(K_{25C}) = 72.652$$

Lactate degradation in the above reactions, i.e., sulfate (Eqn 1) and Fe(III) bireduction (Eqn 2) is assumed to be microbially mediated and the rate R is modeled using a conventional dual-Monod rate law with biomass growth (Spycher et al., 2011; Sengor et al., 2015) as:

$$R = q\ C_b \frac{C_D}{k_D + C_D} \frac{C_A}{k_A + C_A} f_G \quad (3)$$

with

$$R_b = Y_b R - k_{dec} C_b \quad (4)$$

$$f_G = (1 - Q/K) \quad (5)$$

where C is concentration and the subscripts A, D, and b represent electron acceptor, electron donor, and biomass, respectively, k is a half saturation constant in units of C, q is the rate of maximum substrate utilization (in units of moles per time, per biomass), Y_b is the microbial yield coefficient (in units of biomass per substrate), k_{dec} the cell decay rate (in units of per time), and f_G is the affinity term which varies between 1 (far from equilibrium) to 0 (equilibrium). Q is the ion activity product and K is the equilibrium constant of each reaction. Note that although the lactate degradation reaction stoichiometries (Eqns 1 and 2) do not include biomass generation directly, microbial concentrations are still simulated (Spycher et al., 2011; Sengor et al., 2015).

Reaction 3: U(VI) bioreduction (combined abiotic and biotic):

$$4\ UO_2^{+2} + HS^- + 7\ H^+ \rightarrow 4\ U^{+4} + SO_4^{-2} + 4\ H_2O \quad (6)$$

$$\log(K_{25C}) = 2.51$$

where the rate R of the reaction is calculated as:

$$R = r \frac{C_D}{k_D + C_D} f_G \quad (7)$$

where r and k_D were adjusted to reproduce the observed experimental results as described in detail by Spycher et al., 2011.

Reaction 4: U(IV) reoxidation by Fe(III)(abiotic):

$$U^{+4} + 2\ Fe^{+3} + 2\ H_2O \rightarrow UO_2^{+2} + 2\ Fe^{+2} + 4\ H^{+} \quad (8)$$

$$\log(K_{25C}) = 16.972$$

Reaction 5: Sulfide reoxidation by Fe(III) (abiotic):

$$8\ Fe^{+3} + HS^{-} + 4\ H_2O \rightarrow 8\ Fe^{+2} + SO_4^{-2} + 9\ H^{+} \quad (9)$$

$$\log(K_{25C}) = 70.397$$

Reaction 6: Precipitation/dissolution of sulfur:

$$2Fe^{+3} + HS^{-} \rightarrow 2Fe^{+2} + S_{(s)} + H^{+} \quad (10)$$

$$\log(K_{25C}) = 28.12$$

The rates of the reactions defined by Eqns (8)-(10) are determined by:

$$R = r\ f_G, \quad (11)$$

where r (in units of M per time) is assumed to be constant. These reactions are observed to take place close to equilibrium and the direction of the reaction (dissolution or precipitation) might be reversed, depending on whether the ion activity product, Q, is smaller or greater than K. In order to maintain f_G to be between 0 (equilibrium) and 1 (far from equilibrium), this term was written as $f_G = -(1 - K/Q)$ in the case of reaction reversal. The precipitation/dissolution of elemental sulfur ($S_{(s)}$) was considered to be kinetically controlled (Equation 10), in order to yield results consistent with laboratory experiments (Sani et al., 2004).

It should be noted that the available kinetically controlled reaction rates which are obtained from Spycher et al., (2011) were calibrated for laboratory scale (in accordance with laboratory experiments conducted by Sani et al., (2004)). Therefore, the reaction rates would need to have been adjusted to make it more representative for field scale experiments to be used in this study. Laboratory, local and field scale data have been compiled in Bao et al., (2014), where about a two order magnitude of difference between laboratory and field scale reactions rates have been confirmed. Also considering the reaction rates for the experimental kinetics by Sengor et al., 2015, the available kinetically controlled data is adjusted, where the reaction rates are divided by 100 to be consistent for field scale (see Table 3.7.).

Aqueous speciation reactions were assumed to proceed at equilibrium, where these reactions are described using the law of mass action:

$$C_i = K_i^{-1}\gamma_i^{-1}\prod_{j=1}^{N_c}(\gamma_j C_j)^{\nu_{ij}} \tag{12}$$

where C is the concentration (mol/kg_{water}), K is the thermodynamic equilibrium constant, γ is the activity coefficient, ν_{ij} are the stoichiometric coefficients in the reaction, N_c is the number of primary species, and subscripts j and i refer to the primary and secondary species, respectively. The aqueous speciation reactions that are used in the modeling study are listed in Table 3.5.

Inorganic reaction system included biogenic uraninite (UO_2), hematite (Fe_2O_3) which is considered to be the Fe(III)-hydr(oxide) phase, siderite ($FeCO_3$), and disordered mackinawite (FeS_m), all implemented as equilibrium reactions. Hematite is considered to be initially present (as Fe(III)-hydr(oxide) phase as described above), whereas other minerals are initially absent and considered as secondary minerals. The equilibrium

mineral dissolution and precipitation reactions are described using the mass action equation:

$$K_m = \prod_{j=1}^{Nc} (\gamma_j C_j)^{\nu_{mj}} \quad (13)$$

where K_m is the equilibrium constant for the mineral dissolution reaction (assuming unit activity of solid phases), N_c is the number of primary species considered, subscript m refers to minerals, and ν_{mj} are the stoichiometric coefficients of primary species j in mineral m. Simplified conceptual model of the biogeochemical reaction network is illustrated in Figure 3.4.

Table 3.5. Aqueous speciation reactions used in the model simulation (from Spycher et al., (2011) and Sengor et al., (2015))

Aqueous speciation reaction	**LogK**
$H^+ + Acetate^- = H(Acetate)$	4.757
$H^+ + CO_3^{-2} = HCO_3^-$	10.329
$2H^+ + CO_3^{-2} = CO_2 + H_2O$	16.681
$Ca^{+2} + HCO_3^- = CaCO_3 + H^+$	-7.002
$Ca^{+2} + Cl^- = CaCl^+$	-.696
$Ca^{+2} + 2Cl^- = CaCl_2$	-0.644
$Ca^{+2} + HCO_3^- = CaHCO_3^+$	1.047
$Ca^{+2} + H_2O = CaOH^+ + H^+$	-12.85
$Ca^{+2} + Sulfate^{-2} = CaSulfate$	2.111
$Fe^{+2} + 2CO_3^{-2} = Fe(CO_3)_2^{-2}$	7.45
$Fe^{+2} + 3H_2O = Fe(OH)_3^- + 3H^+$	-32.962
$Feii^{+2} + 4H_2O = Fe(OH)_4^{-2} + 4H^+$	-46
$Fe^{+3} + 2\ Sulfate^{-2} = Fe(Sulfate)_2^-$	3.214
$2Fe^{+3} + 2H_2O = Fe_2(OH)_2^{+4} + 2H^+$	-7.283
$3\ Fe^{+3} + 4\ H_2O = Fe_3(OH)_4^{+5} + 4\ H^+$	-6.3
$Fe^{+2} + CO_3^{-2} = FeCO_3$	5.45
$Fe^{+2} + Cl^- = FeCl^+$	-0.16
$Fe^{+3} + Cl^- = FeCl^{+2}$	1.48
$Fe^{+2} + 2Cl^- = FeCl_2$	-2.45
$Fe^{+2} + CO_3^{-2} + H^+ = FeHCO_3^+$	11.799
$Fe^{+2} + H_2O = FeO + 2H^+$	-20.405
$Fe^{+3} + H_2O = FeO^+ + 2H^+$	-5.65

Aqueous speciation reaction	LogK
$Fe^{+3} + 2H_2O = FeO2^- + 4H^+$	-21.62
$Fe^{+2} + H_2O = FeOH^+ + H^+$	-9.315
$Fe^{+3} + H_2O = FeOH^{+2} + H^+$	-4.38
$Fe^{+2} + HS- = FeS + H+$	-2.2
$Fe^{+3} + Sulfate^{-2} = FeSulfate^+$	1.93
$H^+ + HS^- = H_2S$	7.02
$2H^+ + Sulfate^{-2} = H_2Sulfate$	0
$Fe^{+3} + 2H_2O = HFeO_2 + 3H^+$	-12.018
$Fe^{+2} + 2H_2O = HFeO_2^- + 3H^+$	-33.988
$H^+ + Sulfate^{-2} = HSulfate-$	1.99
$4Mg^{+2} + 4H_2O = Mg_4(OH)_4^{+4} + 4H^+$	-39.75
$Mg^{+2} + CO_3^{-2} = MgCO_3$	2.98
$Mg^{+2} + Cl^- = MgCl^+$	-0.1349
$Mg^{+2} + H^+ + CO3^{-2} = MgHCO_3^+$	11.339
$Mg^{+2} + H_2O = MgOH^+ + H^+$	-11.397
$Mg^{+2} + Sulfate^{-2} = MgSulfate$	2.26
$Na^+ + CO_3^{-2} = NaCO_3^-$	1.27
$Na^+ + Cl^- = NaCl$	-0.777
$Na^+ + H^+ + CO_3^{-2} = NaHCO_3$	10.079
$Na^+ + H_2O = NaOH + H^+$	-14.18
$Na^+ + Sulfate^{-2} = NaSulfate^-$	0.73
$HS^- = S^{-2} + H^+$	-12.918
$11Uranyl^{+2} + 6CO_3^{-2} + 12H_2O = (Uranyl)_{11}(CO_3)_6(OH)_{12}^{-2} + 12H^+$	36.12
$2Uranyl^{+2} + 2H_2O = (Uranyl)_{2(}OH)_2^{+2} + 2H^+$	-5.659
$2Uranyl^{+2} + CO_3^{-2} + 3H_2O = (Uranyl)_2(CO_3)(OH)^{3-} + 3H^+$	-0.916
$2Uranyl^{+2} + H_2O = (Uranyl)_2OH^{+3} + H^+$	-2.729
$3Uranyl^{+2} + 6CO_3^{-2} = (Uranyl)_3(CO3)_6^{-6}$	53.88
$3Uranyl^{+2} + 4H_2O = (Uranyl)_3(OH)_4^{+2} + 4H^+$	-11.96
$3Uranyl^{+2} + 5H_2O = (Uranyl)_3(OH)_5^+ + 5H^+$	-15.62
$3Uranyl^{+2} + 7H_2O = (Uranyl)_3(OH)_7^- + 7H^+$	-32.2
$3Uranyl^{+2} + CO_3^{-2} + 3H_2O = (Uranyl)_3O(OH)_2(HCO_3)^+ + 3H^+$	0.583
$4Uranyl^{+2} + 7H_2O = (Uranyl)4(OH)_7^+ + 7H^+$	-21.995
$U^{+4} + 4CO_3^{-2} = U(CO_3)_4^{-4}$	35.05
$U^{+4} + 5CO_3-2 = U(CO_3)_5^{-6}$	33.82
$U^{+4} + 2Sulfate^{-2} = U(Sulfate)^2$	10.5
$Uranyl^{+2} + 2Sulfate^{-2} = Uranyl(Sulfate)_2^{-2}$	4.3
$U^{+4} + Cl^- = UCl^{+3}$	1.697
$Uranyl^{+2} + Cl^- = UranylCl^+$	0.141
$Uranyl^{+2} + 2Cl^- = UranylCl_2$	-1.146
$Uranyl^{+2} + Sulfate^{-2} = UranylSulfate$	3.18
$Uranyl^{+2} + H_2O = UranylOH+ + H^+$	-5.217
$2H_2O + Uranyl^{+2} = Uranyl(OH)_2 + 2H^+$	-12.152
$Uranyl^{+2} + 3H_2O = Uranyl(OH)_3- + 3H^+$	-20.246
$Uranyl^{+2} + 4H_2O = Uranyl(OH)_4^{-2} + 4H^+$	-32.4

Aqueous speciation reaction	**LogK**
$U^{+4} + H_2O = UOH^{+3} + H^+$	-0.541
$U^{+4} + 2H_2O = U(OH)_2^{+2} + 2H^+$	-1.091
$U^{+4} + 3H_2O = U(OH)_3+ + 3H^+$	-4.69
$U^{+4} + Sulfate^{-2} = USulfate^{+2}$	6.6
$Uranyl^{+2} + CO_3^{-2} = UranylCO_3$	9.94
$Uranyl^{+2} + 2CO_3^{-2} = Uranyl(CO_3)_2^{-2}$	16.61
$Uranyl^{+2} + 3CO_3^{-2} = Uranyl(CO_3)_3^{-4}$	21.84
$Ca^{+2} + Uranyl^{+2} + 3CO_3^{-2} = CaUranyl(CO_3)_3^{-2}$	27.18
$2Ca^{+2} + Uranyl^{+2} + 3CO_3^{-2} = Ca_2Uranyl(CO_3)_3$	30.7

Table 3.6. Kinetically controlled reactions in this study (from Spycher et al., (2011) and Sengor et al., (2015))

No	Process	Reaction
1.	Sulfate bioreduction (lactate degradation-biotic)	$2C_3H_5O_3^- + SO_4^{-2} \rightarrow 2CH_3COO^- + 2\ CO_3^{-2} + HS^- + 3H^+$
2.	Fe(III) bioreduction (lactate degradation-biotic)	$C_3H_5O_3^- + 4Fe^{+3} + 2H_2O \rightarrow CH_3COO^- + CO_3^{-2} + 4Fe^{+2} + 6H^+$
3.	U(IV) bioreduction (abiotic & biotic)	$4UO_2^{+2} + HS^- + 7H^+ \rightarrow 4U^{+4} + SO_4^{-2} + 4H_2O$
4.	U(IV) reoxidation by Fe(III) (abiotic)	$U^{+4}\ 2Fe^{+3} + 2H_2O \rightarrow UO_2^{+2} + 2Fe^{+2} + 4H^+$
5.	Sulfide reoxidation by Fe(III) (abiotic)	$8Fe^{+3} + HS^- + 4H_2O \rightarrow 8Fe^{+2} + SO_4^{-2} + 9H^+$
6.	Precipitation of sulfur	$2Fe^{+3} + HS^- \rightarrow 2Fe^{+2} + S_{(s)} + H^+$

Table 3.7. Calibrated kinetic parameters used for the simulation of U(VI) bioreduction in the presence of hematite (from Sengor et al., (2015) and Spycher et al., 2011)

No	Process	Rate Law	q (mol/s/mg_{cells}) or r(mol/s)	k_D (mol/L)	k_A(mol/L)	Y_b(mg_{cells}/mol)	k_{Dec} (1/s)
1.	Sulfate bioreduction (lactate degradation-bioti	$R = qC_b \frac{C_D}{k_D + C_D} \frac{C_A}{k_A + C_A}$	10^{-8} /100	2 x 10^{-2}	2 x 10^{-2}	1600	10^{-8} /100
2.	Fe(III) bioreduction (lactate degradation-bioti	$R = qC_b \frac{C_D}{k_D + C_D} \frac{C_A}{k_A + C_A}$	10^{-11} / 100	2 x 10^{-2}	10^{-20} (a)	1600	10^{-8} /100
3.	U(VI) bioreduction (abiotic & biotic)	$R = r \frac{C_D}{k_D + C_D} f_G$	8 x 10^{-11} /100	4 x 10^{-2}			
4.	U(IV) reoxidation by Fe(III) (abiotic)	$R = rf_G$	0.45 x 10^{-11} /100				
5.	Sulfide reoxidation by Fe(III) (abiotic)	$R = rf_G$	2 x 10^{-11} /100				
6.	Precipitation of sulfur (b)	$R = rf_G$	2 x 10^{-11} /100				

(a) Rate is presumed essentially unlimited by the electron acceptor (donor- limited experiments).
(b) Rate incorporates (and assumes) a constant surface area.

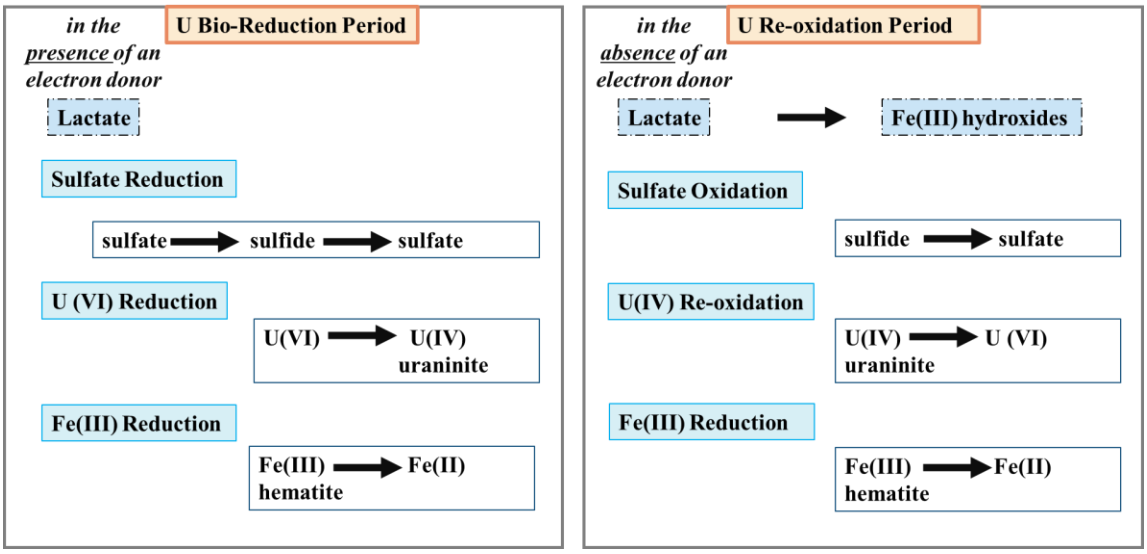

Figure 3.4. Conceptual illustration of biotic and abiotic reactions for uranium transformation

Sorption of uranium onto the Fe(III)-hydr(oxide) phases is implemented as surface complexation reactions, which are also considered to be at equilibrium and modeled using non-electrostatic double layer modeling (Dzombak and Morel, 1990). The surface complexation reactions of uranium used in the study are listed in Table 3.8. below.

Table 3.8. Surface complexation reactions used in this study

Surface Complexation Reactions	Log K	Reference
$UO_2^{2+} + Fe_sOH + 2H_2O = Fe_sOUO_2 + 2H^+$	-2.5	Scheibe et al., 2006
$UO_2^{2+} + Fe_wOH + 2H_2O = Fe_wOUO_2 + 2H^+$	-2.5	Scheibe et al., 2006

3.3.Transport Processes

Reactive transport modeling is a tool for analyzing and monitoring physical, chemical, geological, and biological processes in different environmental systems. Designed models can describe the processes at a certain time scale. In this study, PHT3D V2.17 code (Prommer et al., 2003) is used as the reactive transport simulator to observe the interactions of biogeochemical processes described above. PHT3D is a 3D reactive transport simulator which incorporates MT3DMS (v5.1, Zheng and Wang, 1998) for advective-dispersive multi-species transport; and PHREEQC-2 (v2.17, Parkhurst and Appelo, 1999) for quantification of reactive processes via sequential operator splitting approach. The governing equation for the advective-dispersive reactive transport of i^{th} (mobile) aqueous specie can be described as:

$$\frac{\partial(\theta C_i)}{\partial t} = \nabla \cdot (\theta D \nabla C_i) - \nabla \cdot (\theta v C_i) - q_s C_i^s + \theta r_{react,i} \tag{14}$$

where $\nabla = \left(\frac{\partial}{\partial x}, \frac{\partial}{\partial y}, \frac{\partial}{\partial z} \right)$ and D is the hydrodynamic dispersion coefficient tensor and v is the pore velocity vector $v = (v_x, v_y, v_z)$ with v_x, v_y and v_z are the pore velocities in x,y and z direction.

The rate of change of concentration for immobile species, e.g., bacteria and/or minerals is computed by:

$$\frac{\partial C_i}{\partial t} = r_{react,i} \tag{15}$$

where q_s is a volumetric flow rate per unit volume of aquifer representing fluid sources (positive) and sinks (negative), θ is the porosity, C_i^s is the concentration of the source

or sink flux, $r_{react,i}$ is a source/sink term due to the chemical reaction and C_i is the total aqueous concentration of the i^{th} component (Sengor et al., 2015).

Designing a conceptual model framework of subsurface system is a requirement for conducting a successful numerical groundwater model. The conceptual model is a representative tool which includes the hydrogeological system boundaries, existing data and their relationship between the numerical model. The comprehensive conceptual model for the current study is shown in Figure 3.5.

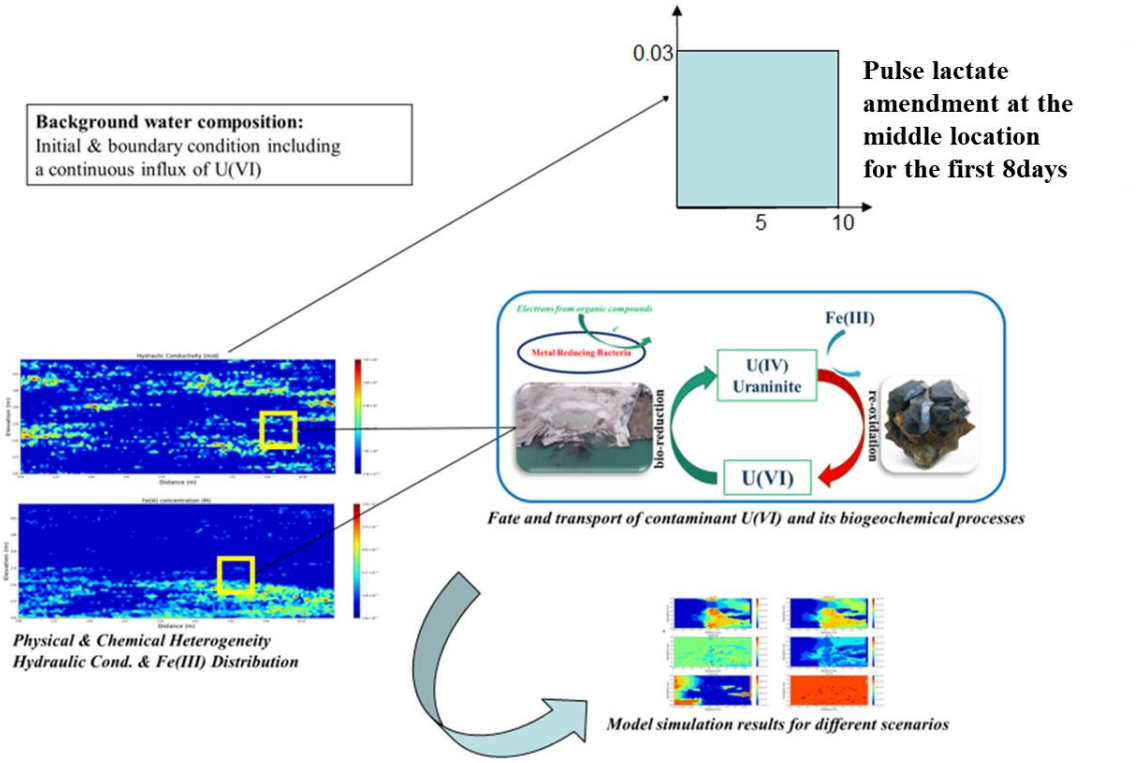

Figure 3.5. Conceptual model scheme of the study

CHAPTER 4

RESULTS AND DISCUSSION

In this section, 2D reactive transport model results are presented and discussed with regards to simulating key biogeochemical reaction processes coupled to the transport of contaminants under field scale heterogeneity, where an example for uranium fate and transport was chosen. The reaction network and model parameters used in the used were described in Chapter 3. The model simulations are set up with various levels of heterogeneity involvement, and each of their results are discussed as under three headings which are detailed below. In the first part of the model runs, the numerical model simulations are run with no adsorption of uranium or any other species onto the aquifer solids (Section 4.1). In the second part, adsorption of uranium onto Fe(III)-(hydr)oxide surfaces are implemented by surface complexation reactions (Section 4.2). In the last part, the numerical model simulations are compared with/without U(IV) reoxidation reaction by Fe(III)- (hydr)oxide minerals (Section 4.3). The list of all model simulations and corresponding different scenarios as described in related chapters are summarized in Table 4.1. below.

Table 4.1. The list of all model simulations and corresponding different scenarios considered in this study

Model Simulations	**Section 4.1**	**Section 4.2**	**Section 4.3**
Heterogeneous K & Heterogeneous Fe(III)	Reactive transport with biogeochemical reaction processes (Table 3.6.) using: -Uniform initial water composition (Table 3.1.)	Reactive transport with biogeochemical reaction processes (Table 3.6.) including surface complexation of U(VI) using: -uniform initial water composition (Table 3.1.) (Section 4.2.1.) - initial water composition after 25 yr of U(VI) loading period with surface complexation (Section 4.2.2.)	Reactive transport with biogeochemical reaction processes (Table 3.6. without reoxidation, i.e., without rxn # 4) including surface complexation of U(VI) using: - initial water composition after 25 yr of U(VI) loading period with surface complexation
Heterogeneous K & Homogeneous Fe(III)	Reactive transport with biogeochemical reaction processes (Table 3.6.) using: -Uniform initial water composition (Table 3.1.)	Reactive transport with biogeochemical reaction processes (Table 3.6.) including surface complexation of U(VI) using: -uniform initial water composition (Table 3.1.) (Section 4.2.1.) - initial water composition after 25 yr of U(VI) loading period with surface complexation (Section 4.2.2.)	Reactive transport with biogeochemical reaction processes (Table 3.6. without reoxidation, i.e., without rxn # 4) including surface complexation of U(VI) using: - initial water composition after 25 yr of U(VI) loading period with surface complexation

Table 4.2. (continued)

Model Simulations	Section 4.1	Section 4.2	Section 4.3
Homogeneous K & Homogeneous Fe(III)	Reactive transport with biogeochemical reaction processes (Table 3.6.) using: -Uniform initial water composition (Table 3.1.)	Reactive transport with biogeochemical reaction processes (Table 3.6.) including surface complexation of U(VI) using: -uniform initial water composition (Table 3.1) (Section 4.2.1.) - initial water composition after 25 yr of U(VI) loading period with surface complexation (Section 4.2.2.)	Reactive transport with biogeochemical reaction processes (Table 3.6. without reoxidation, i.e., without rxn # 4) including surface complexation of U(VI) using: - initial water composition after 25 yr of U(VI) loading period with surface complexation

4.1. Impact of Physical and Chemical Heterogeneity on the Biogeochemical Dynamics of Reactive Transport Model

In order to investigate the impact of physical and chemical heterogeneity on the reaction network of 2D reactive transport model of uranium, 3 different scenario cases were demonstrated, with differing levels of heterogeneity. In the first case, both physical and chemical heterogeneities are considered, where the heterogeneous hydraulic conductivity (Figure 3.2.) and heterogeneous Fe(III) distributions (Figure 3.3.) are assigned throughout the model domain. In the second case, the model domain included only physical heterogeneity with no chemical heterogeneity. Therefore for this case, the hydraulic conductivity representing the physical heterogeneity is distributed heterogeneously throughout the domain, whereas the distribution of Fe (III) hydroxide is homogeneous for each cell, corresponding to 7.25 x 10^{-3} mol/L_{water} of Fe(III) hydr(oxide) mineral concentration. In the third case, the model domain did not include

any physical or chemical heterogeneity. Thus, a unique value of 0.432 m/d for hydraulic conductivity, and a unique value of 7.25 x 10^{-3} mol/L_{water} for Fe(III) hydr(oxide) mineral concentration was assigned for all 6426 cells throughout the domain, based on the previous work of Sengor et al., (2015). In all scenario cases, lactate was injected for a time period of 8 days from an injection well defined from a middle location as seen in Figure 3.1., where a lactate containing solution (see Table 3.3.) was injected at a rate of 0.02 m^3/day into an initially steady-state flow field, resulting in transient flow conditions. The total simulation period was considered to be 40 days (being representative of demonstrating the impact of biotic and abiotic reactions on uranium transformation), where simulation results corresponding to days 8 and 40 are presented of all scenarios for the key species, which are lactate, acetate, sulfate, Fe (II), U(VI) and uraninite (UO_2). The concentrations of Cl (tracer), U(IV), mackinawite (FeS), total aqueous sulfide (S) and sulfur (S(s)) species as well as pH are also presented.

Figures 4.1. and 4.2. show the concentration distribution of key species in heterogeneous hydraulic conductivity and heterogeneous Fe(III) concentration distribution case after 8 and 40 days of simulation period, respectively. Figures 4.3. and 4.4. show the concentration distribution of key species in heterogeneous hydraulic conductivity and homogeneous Fe(III) concentration distribution case after 8 and 40 days of simulation period, respectively. Figure 4.5. shows the concentration distribution of key species in homogeneous hydraulic conductivity and Fe(III) concentration distribution case after 40 days of simulation period. In addition to the areal concentration distributions, key species concentrations have also been plotted along a vertical cross section of the model domain at x=9m, in order to elucidate the concentration changes within the low and high physical and chemical heterogeneity zones (Figure 4.8.- 4.10.). Hydraulic conductivity and Fe (III) hydroxide concentration distribution (namely hematite concentration), along the vertical cross section at x=9m are also shown in Figure 4.6. and Figure 4.7., to compare the heterogeneous zones and corresponding concentration predictions at this

section, as presented for various cases below. As shown in Figure 4.6., a low hydraulic conductivity zone appears between 1.8-2 m and 3-3.6 m, and a high hydraulic conductivity zone appears between 3.8- 5.4 m. For the hematite concentration distribution, a low zone is observed at 2.2-3.6 m and a high zone is seen around 0-1.8 m (Figure 4.7.).

When model simulations are compared as seen in Figure 4.1.-4.5. separately for the heterogeneous and homogeneous cases, the influences of physical and chemical heterogeneity on subsurface transport can be observed. For the homogeneous hydraulic conductivity and Fe(III) concentration distribution case, a uniform and regular concentration distribution is monitored, due to the absence of any spatial variability physically and chemically. However, as the model site becomes more heterogeneous physically, spatial variation in concentration of key species is also observed The spatial variability of concentration of key species confirms that heterogeneity exerts a significant role in terms of groundwater flow and contaminant transport in subsurface, and when the heterogeneity is ignored, this would cause an overestimation of bioreduction processes. In accordance with the present findings, previous studies have demonstrated that heterogeneity has significant control on the groundwater transport and reactive processes (Scheibe et al., 2006 & Li et al., 2010). The comparison between physical and chemical heterogeneity from the model simulations show that the impact of physical heterogeneity is more visible.

When the model predictions are compared for 8 and 40 days of simulation period, the impact of lactate injection, resulting in sulfate bioreduction and acetate generation, along with Fe(III) bioreduction to produce Fe(II) can be monitored from 8 to 40 days of simulation. With the injection of lactate, U(VI) bioreduction to U(IV) forming uraninite mineral, along with the lactate degradation trends can also be seen; demonstrating that the model simulations capture the complex biogeochemical reaction kinetics coupled with transport of aqueous species in the system (Figures 4.1. – 4.5.). Besides the areal

concentration distribution of key species at the model site, vertical cross section distributions at x=9m are also presented to elucidate the concentrations along the heterogeneous zones. Figure 4.8. shows lactate, acetate, sulfate, Fe(II), U(VI), and uraninite distributions; and Figure 4.9. shows pH, mackinawite, total aqueous sulfide, and sulfur distributions along the vertical cross section of the model domain at x=9m. In Figures 4.8. and Figure 4.9. (and subsequent x-section figures presented throughout of Chapter 4), red lines represent the heterogeneous hydraulic conductivity & heterogeneous Fe(III) hydroxide distribution case results; blue lines represent heterogeneous hydraulic conductivity & homogeneous Fe(III) hydroxide distribution case results; green lines represent homogeneous hydraulic conductivity & homogeneous Fe(III) hydroxide distribution case results. The model simulation results across the cross section of the domain indicate the fluctuations of species concentrations, where high concentrations are observed corresponding to relatively high hydraulic conductivity zones and low concentrations are observed corresponding to low conductivity zones within the x-section, due to the preferential transport through areas of high conductivity resulting in high mixing and reaction potential. Therefore, the lowest concentrations (nearly zero) are seen at locations along the 1.8-1.9 m and 3-3.6 m zones which are associated with the lowest hydraulic conductivity (Figure 4.8. -4.10.). Accordingly, mineral formations (i.e. mackinawite, uraninite, sulfur) are also observed at areas of high mixing at the high conductivity zones, following the biogeochemical reaction dynamics (Table 3.6.); and pH values show decreasing trends based on sulfate and Fe(III) reduction reactions resulting in Fe(II) formation and sulfur precipitation (Figure 4.10.). The uranyl concentrations on the other hand, show the highest distributions along the lowest hydraulic conductivity zones due to the initially uniform 1 μM concentration distributions throughout the domain (Figure 4.8a). The transport of solution and dissolved species within the low hydraulic conductivity zones would be limited within these low conductivity lenses with enhanced mixing limitations, resulting in limited reaction potential. The results thus demonstrate the strong impact of spatial variations of

hydraulic conductivity on the overall fate and transport of dissolved constituents in the porewater, pointing out the fact that physical heterogeneity is a key challenge for reliable contaminant transport predictions in subsurface.

When the model results with heterogeneous hydraulic conductivity and Fe(III) distribution case is compared with heterogeneous hydraulic conductivity and homogeneous Fe(III) distribution, the concentration distributions are observed to be nearly identical. These results demonstrate that physical heterogeneity has a greater impact than chemical heterogeneity with respect to the model predictions of biogeochemical reaction dynamics coupled to subsurface transport. Comparing the model predictions of heterogeneous hydraulic conductivity and Fe(III) distribution case with homogeneous hydraulic conductivity and Fe(III) distribution results, it is seen that uranium concentrations are significantly lower in the homogeneous case, indicating that assuming homogeneity would lead to an overestimation of bioreduction or bioremediation of the contaminant of concern in the subsurface environment.

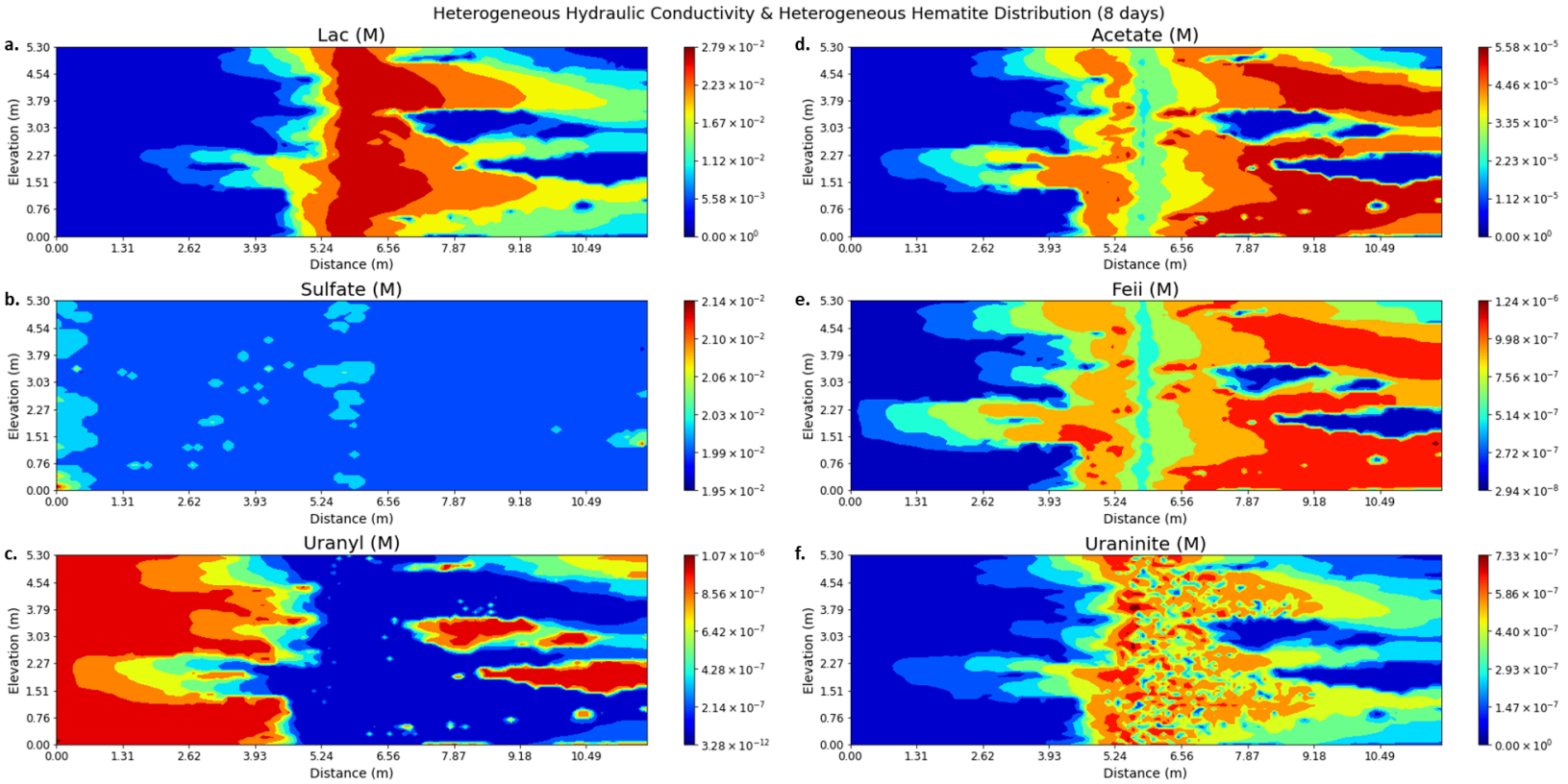

Figure 4.1. Concentration distribution of key species in heterogeneous hydraulic conductivity and heterogeneous Fe(III) hydroxide concentration distribution case for 8 days

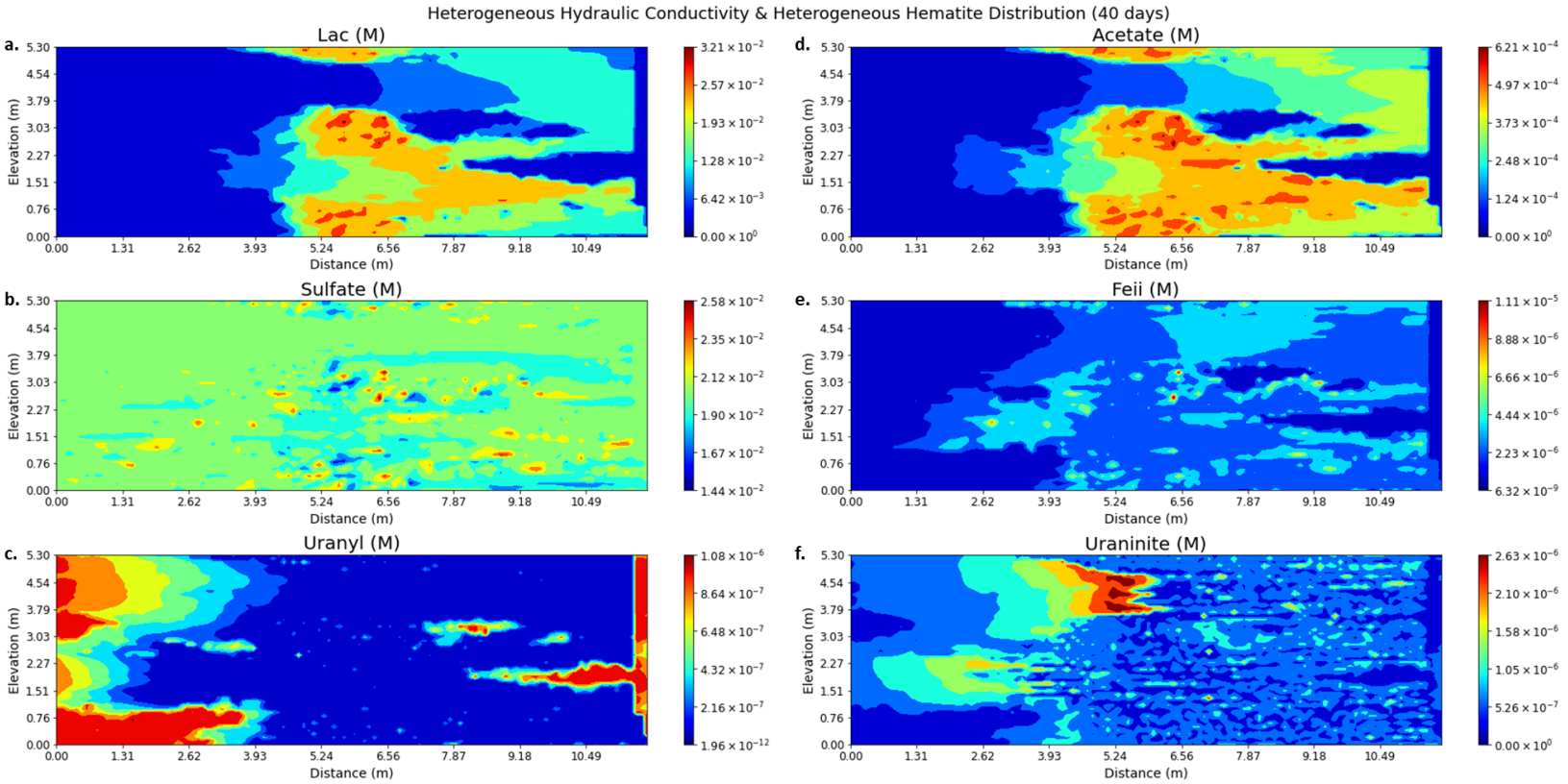

Figure 4.2. Concentration distribution of key species in heterogeneous hydraulic conductivity and heterogeneous Fe(III) hydroxide concentration distribution case for 40 days

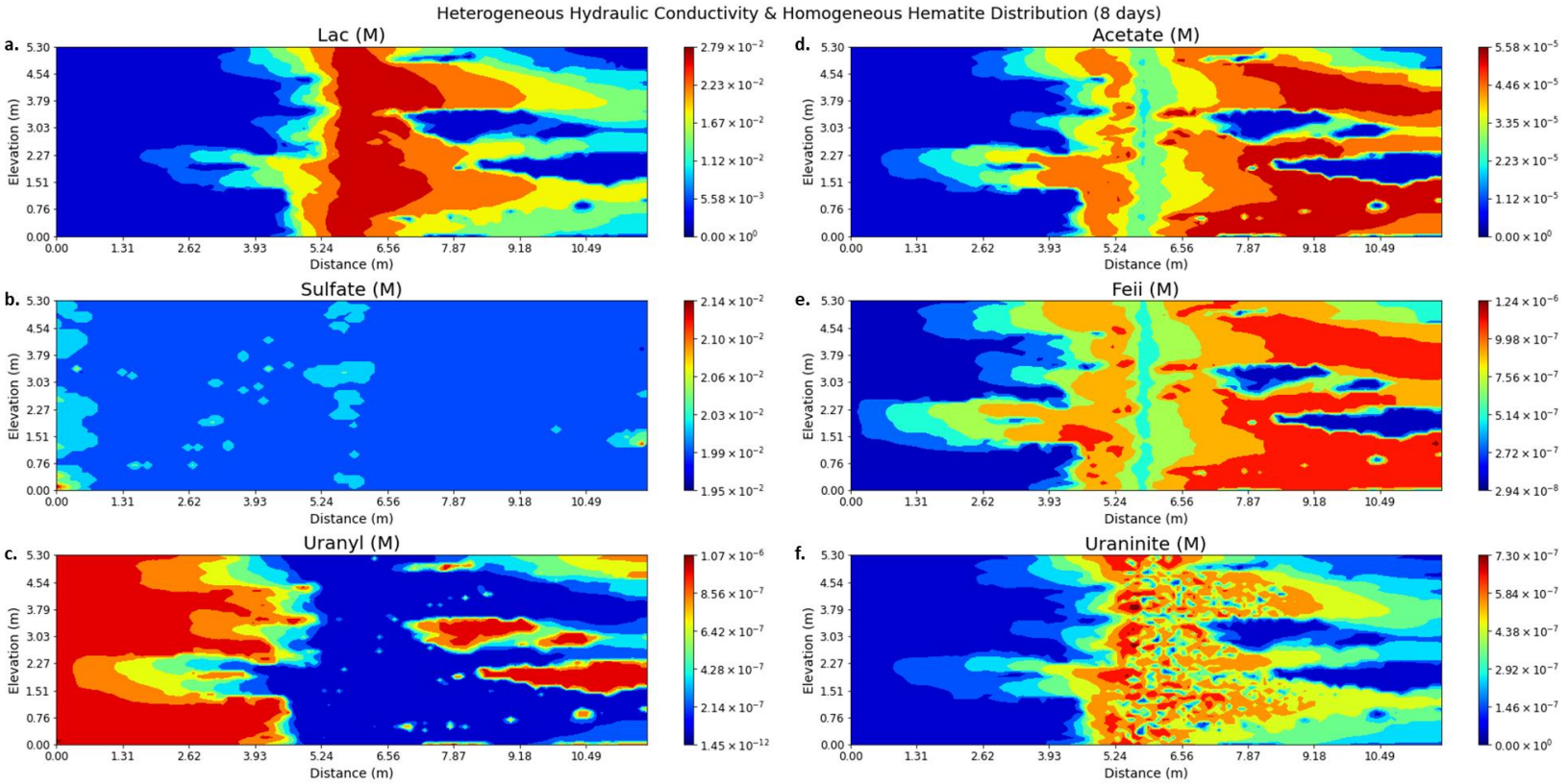

Figure 4.3. Concentration distribution of key species in heterogeneous hydraulic conductivity and homogeneous Fe(III) hydroxide concentration distribution case for 8 days

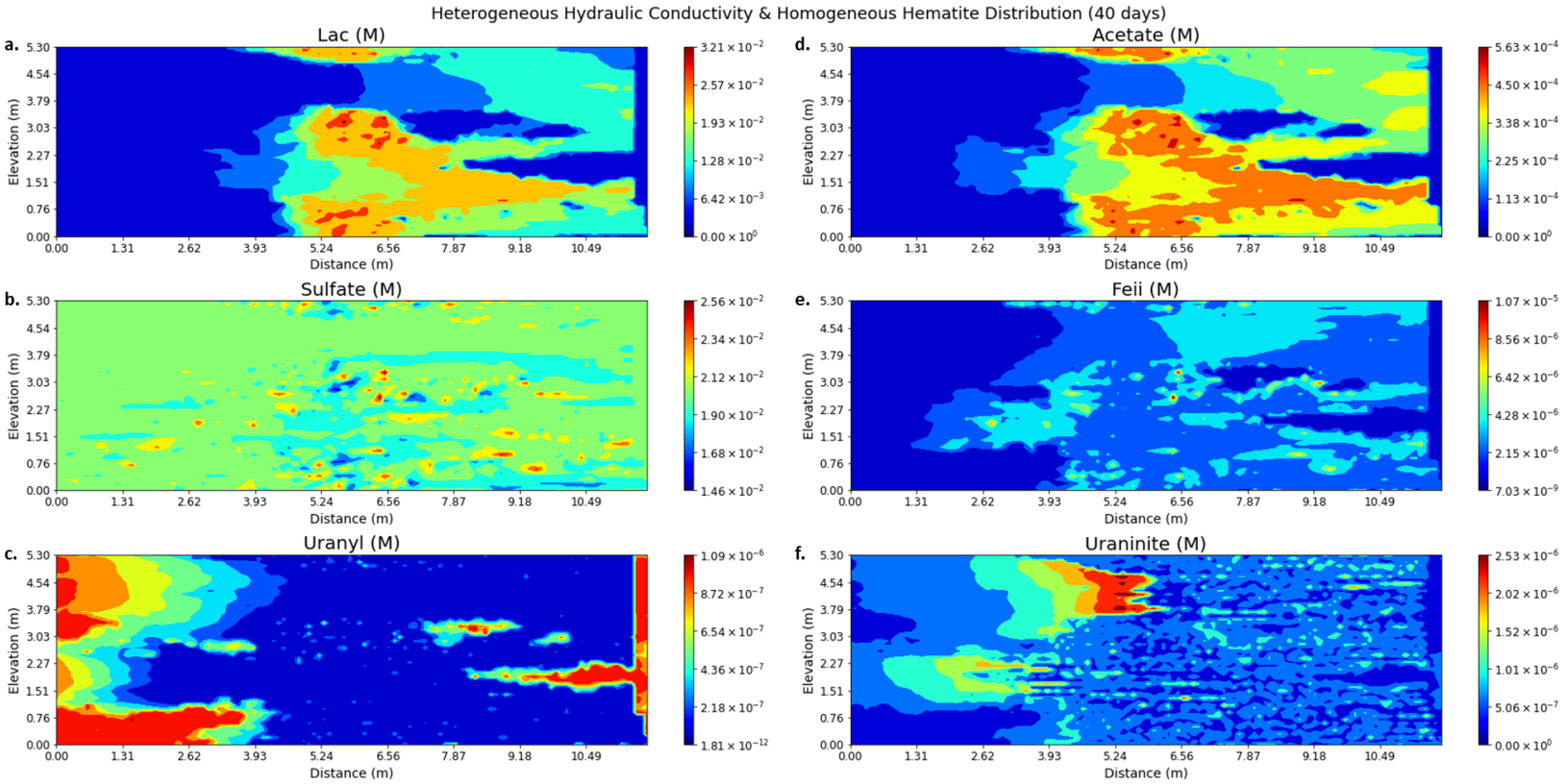

Figure 4.4. Concentration distribution of key species in heterogeneous hydraulic conductivity and homogeneous Fe(III) hydroxide concentration distribution case for 40 days

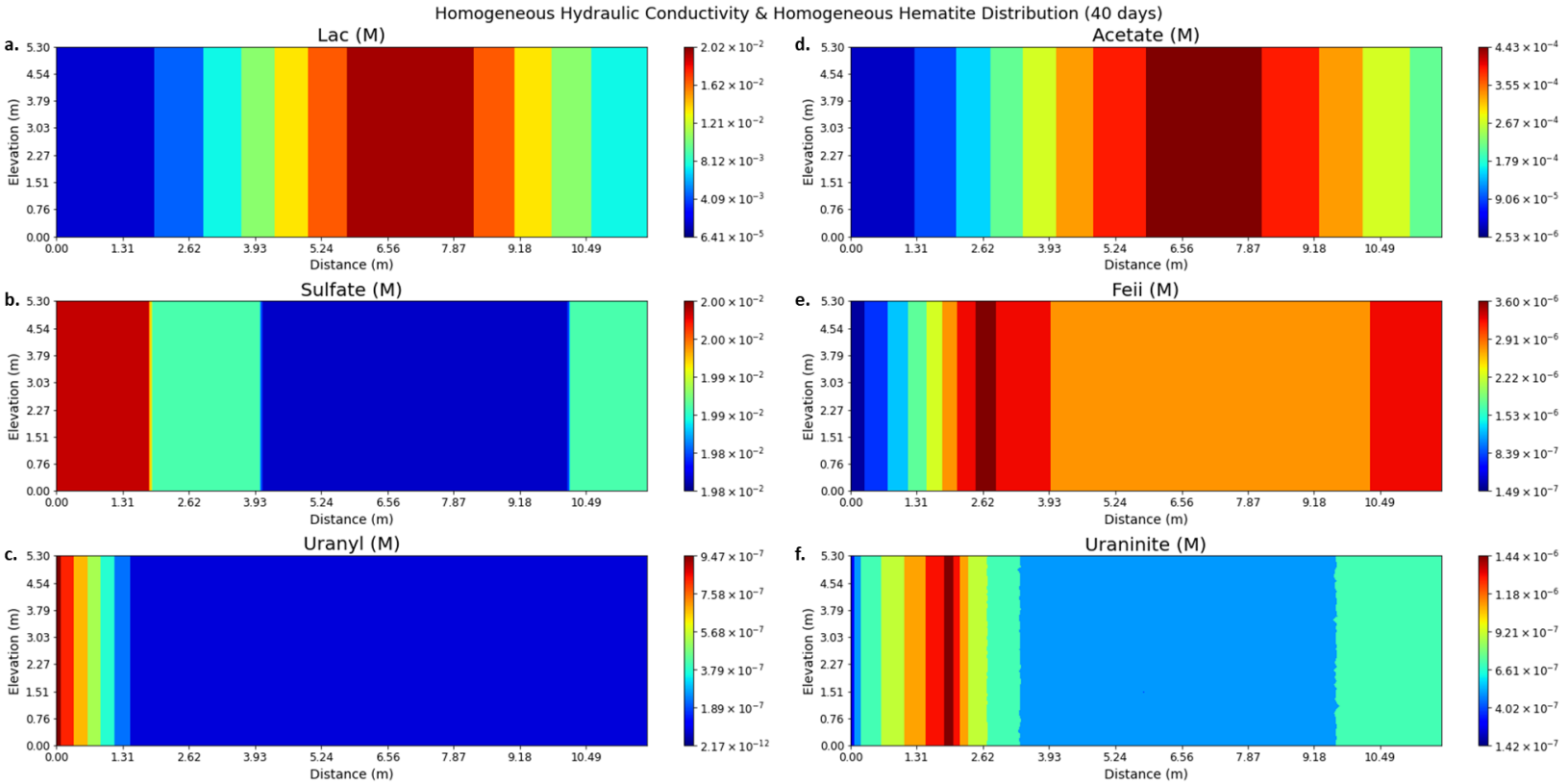

Figure 4.5. Concentration distribution of key species in homogeneous hydraulic conductivity and homogeneous Fe(III) hydroxide concentration distribution case for 8 days

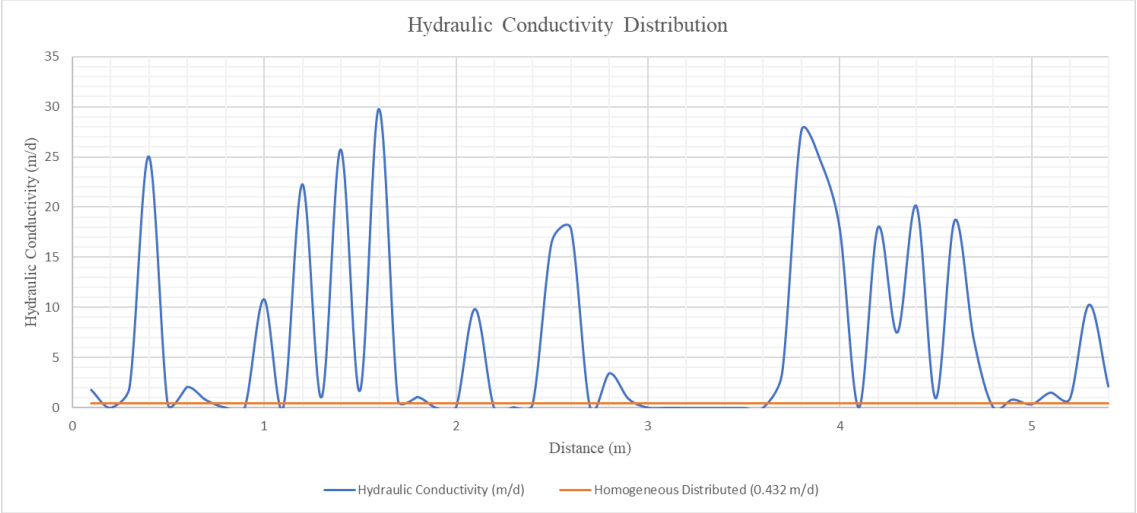

Figure 4.6. Homogeneously and heterogeneously distributed hydraulic conductivity from the section x=9 m

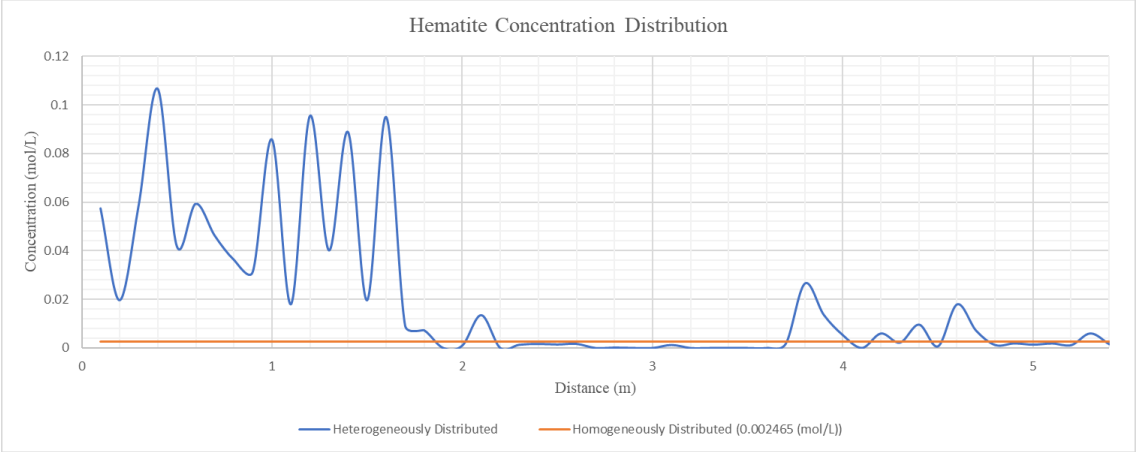

Figure 4.7. Homogeneously and heterogeneously distributed Fe(III) hydroxides concentration from the section x=9 m

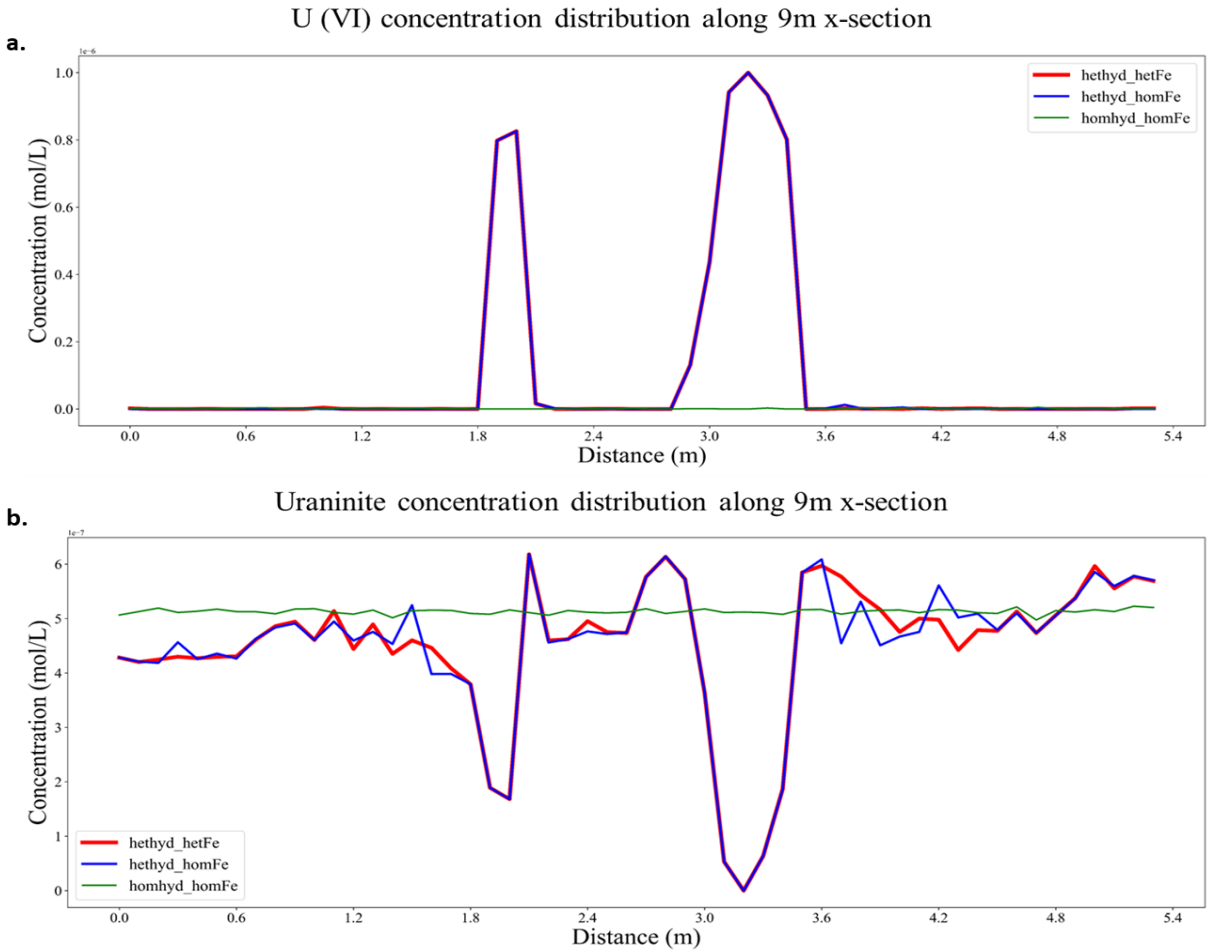

Figure 4.8. U(VI) and Uraninite concentration distribution along 9m x-section for 30 days

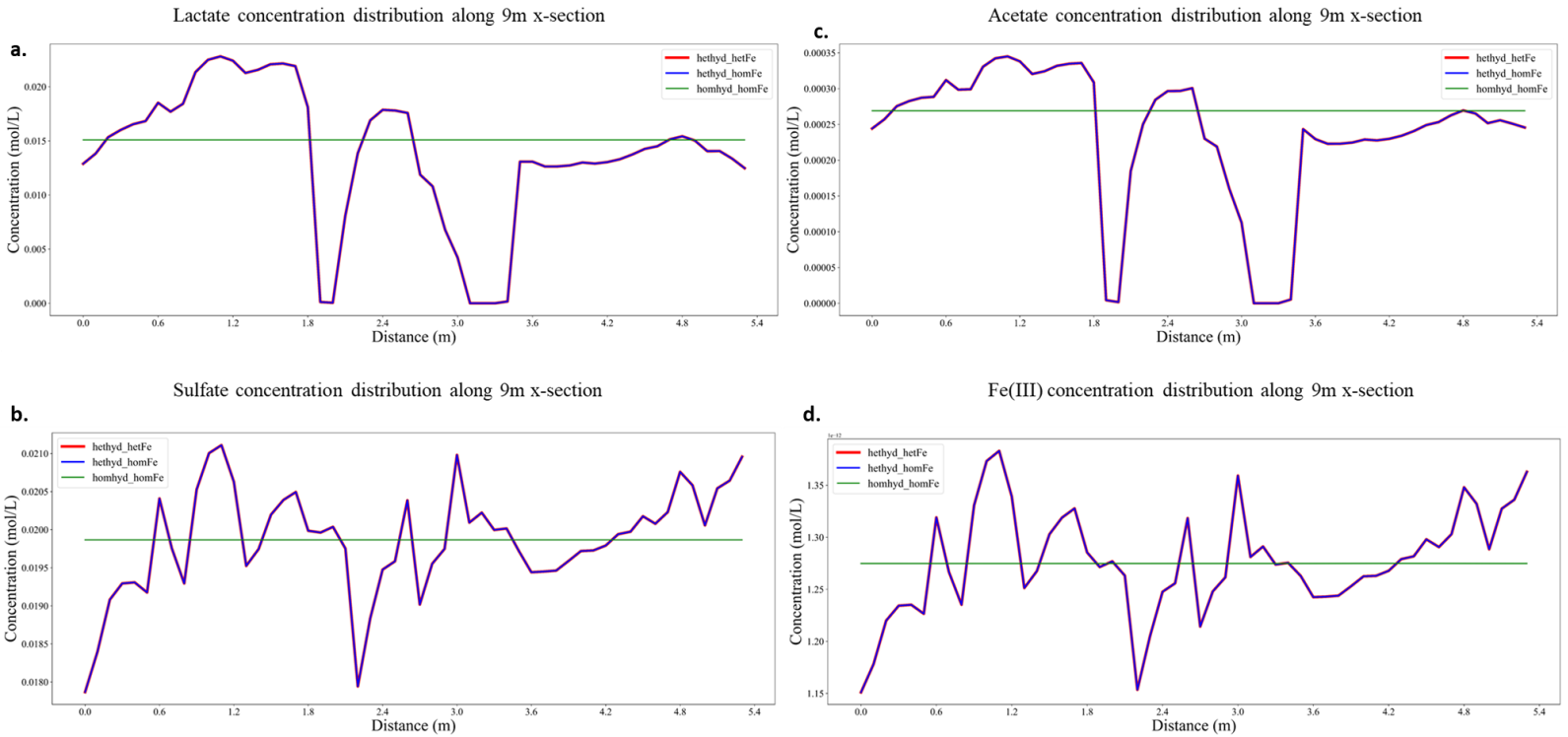

Figure 4.9. Concentration distribution of key species (lactate,acetate, sulfate and Fe(III)) along 9m x-section for 30 days

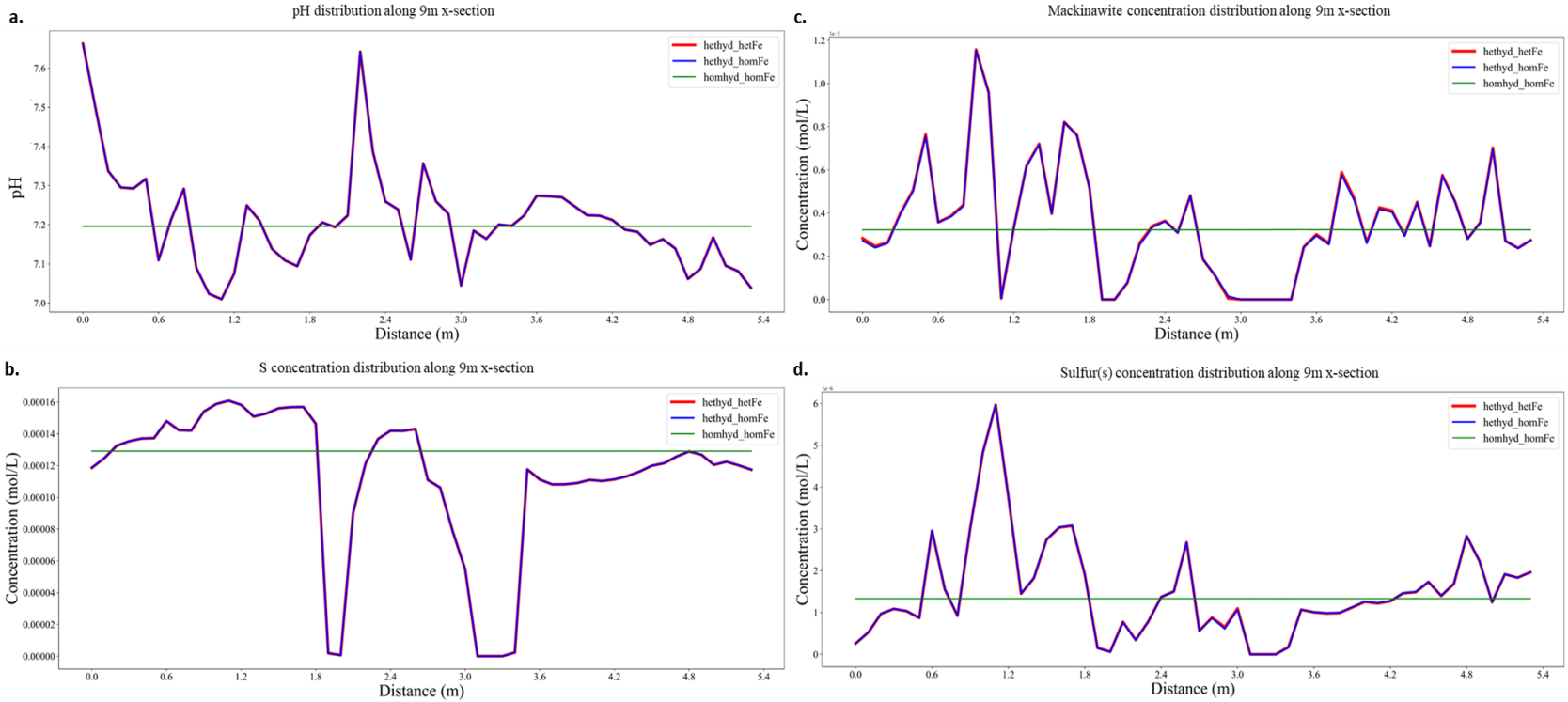

Figure 4.10. Concentration and pH distribution of key species (mackinawite, S and Sulfur(s)) along 9m x-section for 30 days

4.2. Impact of Physical and Chemical Heterogeneity on the Biogeochemical Dynamics of Reactive Transport Model with Surface Complexation of U(VI)

The results of previous part of the study demonstrated that the physical heterogeneity compared to chemical heterogeneity has more remarkable impact on groundwater transport in the absence of surface complexation. In this part, the 2D transport model was set up by the incorporation of surface complexation reactions, particularly U(VI) sorption onto Fe(hydr)oxide solids, to see the impact of all biogeochemical reaction network including sorption reactions on uranium fate and transport. Uranium adsorption reactions are implemented in the model by surface complexation using non-electrostatic double layer modeling (Dzombak and Morel, 1990).

Iron (hydr)oxide phases are often associated with the solid matrix composition within the aquifer environment in the subsurface. Iron (hydr)oxide nanoparticle phases may also form in natural waters and at oxic-anoxic boundaries in sediments, and it is well established that they can control the solid-solution partitioning of numerous toxic metal species in near-surface aqueous regimes (Amde et al., 2017). Thus, iron (hydr)oxide compounds and their colloidal counterparts have significant applications in soil and groundwater remediation due to their large surface areas, self-assembly potential, high specificity, and high reactivity characteristics, which can lead to spontaneous adsorption and co-precipitation of heavy metals, including uranium. Therefore, understanding and integration of sorption processes into model simulations are highly important for accurate representation of (bio)geochemical reaction dynamics occurring in the environment of concern and to properly justify reactive transport modeling predictions.

4.2.1 Reactive Transport Simulations Using Uniform Initial Water Composition

Reactive transport simulations including surface complexation of U(VI) onto Fe(III)hydroxide surfaces are carried out using uniform initial water composition (see Table 3.1.) at t=0, as in the previous section (Section 4.1) model simulations. The model results are therefore compared for the three case scenarios along with the previous section results without surface complexation, in order to elucidate the impact of surface complexation. The simulation results are given in 10 through 6 for each scenario case. Figure 4.11. and Figure 4.12. shows the concentration distribution of key species in heterogeneous hydraulic conductivity and heterogeneous Fe(III) concentration distributions for 8 and 40 days, respectively. Figure 4.13. and Figure 4.14. shows the concentration distribution of key species in heterogeneous hydraulic conductivity and homogeneous Fe(III) concentration distributions for 8 and 40 days, respectively. Figure 4.15. shows the concentration distribution of key species in homogeneous hydraulic conductivity and homogeneous Fe(III) concentration distributions after 40 days of simulation period. The numerical model simulations including surface complexation again capture the biogeochemical dynamics of the system coupled with transport of species in the model domain. The all reaction mechanism are same with the previous scenario. With the injection of lactate, U(VI) reduction, acetate and sulfate generation and Fe(III) reduction processes are simulated as seen in the Figures 4.11. – 4.15., following the same reaction network as in the previous section. When surface complexation of U(VI) species onto Fe(III) hyroxide solids are included in the model, the results show higher amount of U(VI) to be retained in the system, leading to form higher amounts of uraninite (and correspondingly low amounts of soluble U(IV)) at the model site, compared to previous model simulations without surface complexation, whereas the concentrations of other key species show almost the same distribution. When the heterogeneous K-heterogeneous Fe(III) distribution and the heterogeneous K-homogeneous Fe(III) distributions are compared, it is observed that the surface complexation impact is more pronounced in the presence of chemical heterogeneity

(Figures 4.18.-4.20.), which is due to the heterogeneous distribution of hematite at the site, where hematite concentration values are relatively higher compared to the homogeneous average hematite of 7.25 x 10^{-3} moles/L_{water} (see Figure 4.7.)

To demonstrate the difference between the physical and chemical heterogeneity in the presence of surface complexation, the concentration distributions of key species along the 9 m x-section are presented (Figure 4.16. -4.18.). As seen from the results (Figure 4.16.), when surface complexation is included in the biogeochemical reaction dynamics, especially the soluble uranium U(VI) and bioreduced uranium (i.e., uraninite mineral) concentrations are observed to be significantly higher in the system when both physical and chemical heterogeneity is involved (compared to only physical heterogeneity case, as well as homogeneous K and Fe distribution cases). The sorption of uranium ions in the system results in higher retention of the species in the system, resulting in higher soluble concentrations, and higher potential of reacting with other compounds, especially with Fe(hydr)oxide mineral surfaces with higher potential of reduction to uraninite mineral; ending up in higher uraninite mineral distribution in the system. This impact is observed to be significantly enhanced in the presence of chemical heterogeneity, due to the high potential of uranium and Fe(hydr)oxide mineral surface interactions. Therefore, these results reveal that when potential sorption of uranium contaminants are ignored in reactive transport models in a relatively chemically heterogeneous environment, the contaminant concentrations might be underestimated. The underestimation is seen to be more pronounced especially in the low hydraulic conductivity zones, where highest peaks of U(VI) and corresponding low peaks of uraninite mineral concentrations are observed along the 1.8-1.9 m and 3-3.6 m zones within the 9 m x-section profiles (Figure 4.16.), which are associated with the lowest hydraulic conductivity areas within the x-section (Figure 4.18.).Therefore the model results imply that chemical heterogeneity is more pronounced in low physical heterogeneity zones due to the mixing limitations. Ignoring the potential adsorption

reactions in chemically heterogeneous environments might lead to the overestimation of bioremediation/bioreduction processes in the subsurface environment.

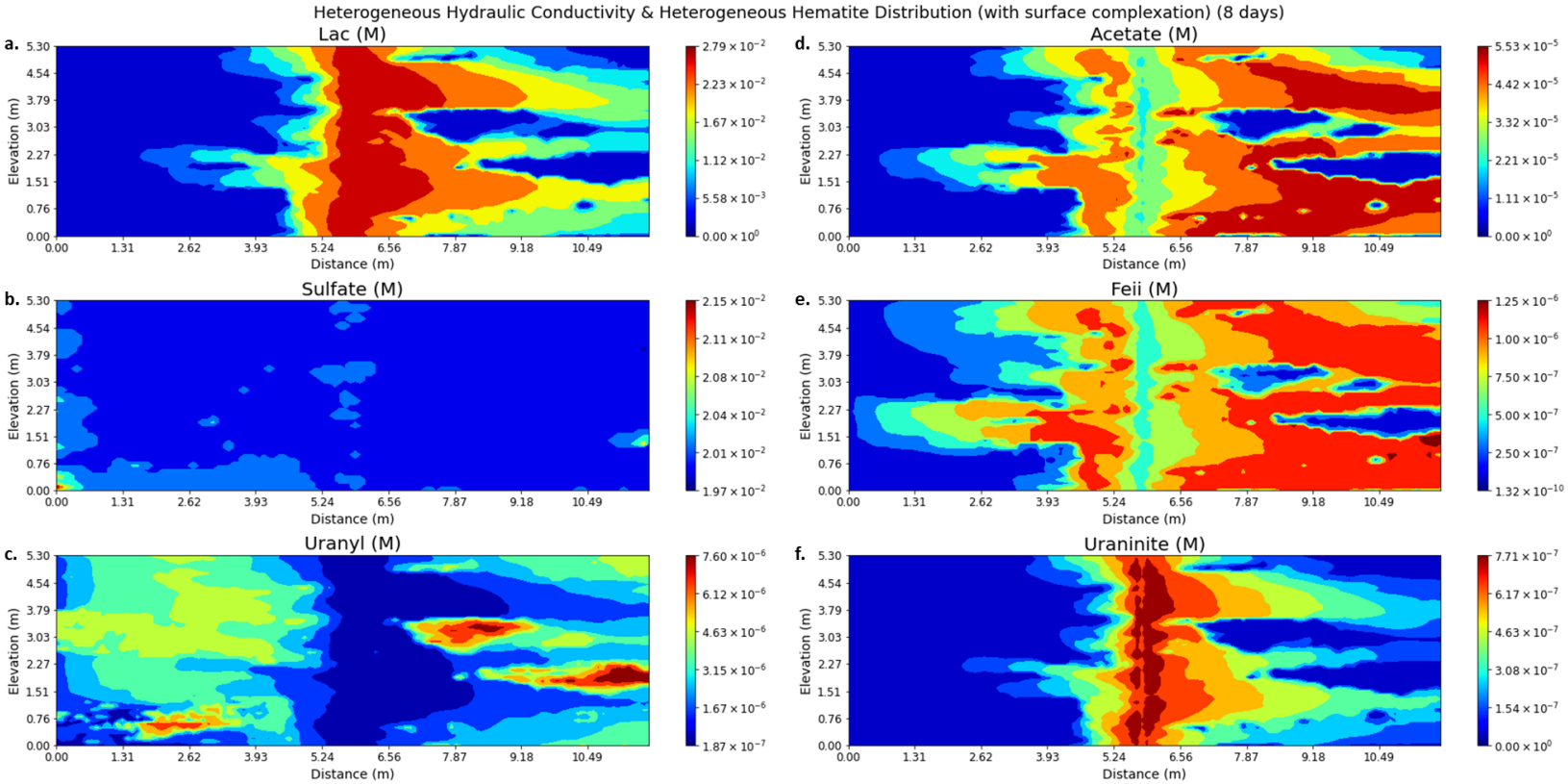

Figure 4.11. Concentration distribution of key species in heterogeneous hydraulic conductivity and heterogeneous Fe(III) hydroxide concentration distribution with surface complexation case for 8 days

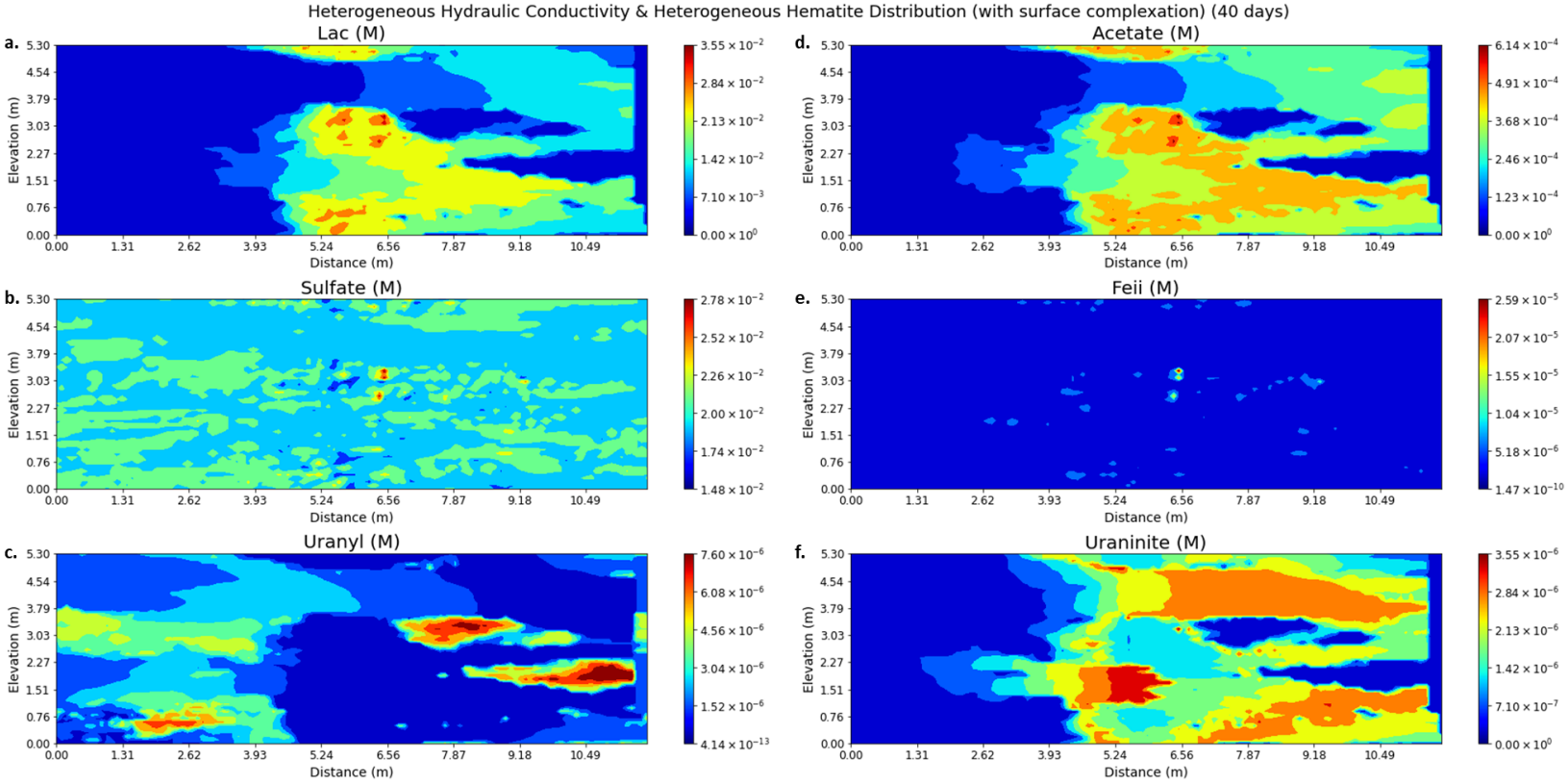

Figure 4.12. Concentration distribution of key species in heterogeneous hydraulic conductivity and heterogeneous Fe(III) hydroxide concentration distribution with surface complexation case for 40 days

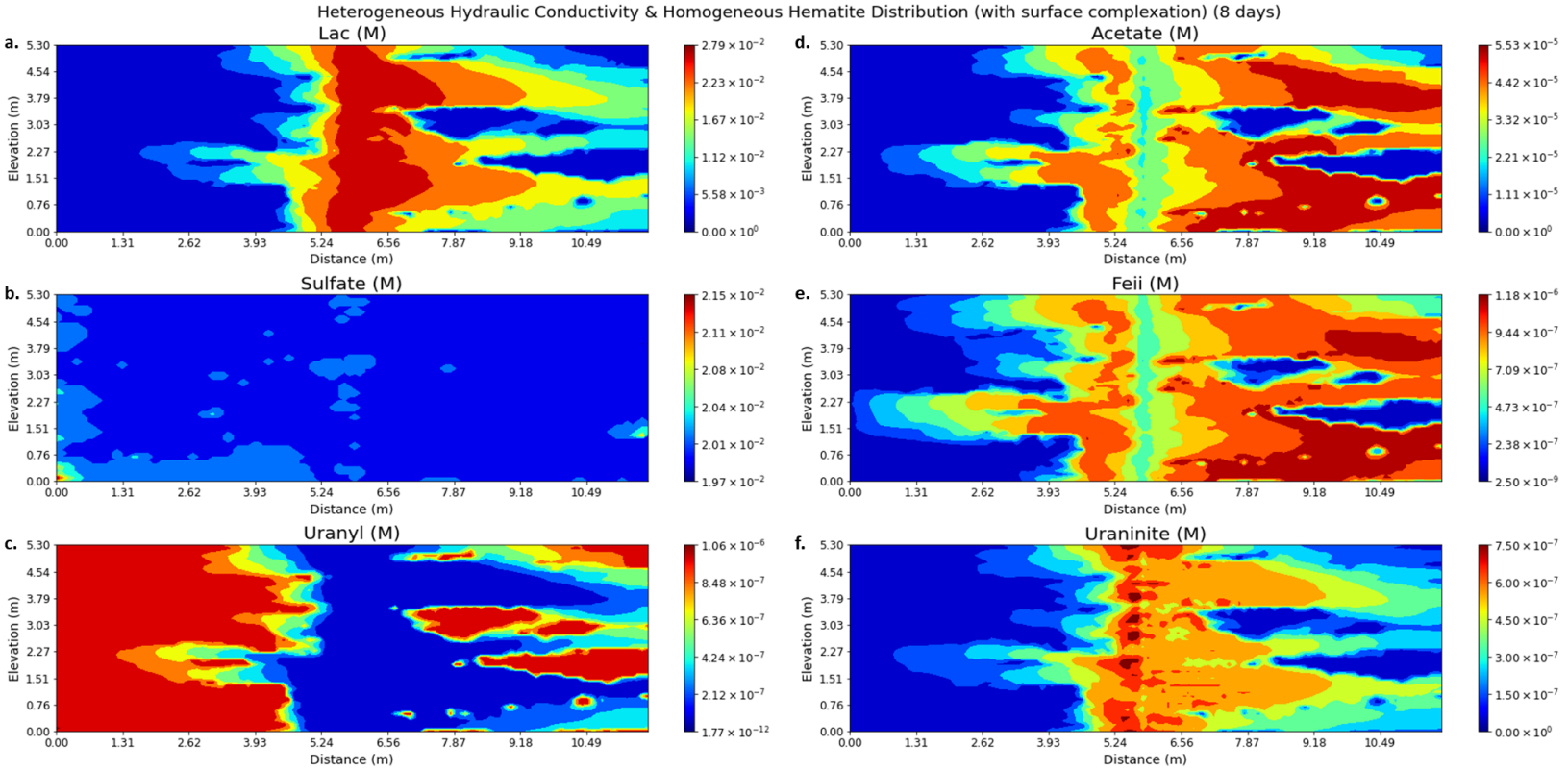

Figure 4.13. Concentration distribution of key species in heterogeneous hydraulic conductivity and homogeneous Fe(III) hydroxide concentration distribution with surface complexation case for 8 days

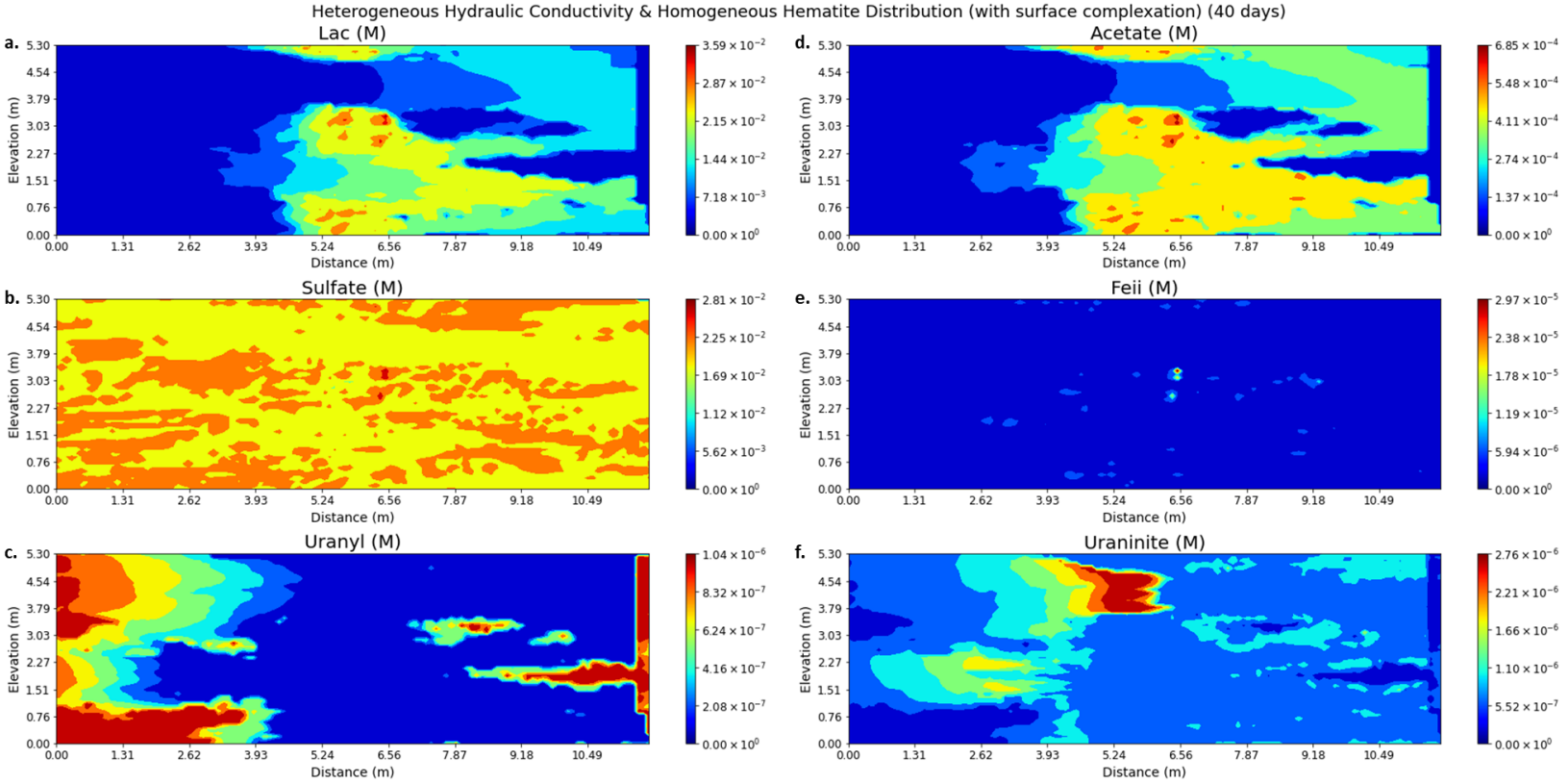

Figure 4.14. Concentration distribution of key species in heterogeneous hydraulic conductivity and homogeneous Fe(III) hydroxide concentration distribution with surface complexation case for 40 days

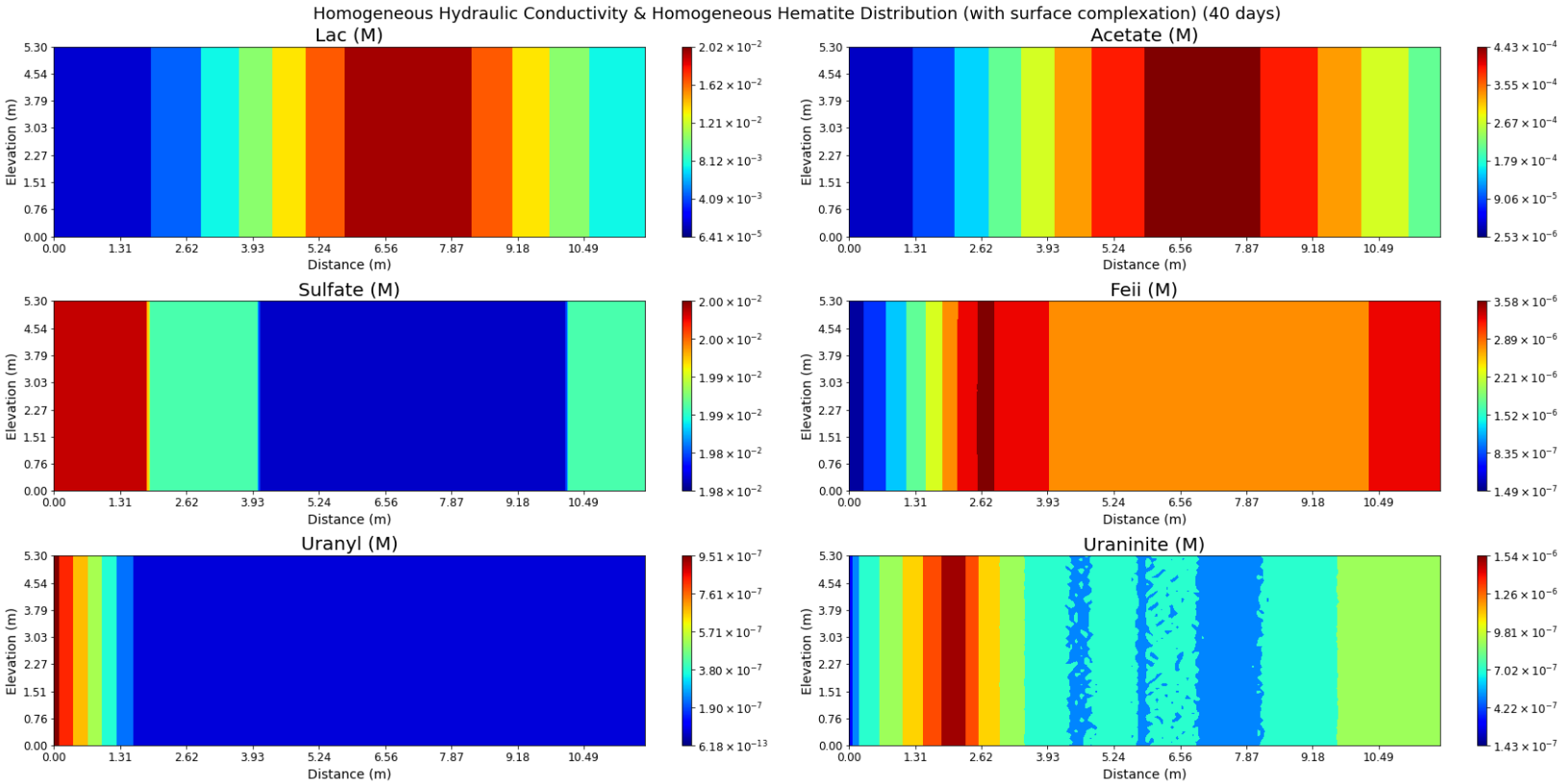

Figure 4.15. Concentration distribution of key species in homogeneous hydraulic conductivity and homogeneous Fe(III) hydroxide concentration distribution with surface complexation case for 40 days

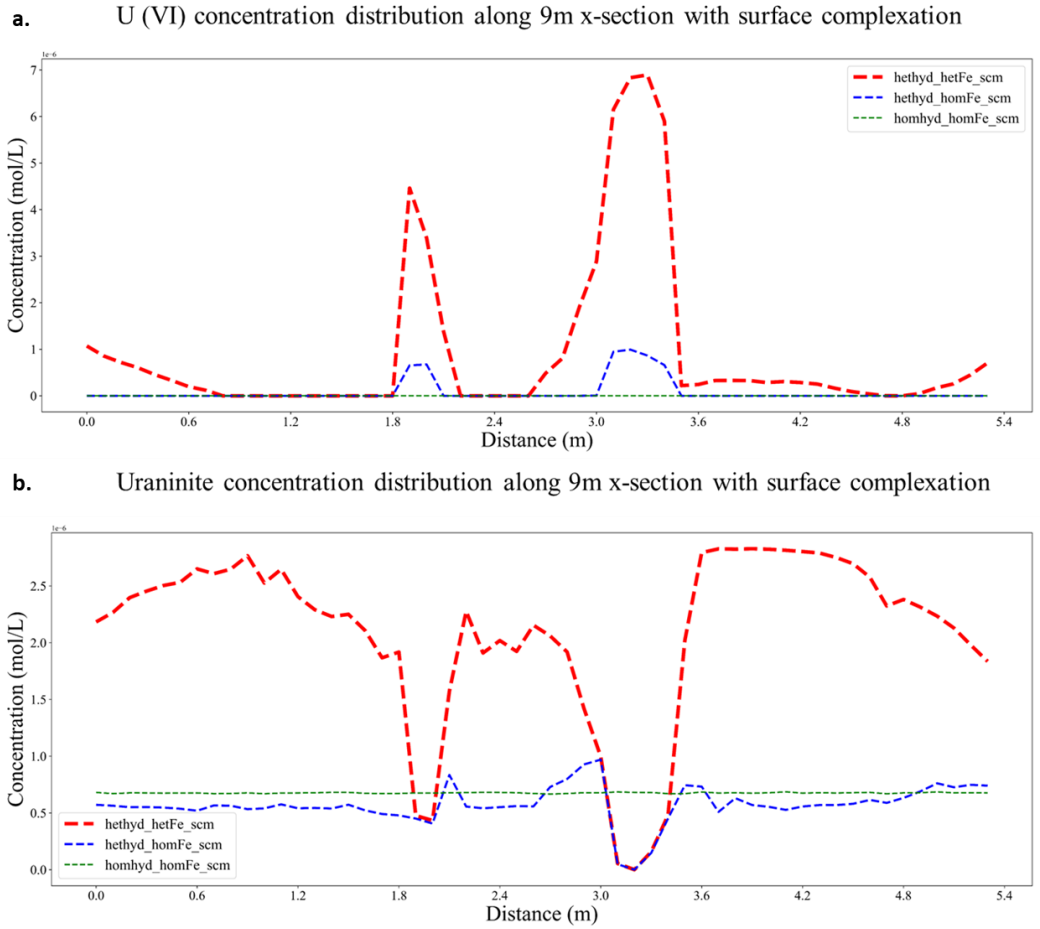

Figure 4.16. U(VI) and Uraninite concentration distribution along 9m x-section for 30 days

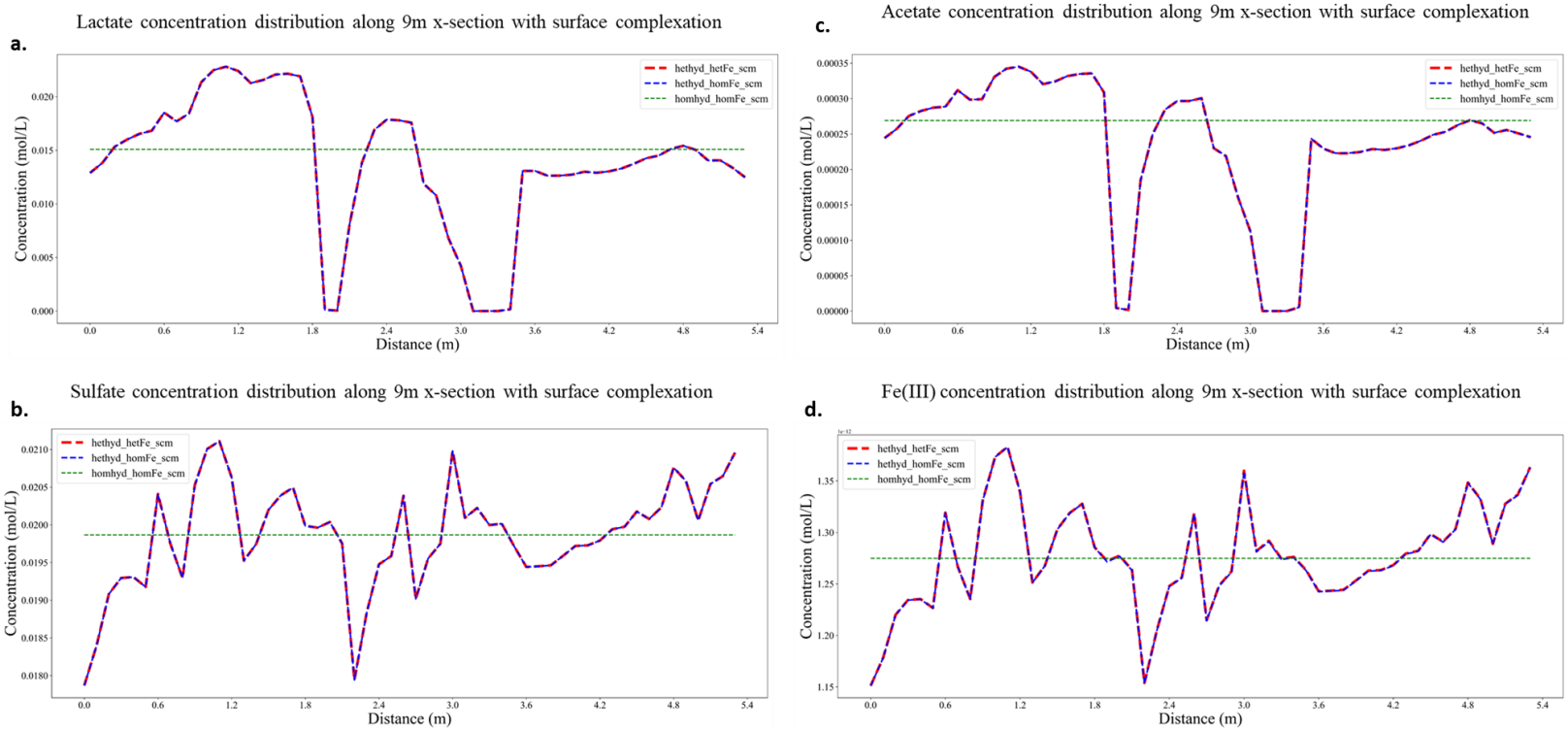

Figure 4.17. Concentration distribution of key species (lactate,acetate, sulfate and Fe(III)) along 9m x-section for 30 days

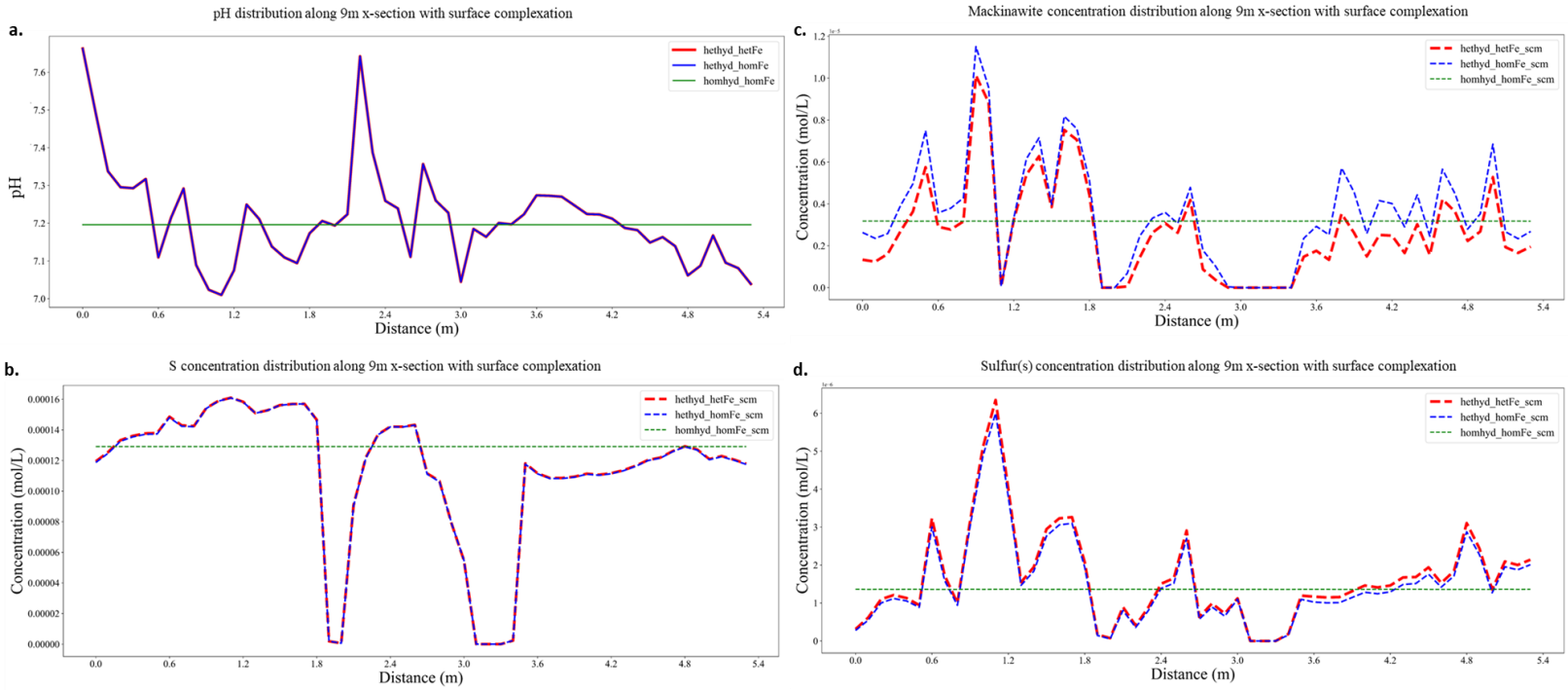

Figure 4.18. Concentration and pH distribution of key species (mackinawite, S and Sulfur(s)) along 9m x-section for 30 days

4.2.2. Reactive Transport Simulations Using Initial Water Composition after 25 yr of U(VI) Loading Period with Surface Complexation

Reactive transport simulations including surface complexation of U(VI) onto Fe(III)hydroxide surfaces are also carried out using initial water composition after 25 yr of U(VI) loading period with surface complexation at t=0, being more representative of natural field conditions when considering the influence of surface complexation. In these runs, model site is first loaded with uranium from an upgradient source at a uniform concentration of $1x10^{-6}$ μmol/L for 25 years to obtain quasi-equilibrium state of uranium concentration (aqueous and sorbed U(VI)) distribution. Then the distribution of uranium concentration is used as the initial condition for transient flow runs. During these runs only equilibrium surface complexation reaction of U(VI) onto hematite surfaces are included, whereas all other reaction network (of Table 3.6.) is ignored.

The initial uranium concentration distributions for each scenario case are given in Figure 4.19.

When the simulation results for all key species are compared with the results of Section 4.2.1., the same concentration trends are observed; supporting the same conclusions drawn as in Section 4.2.1. The initial condition effect just results in higher U(VI) concentration distribution at low hydraulic conductivity zones, as seen in Figure 4.20., which shows the U(VI) concentration distribution after 40 days of simulation period at the x=9m cross-section. The higher U(VI) concentrations are expected, as the adsorption of higher concentration ions within the limited mixing zones results in their enhanced retention with increased concentration effect.

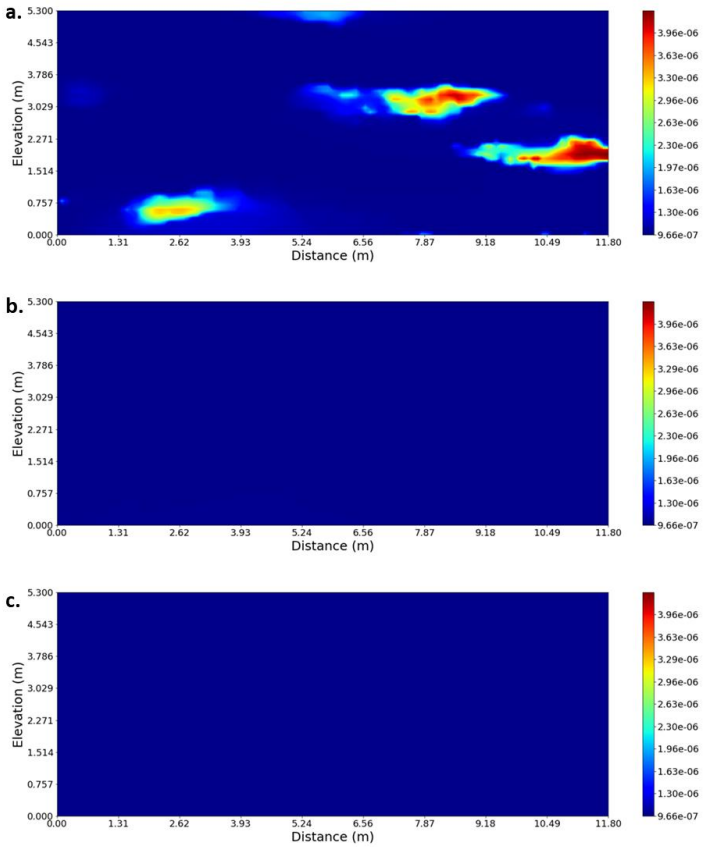

Figure 4.19. The initial uranium concentration distributions after reaching quasi-equilibrium at 25 yr (a) Heterogeneous K-heterogeneous Fe, (b) Heterogeneous K- homogeneous Fe, (c) Homogeneous K- homogeneous Fe case (Since the values of Heterogeneous K-homogeneous Fe scenario are very close, color distribution is not observed in this graph.)

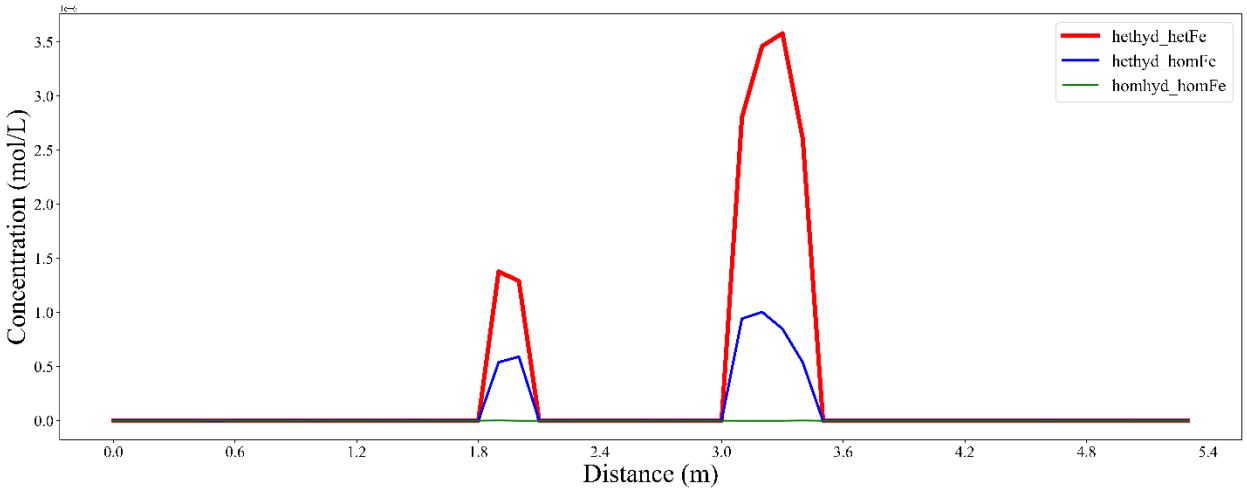

Figure 4.20. U (VI) concentration distribution along 9m x-section for 40 days

4.3.Impact of Physical and Chemical Heterogeneity on the Biogeochemical Dynamics of Reactive Transport Model Transport Model without U(IV)reoxidation Reaction

In this part, the impact of U(IV) (i.e. in the form of uraninite mineral) reoxidation reaction back to soluble U(VI), in the presence of Fe(hydr)oxide minerals is investigated, to elucidate reoxidation and hence solubilization potential of bioreduced uranium in the presence of physical and chemical heterogeneity in an example of subsurface environmental setting. As mentioned in Chapter 2, Sani et al., (2004) has indicated that the reduction of U(VI) to U(IV) being the promising approach in terms of bioremediation strategies, can be reversed in the absence of electron donor: where the precipitated uraninite can be reoxidized with using Fe (III) hydroxides as an electron acceptor. Therefore, it is aimed to put forth the relationship between the overall reaction network and reoxidation processes in this part.

In a reducing environment, reoxidation potential of available species in the system (e.g. U(IV) or HS^-) with the Fe(III) hydroxide is critical in terms of predicting the mobilization and/or immobilization potential of pollutants in the porewater. Concomitant reduction and oxidation processes considered in this study are listed in Table 3.6. To delineate the influence of reoxidation on biogeochemical processes, the same reaction system as described in sections 4.1 and 4.2 were simulated, but without the U(VI) reoxidation reaction (i.e., reaction # 6 as shown in Table 3.6.) for homogeneous and heterogeneous scenarios separately. In this regard, the differences in the concentration distribution of key species in these scenarios, especially U(VI) and U(IV) (and hence uraninite) were monitored. Model simulations without reoxidation were conducted, and their concentration distribution schemes are given below in Figures 4.21. through 4.25. Figure 4.21. and Figure 4.22. shows the concentration distribution of key species in heterogeneous hydraulic conductivity and heterogeneous Fe(III)

concentration distribution without reoxidation case after 8 and 40 days of simulation period, respectively. Figure 4.23. and Figure 4.24. shows the concentration distribution of key species in heterogeneous hydraulic conductivity and homogeneous Fe(III) concentration distribution without reoxidation case after 8 and 40 days of simulation period, respectively. Figure 4.25. shows the concentration distribution of key species in homogeneous hydraulic conductivity and Fe(III) concentration distribution without reoxidation case after 40 days of simulation period. Figure 4.26. -4.28. presents the concentration profile of key species in different scenarios without reoxidation case after 30 days of simulation period along the 9 m x-section.

The simulation results show that when U(VI) reoxidation process is not implemented in the biogeochemical reaction dynamics, higher U(VI) concentrations are observed in the system for all homogeneous and heterogenous heterogeneity cases. When U(VI) reoxidation reaction is turned off (reaction #4 in Table 3.6.), all Fe(III)oxides become available to oxidize HS- abiotically (reaction #5 in Table 3.6.) instead of oxidizing U(VI)), resulting in higher Fe(II) ions in the porewater with lower amounts of HS- concentrations. The relatively lower amounts of soluble HS-ions in solution would result in less S(s) precipitation (reaction #6 in Table 3.6.) as well as reduced U(IV) bioreduction (reaction #3 in Table 3.6.), thus resulting in higher amounts of U(VI) ions in the porewater solution. FeS and S are predicted to precipitate within the system, whereas siderite is not predicted to form, in conjunction with the results presented by Spycher et al., (2011) for modeling the laboratory experiments. When the model simulation results for U(VI) and uraninite in the 9 m cross-section part of the site are compared with the heterogeneous hydraulic conductivity and Fe distributions in the 9 m cross-section (Figures 4.26. -4.28.), it is seen that the impact of the oxidation and reduction reactions are particularly enhanced in the zones with highest mixing. The highest potential of mixing is observed to result mostly in the zones especially corresponding to the transition of high to low hydraulic conductivity, where preferential

flow of species through the high hydraulic conductivity zones are captured in the subsequent low hydraulic conductivity zones with the highest potential to react. This impact can be seen from the highest variation of U(VI) and uraninite concentrations between reoxidation and no-reoxidation cases observed along the 1.8 – 2 m and 2.5 - 3.6 m zones within the 9 m x-section, which corresponds to the transition of very high to low hydraulic conductivity regions (Figure 4.26.).

The biogeochemical reactions include a delicate balance among competing reactions within the U – Fe- S system, demonstrating the complex interplay between various biotic and abiotic reactions under the presence of a physically and chemically heterogeneous environment. The reoxidation of U(VI) depends on the competing rates of U(IV) versus sulfide oxidation by Fe(III)hydroxides, which further depends on kinetic and thermodynamic constraints. It should be noted that the presented model here is not intended to reproduce a specific field data, but to investigate the understanding of field scale heterogeneity (both physical and chemical heterogeneity) on the biogeochemical reaction dynamics in the context of natural advective and dispersive transport with mixing limitations, as an extension of the studies presented by Spycher et al. (2011) and Sengor et al. (2015).

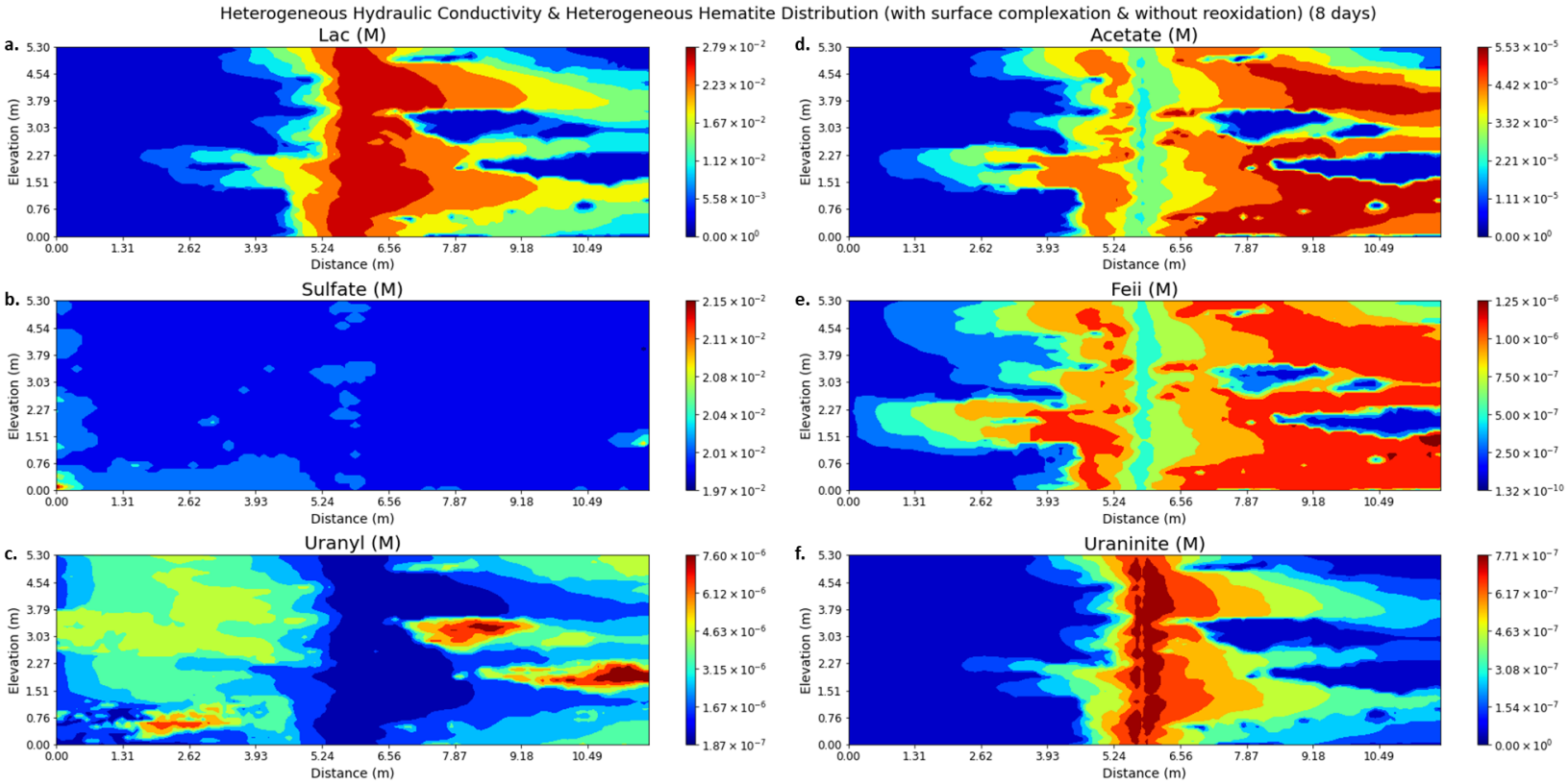

Figure 4.21. Concentration distribution of key species in heterogeneous hydraulic conductivity and heterogeneous Fe(III) hydroxide concentration distribution without U(IV) reoxidation reaction case for 8 days

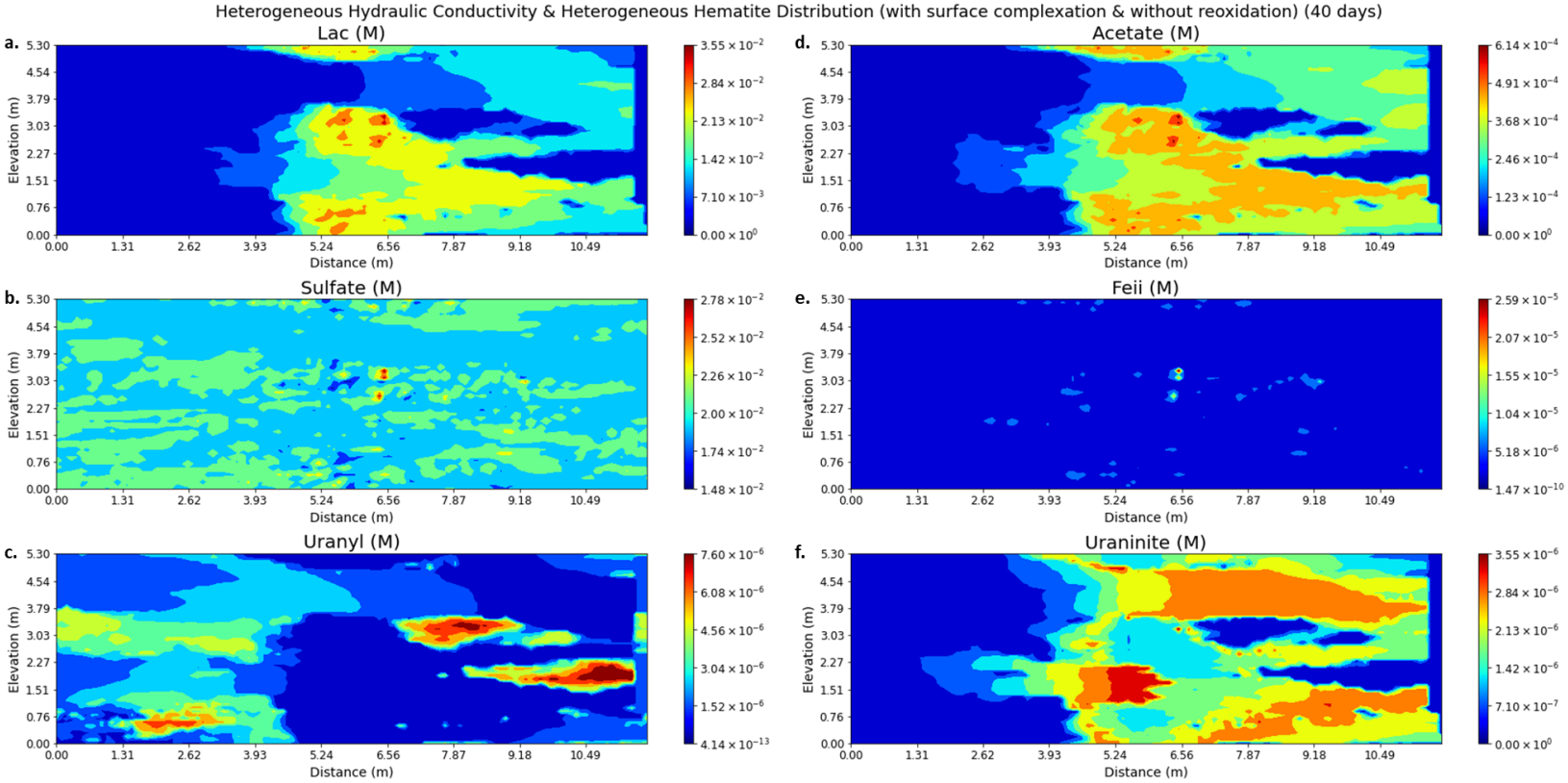

Figure 4.22. Concentration distribution of key species in heterogeneous hydraulic conductivity and heterogeneous Fe(III) hydroxide concentration distribution without U(IV) reoxidation reaction case for 40 days

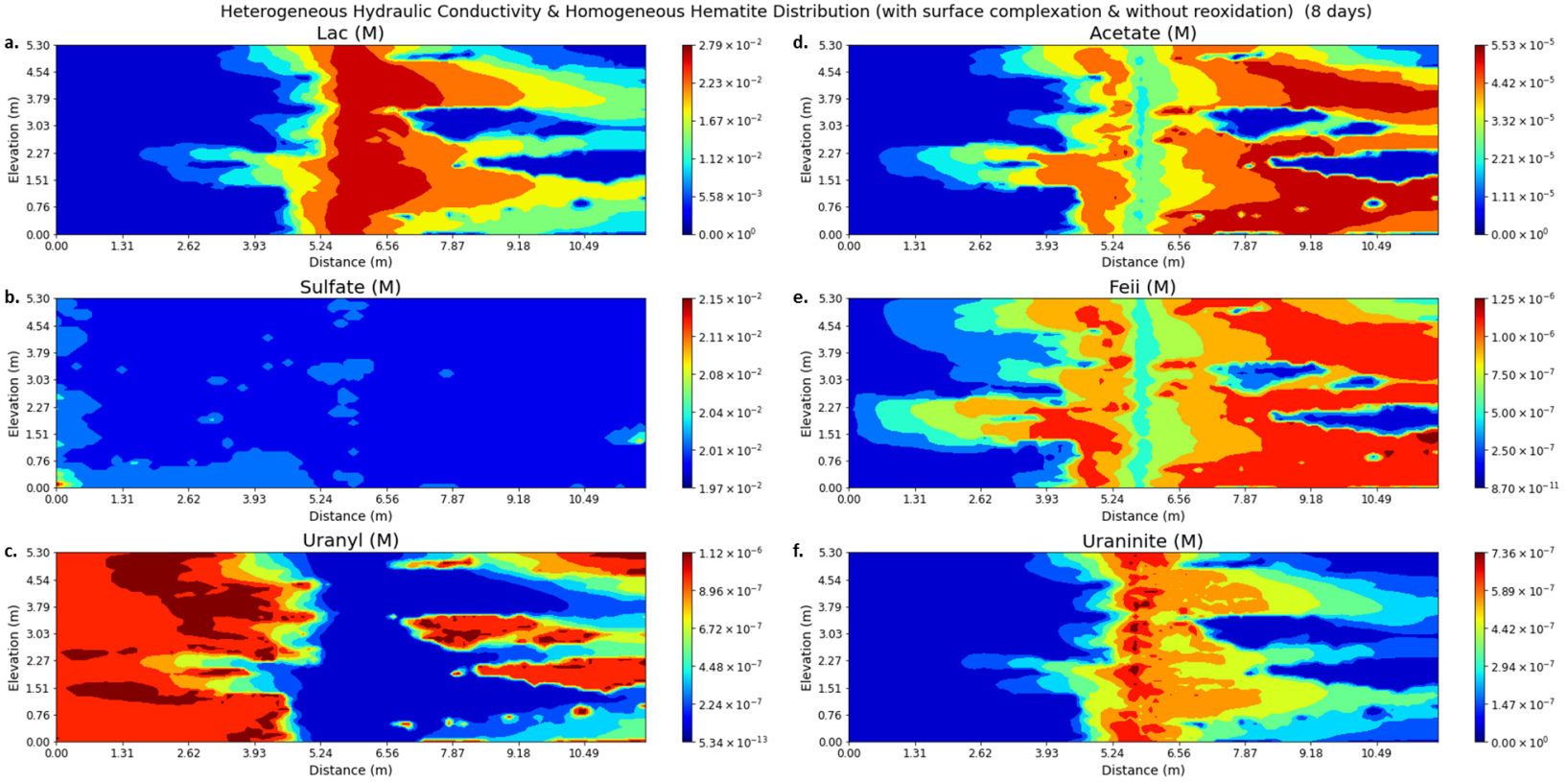

Figure 4.23. Concentration distribution of key species in heterogeneous hydraulic conductivity and homogeneous Fe(III) hydroxide concentration distribution without U(IV) reoxidation reaction case for 8 days

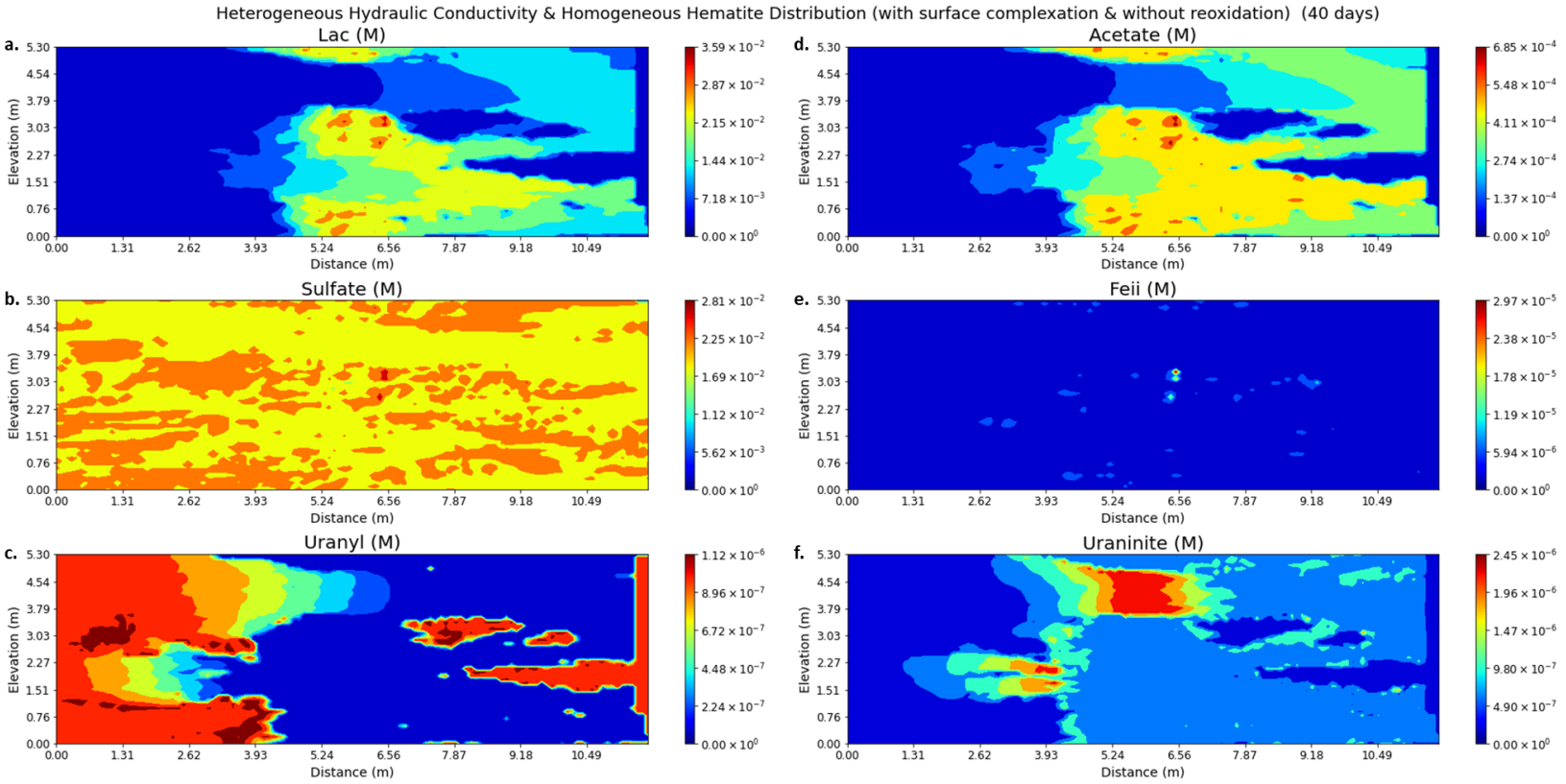

Figure 4.24. Concentration distribution of key species in heterogeneous hydraulic conductivity and homogeneous Fe(III) hydroxide concentration distribution without U(IV) reoxidation reaction case for 40 days

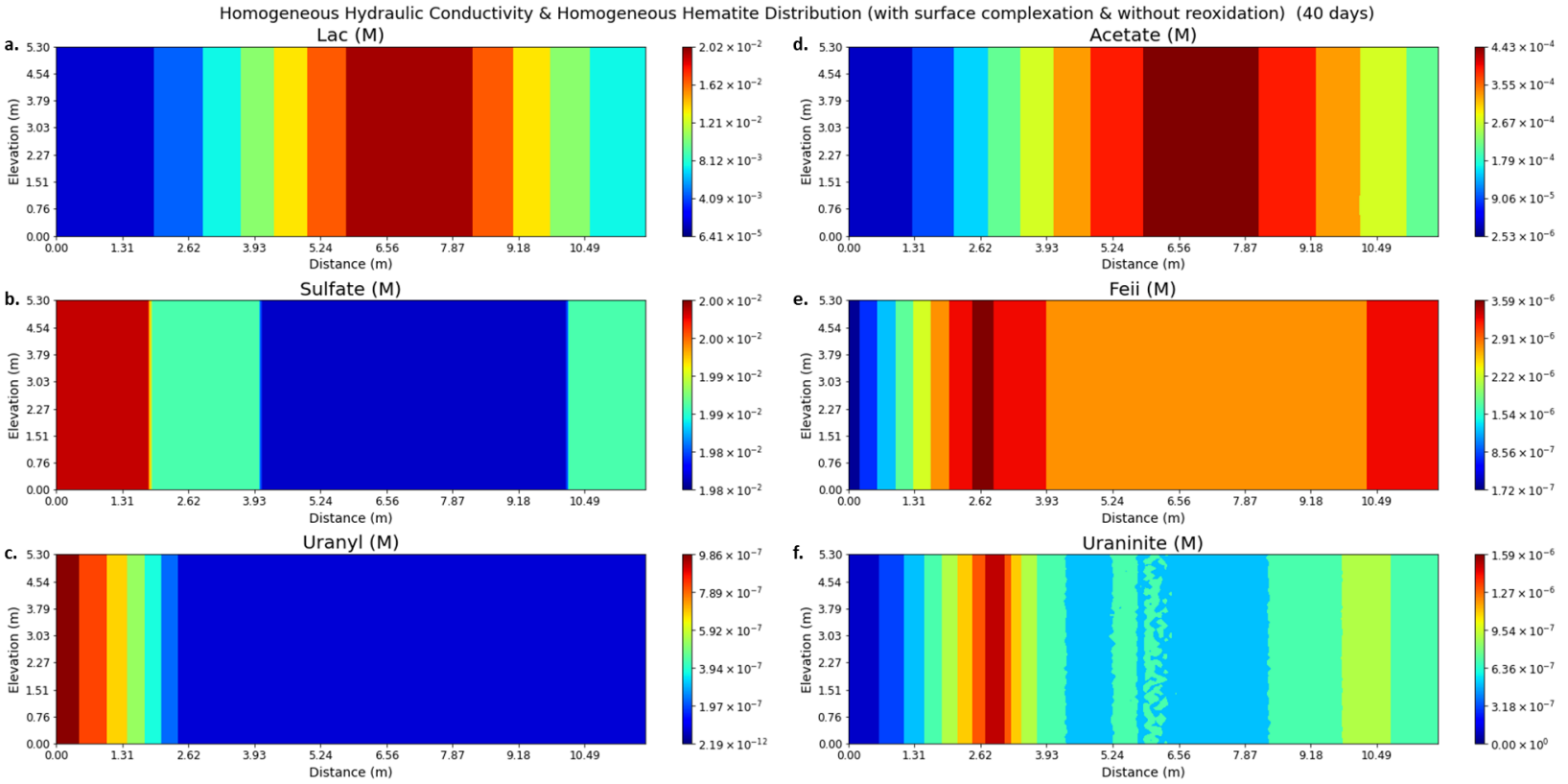

Figure 4.25. Concentration distribution of key species in heterogeneous hydraulic conductivity and homogeneous Fe(III) hydroxide concentration distribution without U(IV) reoxidation reaction case for 40 days

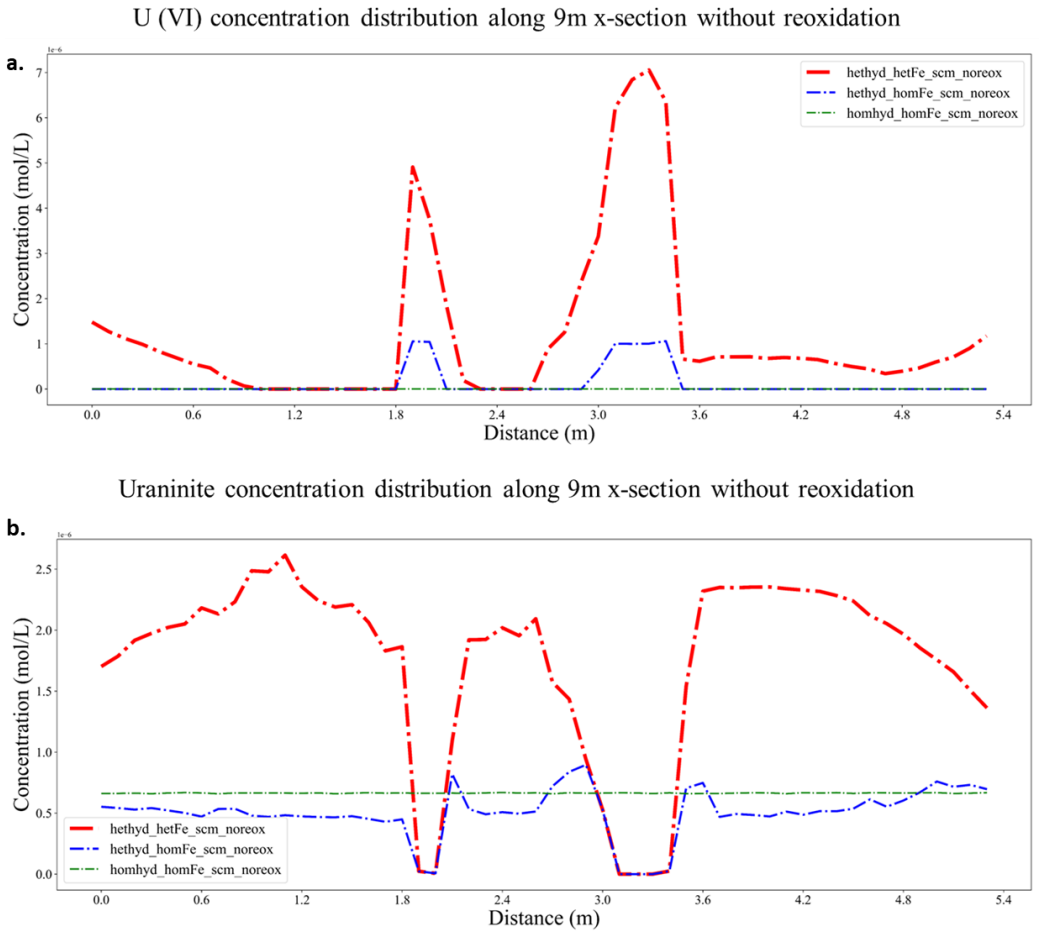

Figure 4.26. U(VI) and Uraninite concentration distribution along 9m x-section for 30 days

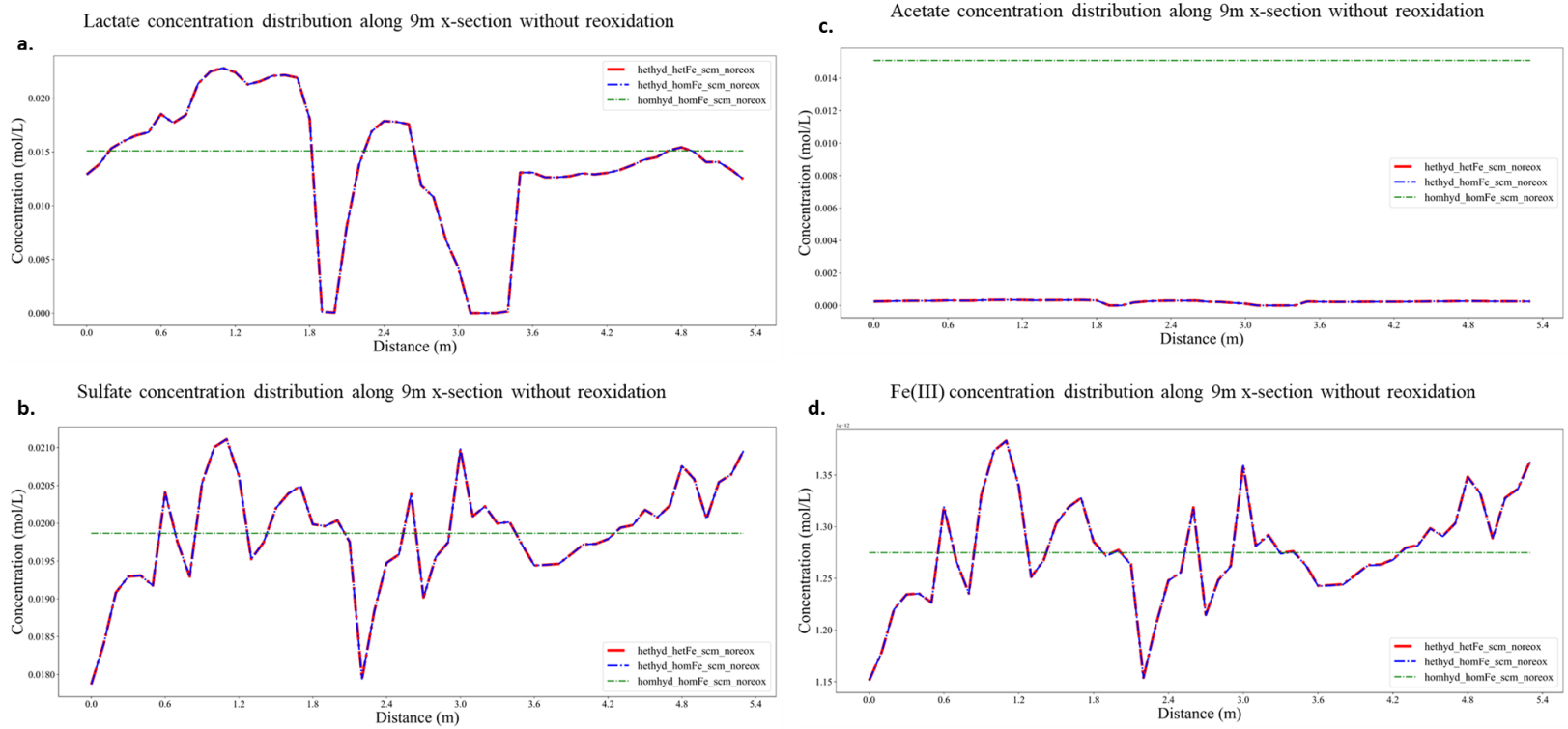

Figure 4.27. Concentration distribution of key species (lactate, acetate, sulfate and Fe(III)) along 9m x-section for 30 days

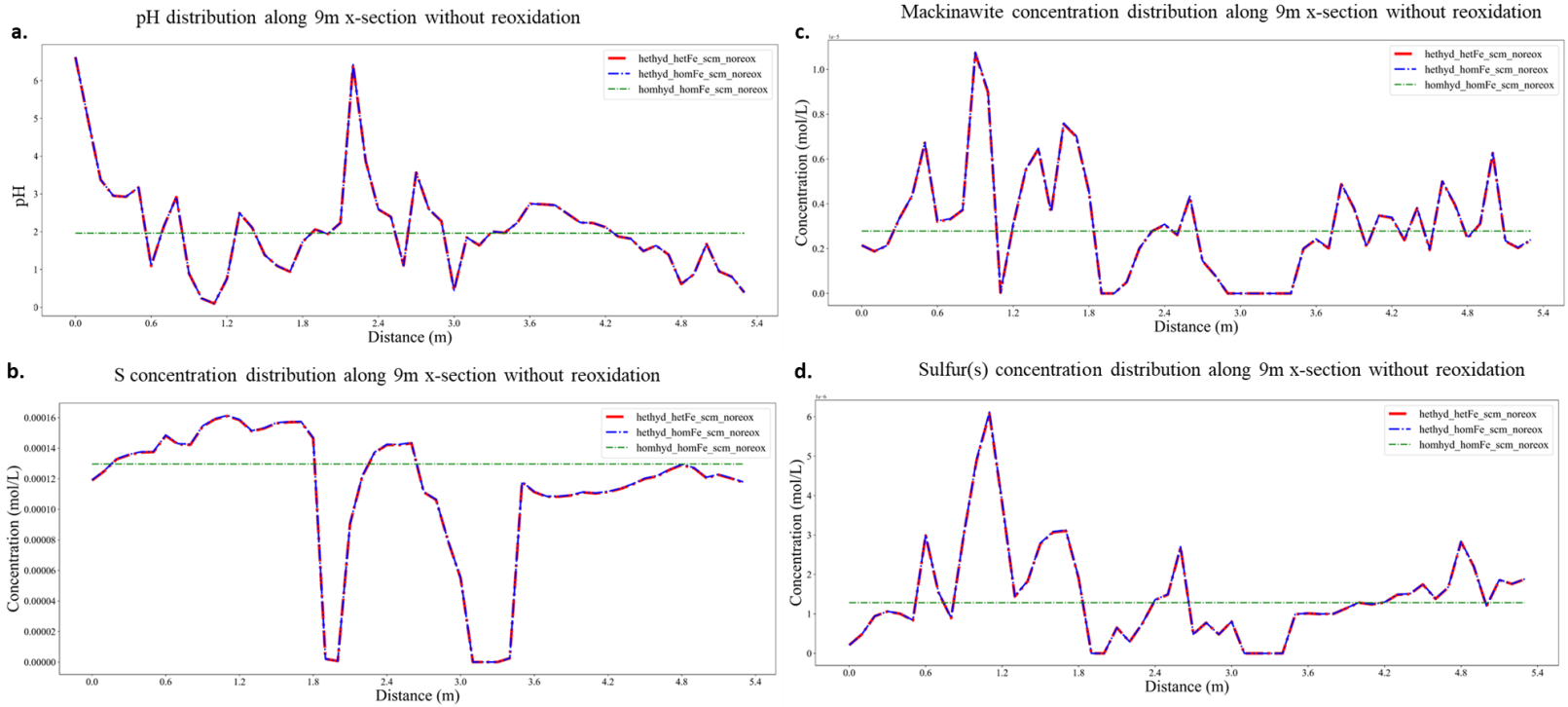

Figure 4.28. Concentration and pH distribution of key species (mackinawite, S and Sulfur(s)) along 9m x-section for 30 days

CHAPTER 5

CONCLUSION AND FUTURE RECOMMENDATIONS

5.1. Conclusions and Summary

In this study, a 2D numerical reactive transport model has been developed for predicting the transport behavior of contaminants in the presence of physical and chemical heterogeneity considering a complex interplay of biogeochemical processes. Within in this scope, uranium has been selected as an example, where its biogeochemical and reoxidation processes has been considered. The system was simulated for a period of 40 days, where a lactate containing solution was injected for the 1st 8 days into an initially steady state flow field, leading to transient flow conditions. In order to delineate the impact of physical and chemical heterogeneity on the overall biogeochemical processes of uranium, numerical model simulations have been set-up with increasing levels of heterogeneity in three cases as follows:

1. Reactive transport simulations are carried out with no physical or chemical heterogeneity (i.e., homogeneous K and homogeneous Fe case),
2. Reactive transport simulations are carried out with physical but no chemical heterogeneity (i.e., heterogeneous K and homogeneous Fe case),
3. Reactive transport simulations are carried out with both physical and chemical heterogeneity (i.e., heterogeneous K and heterogeneous Fe case).

In the first part of the model runs, the numerical model simulations were run with no surface complexation of uranium or any other species onto the aquifer solids. In the

second part, adsorption of uranium onto Fe(III)-(hydr)oxide surfaces were implemented by surface complexation reactions. All model simulations have also been carried out with- and without the U(IV) reoxidation reaction by Fe(III)-(hydr)oxide minerals, to investigate the impact of U(IV) reoxidation specifically on the overall biogeochemical dynamics.

The main findings of this study are summarized as follows:

- Model simulation results have shown that assuming spatial homogeneity might lead to an overestimation of bioreduction or bioremediation of the contaminant of concern in the subsurface environment. The comparison of model results reveal that physical heterogeneity has a greater impact than chemical heterogeneity with respect to the model predictions of biogeochemical reaction dynamics coupled to subsurface transport in the absence of adsorption reaction incorporations.
- On the other hand, incorporation of adsorption via surface complexation processes in predictive models highlights the significance of chemical heterogeneity in the subsurface environment. Model results reveal that when potential adsorption of contaminants is ignored in reactive transport models in a relatively chemically heterogeneous environment, the contaminant concentrations might be underestimated. The underestimation is seen to be more pronounced especially in the low hydraulic conductivity zones.
- The biogeochemical reactions include a delicate balance among competing reactions within the U – Fe- S system, demonstrating the complex interplay between various biotic and abiotic reactions under the presence of a physically and chemically heterogeneous environment.
- The simulation results show that when U(VI) reoxidation process is not implemented in the biogeochemical reaction dynamics, slightly higher U(VI)

concentrations are observed in the system for all homogeneous and heterogeneous heterogeneity cases.

- The impact of the oxidation and reduction reactions are particularly enhanced in the zones with highest mixing. The highest potential of mixing is observed to result mostly in the zones especially corresponding to the transition of high to low hydraulic conductivity, where preferential flow of species through the high hydraulic conductivity zones results to have the highest potential to react, leading to increased concentration of reaction products. The limited mixing within the low hydraulic conductivity zones on the other hand, remain with limited or no reaction potential. This mixing limitation impact is especially highly pronounced in chemically heterogeneous environments. Thus ignoring potential adsorption reactions in the chemically heterogeneous subsurface environment might lead to overestimation of bioremediation/bioreduction processes.

5.2. Future Recommendations

The 2D reactive transport modeling study conducted for this thesis can be expanded for other field scale applications which would involve reactive transport of contaminants in the subsurface under heterogeneous environments. Due to the limited data, the study has been carried out depending on previous literature works.

In particular, there is a lack of information about the field scale reaction rates, especially with the involvement of Fe(III)-(hydr)oxide oxidation rates. Up to now, reoxidation of uranium with Fe(III) hydroxides has been received little attention, since there is a lack of information and study on this. This study, which includes both bioreduction and reoxidation processes of uranium, provides a broad overview of the impacts of physical and chemical heterogeneity on bioreduction and reoxidation processes for uranium fate and transport in a natural subsurface setting environment.

Various challenges can be highlighted in terms of reactive transport simulation studies for contaminant fate and transport for in-situ activities. Although geostatistical methods have been available for compilation of in-situ heterogeneity data, it is still a challenge to fully characterize small-scale heterogeneity at practical field sites. Therefore, stochastic approaches are needed that explicitly recognize the uncertainty in predicting mixing-controlled reactions.

REFERENCES

[1] Abdelouas, A., Lutze, W., Gong, W., Nuttall, E. H., Strietelmeier, B. A., & Travis, B. J. (2000). Biological reduction of uranium in groundwater and subsurface soil. In *The Science of the Total Environment* (Vol. 250).

[2] Akob, D. M., Mills, H. J., & Kostka, J. E. (2007). Metabolically active microbial communities in uranium-contaminated subsurface sediments. *FEMS Microbiology Ecology*, *59*(1), 95–107. https://doi.org/10.1111/j.1574-6941.2006.00203.x

[3] Aksoy, A., Asce, A. M., & Culver, T. B. (n.d.). *Impacts of Physical and Chemical Heterogeneities on Aquifer Remediation Design*. https://doi.org/10.1061/ASCE0733-94962004130:4311

[4] Amde, M., Liu, J., Tan, Z.-Q., & Bekana, D. (2017). Transformation and bioavailability of metal oxide nanoparticles in aquatic and terrestrial environments. A review. Environmental Pollution, 230, 250–267. doi:10.1016/j.envpol.2017.06.064

[5] Anderson, R. T., Vrionis, H. A., Ortiz-Bernad, I., Resch, C. T., Long, P. E., Dayvault, R., Karp, K., Marutzky, S., Metzler, D. R., Peacock, A., White, D. C., Lowe, M., & Lovley, D. R. (2003a). Stimulating the In Situ Activity of Geobacter Species to Remove Uranium from the Groundwater of a Uranium-Contaminated Aquifer. *Applied and Environmental Microbiology*, *69*(10), 5884–5891. https://doi.org/10.1128/AEM.69.10.5884-5891.2003

[6] Appelo, C. A. J., & Rolle, M. (2010). PHT3D: A reactive multicomponent transport model for saturated porous media. In *Ground Water* (Vol. 48, Issue 5, pp. 627–632). https://doi.org/10.1111/j.1745-6584.2010.00732.x

[7] Atchley, A. L., Navarre-Sitchler, A. K., & Maxwell, R. M. (2014a). The effects of physical and geochemical heterogeneities on hydro-geochemical

transport and effective reaction rates. *Journal of Contaminant Hydrology*, *165*, 53–64. https://doi.org/10.1016/j.jconhyd.2014.07.008

[8] Baba, A., & Tayfur, G. (2011). Groundwater contamination and its effect on health in Turkey. *Environmental Monitoring and Assessment*, *183*(1–4), 77–94. https://doi.org/10.1007/s10661-011-1907-z

[9] Barber Ii A'b, L. B., Thurman, E. M., & Runnells, D. D. (1992). *Geochemical heterogeneity in a sand and gravel aquifer: Effect of sediment mineralogy and particle size on the sorption of chlorobenzenes*.

[10] Berg, S. J., & Illman, W. A. (2011). Capturing aquifer heterogeneity: Comparison of approaches through controlled sandbox experiments. *Water Resources Research*, *47*(9). https://doi.org/10.1029/2011WR010429

[11] Boonchayaanant, B., Nayak, D., Du, X., & Criddle, C. S. (2009). Uranium reduction and resistance to reoxidation under iron-reducing and sulfate-reducing conditions. *Water Research*, *43*(18), 4652–4664. https://doi.org/10.1016/j.watres.2009.07.013

[12] Campbell, K. M., Gallegos, T. J., & Landa, E. R. (2015). Biogeochemical aspects of uranium mineralization, mining, milling, and remediation. In *Applied Geochemistry* (Vol. 57, pp. 206–235). Elsevier Ltd. https://doi.org/10.1016/j.apgeochem.2014.07.022

[13] Chang, Y. J., Peacock, A. D., Long, P. E., Stephen, J. R., McKinley, J. P., Macnaughton, S. J., Anwar Hussain, A. K. M., Saxton, A. M., & White, D. C. (2001). Diversity and Characterization of Sulfate-Reducing Bacteria in Groundwater at a Uranium Mill Tailings Site. *Applied and Environmental Microbiology*, *67*(7), 3149–3160. https://doi.org/10.1128/AEM.67.7.3149-3160.2001

[14] Chen, J. P., & Yiacoumi, S. (2002). *MODELING OF DEPLETED URANIUM TRANSPORT IN SUBSURFACE SYSTEMS*.

[15] Chen, J. Y., Ko, C.-H., Bhattacharjee, S., & Elimelech, M. (2001). Role of spatial distribution of porous medium surface charge heterogeneity in colloid transport. In *Colloids and Surfaces A: Physicochemical and Engineering Aspects* (Vol. 191). www.elsevier.nl/locate/colsurfa

[16] Cheng, Y., Arora, B., Sevinç Şengör, S., Druhan, J. L., Wanner, C., van Breukelen, B. M., & Steefel, C. I. (n.d.). *Microbially Mediated Kinetic Sulfur Isotope Fractionation: Reactive Transport Modeling Benchmark 2 3*.

[17] Chrysikopoulos, C. v, Kitanidis, P. K., & Roberts, P. v. (1990). Analysis of One-Dimensional Solute Transport Through Porous Media With Spatially Variable Retardation Factor. In *WATER RESOURCES RESEARCH* (Vol. 26, Issue 3).

[18] Cozzarelli, I. M., Herman, J. S., Baedecker, M. J., & Fischer, J. M. (1999). Geochemical heterogeneity of a gasoline-contaminated aquifer. In *Journal of Contaminant Hydrology* (Vol. 40). www.elsevier.comrlocaterjconhyd

[19] Cunningham, J. A., & Fadel, Z. J. (2007a). Contaminant degradation in physically and chemically heterogeneous aquifers. *Journal of Contaminant Hydrology*, *94*(3–4), 293–304. https://doi.org/10.1016/j.jconhyd.2007.07.011

[20] Dagan, G. (n.d.). Time-Dependent Macrodispersion for Solute Transport in Anisotropic Heterogeneous Aquifers. In *WATER RESOURCES RESEARCH* (Vol. 24, Issue 9).

[21] Dzombak, D.A. and Morel, F.M.M. (1990) Surface Complexation Modeling: Hydrous Ferric Oxide. John Wiley & Sons, New York.

[22] Edwards, E. C. (2016). What lies beneath? Aquifer heterogeneity and the economics of groundwater management. *Journal of the Association of Environmental and Resource Economists*, *3*(2), 453–491. https://doi.org/10.1086/685389

[23] Englert, A., Hubbard, S. S., Williams, K. H., Li, L., & Steefel, C. I. (2009). Feedbacks between hydrological heterogeneity and bioremediation induced biogeochemical transformations. *Environmental Science and Technology*, *43*(14), 5197–5204. https://doi.org/10.1021/es803367n

[24] Fakhreddine, S., Lee, J., Kitanidis, P. K., Fendorf, S., & Rolle, M. (2016). Imaging geochemical heterogeneities using inverse reactive transport modeling: An example relevant for characterizing arsenic mobilization and distribution. *Advances in Water Resources*, *88*, 186–197. https://doi.org/10.1016/j.advwatres.2015.12.005

[25] Finneran, K. T., Anderson, R. T., Nevin, K. P., & Lovley, D. R. (2002). Potential for bioremediation of uranium-contaminated aquifers with microbial U(VI) reduction. *Soil and Sediment Contamination*, *11*(3), 339–357. https://doi.org/10.1080/20025891106781

[26] Flynn, R. M., Mallèn, G., Engel, M., Ahmed, A., & Rossi, P. (2015). Characterizing Aquifer Heterogeneity Using Bacterial and Bacteriophage Tracers. *Journal of Environmental Quality*, *44*(5), 1448–1458. https://doi.org/10.2134/jeq2015.02.0117

[27] Gihring, T. M., Zhang, G., Brandt, C. C., Brooks, S. C., Campbell, J. H., Carroll, S., Criddle, C. S., Green, S. J., Jardine, P., Kostka, J. E., Lowe, K., Mehlhorn, T. L., Overholt, W., Watson, D. B., Yang, Z., Wu, W. M., & Schadt, C. W. (2011). A limited microbial consortium is responsible for extended bioreduction of uranium in a contaminated aquifer. *Applied and Environmental Microbiology*, *77*(17), 5955–5965. https://doi.org/10.1128/AEM.00220-11

[28] Griebler, C., & Lueders, T. (2009a). Microbial biodiversity in groundwater ecosystems. In *Freshwater Biology* (Vol. 54, Issue 4, pp. 649–677). https://doi.org/10.1111/j.1365-2427.2008.02013.x

[29] Gu, B., Wu, W. M., Ginder-Vogel, M. A., Yan, H., Fields, M. W., Zhou, J., Fendorf, S., Criddle, C. S., & Jardine, P. M. (2005). Bioreduction of uranium in a contaminated soil column. *Environmental Science and Technology*, *39*(13), 4841–4847. https://doi.org/10.1021/es050011y

[30] Haberer, C. M., Rolle, M., Cirpka, O. A., & Grathwohl, P. (2015). Impact of Heterogeneity on Oxygen Transfer in a Fluctuating Capillary Fringe. *Groundwater*, *53*(1), 57–70. https://doi.org/10.1111/gwat.12149

[31] Harbaugh, A.W., Langevin, C.D., Hughes, J.D., Niswonger, R.N., and Konikow, L. F., 2017, MODFLOW-2005 version 1.12.00, the U.S. Geological Survey modular groundwater model: U.S. Geological Survey Software Release, 03 February 2017, http://dx.doi.org/10.5066/F7RF5S7G

[32] Harvey, R. W., Kinner, N. E., MacDonald, D., Metge, D. W., & Bunn, A. (1993). Role of physical heterogeneity in the interpretation of small-scale laboratory and field observations of bacteria, microbial-sized microsphere, and bromide transport through aquifer sediments. *Water Resources Research*, *29*(8), 2713–2721. https://doi.org/10.1029/93WR00963

[33] Holmes, D. E., Finneran, K. T., O'Neil, R. A., & Lovley, D. R. (2002). Enrichment of members of the family Geobacteraceae associated with stimulation of dissimilatory metal reduction in uranium-contaminated aquifer sediments. *Applied and Environmental Microbiology*, *68*(5), 2300–2306. https://doi.org/10.1128/AEM.68.5.2300-2306.2002

[34] Hyun, S. P., Davis, J. A., & Hayes, K. F. (2014). Abiotic U(VI) reduction by aqueous sulfide. *Applied Geochemistry*, *50*, 7–15. https://doi.org/10.1016/j.apgeochem.2014.07.021

[35] Istok, J. D., Senko, J. M., Krumholz, L. R., Watson, D., Bogle, M. A., Peacock, A., Chang, Y. J., & White, D. C. (2004a). In Situ Bioreduction of Technetium and Uranium in a Nitrate-Contaminated Aquifer.

Environmental Science and Technology, *38*(2), 468–475. https://doi.org/10.1021/es034639p

[36] Jang, E., He, W., Savoy, H., Dietrich, P., Kolditz, O., Rubin, Y., Schüth, C., & Kalbacher, T. (2017a). Identifying the influential aquifer heterogeneity factor on nitrate reduction processes by numerical simulation. *Advances in Water Resources*, *99*, 38–52. https://doi.org/10.1016/j.advwatres.2016.11.007

[37] Jang, E., Ulsan, in, Korea Supervisor -Ing Olaf Kolditz, S., Schüth, C., Yun, S.-T., University, K., & Korea, S. (n.d.). *Reactive transport simulation of contaminant fate and redox transformation in heterogeneous aquifer systems*.

[38] Komlos, J., Moon, H. S., & Jaffé, P. R. (2008). Effect of Sulfate on the Simultaneous Bioreduction of Iron and Uranium. *Journal of Environmental Quality*, *37*(6), 2058–2062. https://doi.org/10.2134/jeq2007.0665

[39] Li, B., Wu, W. M., Watson, D. B., Cardenas, E., Chao, Y., Phillips, D. H., Mehlhorn, T., Lowe, K., Kelly, S. D., Li, P., Tao, H., Tiedje, J. M., Criddle, C. S., & Zhang, T. (2018). Bacterial community shift and coexisting/coexcluding patterns revealed by network analysis in a uranium-contaminated site after bioreduction followed by reoxidation. *Applied and Environmental Microbiology*, *84*(9). https://doi.org/10.1128/AEM.02885-17

[40] Li, D., Liu, Y., Chen, Y., Wang, K., & Huang, G. (2011). *Impact of Hydraulic Conductivity on Solute Transport in Highly Heterogeneous Aquifer* (Vol. 344).

[41] Li, L., Gawande, N., Kowalsky, M. B., Steefel, C. I., & Hubbard, S. S. (2011). Physicochemical heterogeneity controls on uranium bioreduction rates at the field scale. *Environmental Science and Technology*, *45*(23), 9959–9966. https://doi.org/10.1021/es201111y

[42] Li, L., Steefel, C. I., Kowalsky, M. B., Englert, A., & Hubbard, S. S. (2010). Effects of physical and geochemical heterogeneities on mineral transformation and biomass accumulation during biostimulation experiments at Rifle, Colorado. *Journal of Contaminant Hydrology*, *112*(1–4), 45–63. https://doi.org/10.1016/j.jconhyd.2009.10.006

[43] Liu, G., Butler, J. J., Bohling, G. C., Reboulet, E., Knobbe, S., & Hyndman, D. W. (2009). A new method for high-resolution characterization of hydraulic conductivity. *Water Resources Research*, *45*(8). https://doi.org/10.1029/2009WR008319

[44] Lovley, D. R., Roden, E. E., Phillips, E. J. P., & Woodward, J. C. (1993a). Enzymatic iron and uranium reduction by sulfate-reducing bacteria. *Marine Geology*, *113*(1–2), 41–53. https://doi.org/10.1016/0025-3227(93)90148-O

[45] Luo, J., Weber, F. A., Cirpka, O. A., Wu, W. M., Nyman, J. L., Carley, J., Jardine, P. M., Criddle, C. S., & Kitanidis, P. K. (2007). Modeling in-situ uranium(VI) bioreduction by sulfate-reducing bacteria. *Journal of Contaminant Hydrology*, *92*(1–2), 129–148. https://doi.org/10.1016/j.jconhyd.2007.01.004

[46] Ma, M., Wang, R., Xu, L., Xu, M., & Liu, S. (2020). Emerging health risks and underlying toxicological mechanisms of uranium contamination: Lessons from the past two decades. In *Environment International* (Vol. 145). Elsevier Ltd. https://doi.org/10.1016/j.envint.2020.106107

[47] Maamar, S. ben, Aquilina, L., Quaiser, A., Pauwels, H., Michon-Coudouel, S., Vergnaud-Ayraud, V., Labasque, T., Roques, C., Abbott, B. W., & Dufresne, A. (2015). Groundwater isolation governs chemistry and microbial community structure along hydrologic flowpaths. *Frontiers in Microbiology*, *6*(DEC). https://doi.org/10.3389/fmicb.2015.01457

[48] Mailloux, B. J., Fuller, M. E., Onstott, T. C., Hall, J., Dong, H., DeFlaun, M. F., Streger, S. H., Rothmel, R. K., Green, M., Swift, D. J. P., & Radke, J. (2003). The role of physical, chemical, and microbial heterogeneity on the field-scale transport and attachment of bacteria. *Water Resources Research*, *39*(6). https://doi.org/10.1029/2002WR001591

[49] Maliva, R. G. (2016). *Aquifer Characterization and Properties* (pp. 1–24). https://doi.org/10.1007/978-3-319-32137-0_1

[50] Michael, H. A., & Khan, M. R. (2016). Impacts of physical and chemical aquifer heterogeneity on basin-scale solute transport: Vulnerability of deep groundwater to arsenic contamination in Bangladesh. *Advances in Water Resources*, *98*, 147–158. https://doi.org/10.1016/j.advwatres.2016.10.010

[51] Mićić, V., Bossa, N., Schmid, D., Wiesner, M. R., & Hofmann, T. (2020). Groundwater Chemistry Has a Greater Influence on the Mobility of Nanoparticles Used for Remediation than the Chemical Heterogeneity of Aquifer Media. *Environmental Science and Technology*, *54*(2), 1250–1257. https://doi.org/10.1021/acs.est.9b06135

[52] Miralles-Wilhelm, F. (2000). Stochastic analysis of oxygen-limited biodegradation in heterogeneous aquifers with transient microbial dynamics. In *Gelharr Journal of Contaminant Hydrology* (Vol. 42). www.elsevier.comrlocaterjconhyd

[53] Mohamed, M., Hatfield, K., Hassan, A., & Klammler, H. (2010). Stochastic evaluation of subsurface contaminant discharges under physical, chemical, and biological heterogeneities. *Advances in Water Resources*, *33*(7), 801–812. https://doi.org/10.1016/j.advwatres.2010.04.010

[54] Mohamed, M. M. A., Hatfield, K., & Hassan, A. E. (2006). Monte Carlo evaluation of microbial-mediated contaminant reactions in heterogeneous aquifers. *Advances in Water Resources*, *29*(8), 1123–1139. https://doi.org/10.1016/j.advwatres.2005.09.008

[55] Murphy, E. M., Ginn, T. R., & Hall, E. (2000). Modeling microbial processes in porous media. In *Hydrogeology Journal* (Vol. 8). Springer-Verlag.

[56] Newsome, L., Morris, K., & Lloyd, J. R. (2014a). The biogeochemistry and bioremediation of uranium and other priority radionuclides. *Chemical Geology*, *363*, 164–184. https://doi.org/10.1016/j.chemgeo.2013.10.034

[57] Nolan, J., & Weber, K. A. (2015). Natural Uranium Contamination in Major U.S. Aquifers Linked to Nitrate. *Environmental Science and Technology Letters*, *2*(8), 215–220. https://doi.org/10.1021/acs.estlett.5b00174

[58] Nyyssönen, M., Hultman, J., Ahonen, L., Kukkonen, I., Paulin, L., Laine, P., Itävaara, M., & Auvinen, P. (2014). Taxonomically and functionally diverse microbial communities in deep crystalline rocks of the Fennoscandian shield. *ISME Journal*, *8*(1), 126–138. https://doi.org/10.1038/ismej.2013.125

[59] Prommer, H., Barry, D.A. and Zheng, C. (2003), MODFLOW/MT3DMS-Based Reactive Multicomponent Transport Modeling. Groundwater, 41: 247-257. https://doi.org/10.1111/j.1745-6584.2003.tb02588.x

[60] Renshaw, J. C., Butchins, L. J. C., Livens, F. R., May, I., Charnock, J. M., & Lloyd, J. R. (2005a). Bioreduction of uranium: Environmental implications of a pentavalent intermediate. *Environmental Science and Technology*, *39*(15), 5657–5660. https://doi.org/10.1021/es048232b

[61] Roden, E. E., & Scheibe, T. D. (2005). Conceptual and numerical model of uranium(VI) reductive immobilization in fractured subsurface sediments. *Chemosphere*, *59*(5), 617–628. https://doi.org/10.1016/j.chemosphere.2004.11.007

[62] Roh, Y., Lee, S. Y., Elless, M. P., & Cho, K. S. (2000). Electro-enhanced remediation of radionuclide-contaminated groundwater using zero-valent iron. *Journal of Environmental Science and Health - Part A Toxic/Hazardous Substances and Environmental Engineering*, *35*(7), 1043–1059. https://doi.org/10.1080/10934520009377019

[63] Sani, R. K., Peyton, B. M., Amonette, J. E., & Geesey, G. G. (2004a). Reduction of uranium(VI) under sulfate-reducing conditions in the presence of Fe(III)-(hydr)oxides. *Geochimica et Cosmochimica Acta*, *68*(12), 2639–2648. https://doi.org/10.1016/j.gca.2004.01.005

[64] Sarris, T. S., Close, M. E., & Moore, C. (2019). Uncertainty assessment of nitrate reduction in heterogeneous aquifers under uncertain redox conditions. *Stochastic Environmental Research and Risk Assessment*, *33*(8–9), 1609–1627. https://doi.org/10.1007/s00477-019-01715-w

[65] Scheibe, T. D., Fang, Y., Murray, C. J., Roden, E. E., Chen, J., Chien, Y. J., Brooks, S. C., & Hubbard, S. S. (2006). Transport and biogeochemical reaction of metals in a physically and chemically heterogeneous aquifer. *Geosphere*, *2*(4), 220–235. https://doi.org/10.1130/GES00029.1

[66] Şengör, S. S., Ginn, T. R., Brugato, C. J., & Gikas, P. (2013). Anaerobic microbial growth near thermodynamic equilibrium as a function of ATP/ADP cycle: The effect of maintenance energy requirements. *Biochemical Engineering Journal*, *81*, 65–72. https://doi.org/10.1016/j.bej.2013.10.006

[67] Şengör, S. S., Mayer, K. U., Greskowiak, J., Wanner, C., Su, D., & Prommer, H. (2015a). A reactive transport benchmark on modeling biogenic uraninite re-oxidation by Fe(III)-(hydr)oxides. *Computational Geosciences*, *19*(3), 569–583. https://doi.org/10.1007/s10596-015-9480-0

[68] Şengör, S. S., Singh, G., Dohnalkova, A., Spycher, N., Ginn, T. R., Peyton, B. M., & Sani, R. K. (2016). Impact of different environmental

conditions on the aggregation of biogenic U(IV) nanoparticles synthesized by Desulfovibrio alaskensis G20. *BioMetals*, *29*(6), 965–980. https://doi.org/10.1007/s10534-016-9969-6

[69] Senko, J. M., Istok, J. D., Suflita, J. M., & Krumholz, L. R. (2002a). In-situ evidence for uranium immobilization and remobilization. *Environmental Science and Technology*, *36*(7), 1491–1496. https://doi.org/10.1021/es011240x

[70] Singh, G., Şengör, S. S., Bhalla, A., Kumar, S., De, J., Stewart, B., Spycher, N., Ginn, T. M., Peyton, B. M., & Sani, R. K. (2014). Reoxidation of biogenic reduced uranium: A challenge toward bioremediation. *Critical Reviews in Environmental Science and Technology*, *44*(4), 391–415. https://doi.org/10.1080/10643389.2012.728522

[71] Sitte, J., Akob, D. M., Kaufmann, C., Finster, K., Banerjee, D., Burkhardt, E. M., Kostka, J. E., Scheinost, A. C., Büchel, G., & Küsel, K. (2010). Microbial links between sulfate reduction and metal retention in uranium- and heavy metal-contaminated soil. *Applied and Environmental Microbiology*, *76*(10), 3143–3152. https://doi.org/10.1128/AEM.00051-10

[72] Spycher, N. F., Issarangkun, M., Stewart, B. D., Sevinç Şengör, S., Belding, E., Ginn, T. R., Peyton, B. M., & Sani, R. K. (2011a). Biogenic uraninite precipitation and its reoxidation by iron(III) (hydr)oxides: A reaction modeling approach. *Geochimica et Cosmochimica Acta*, *75*(16), 4426–4440. https://doi.org/10.1016/j.gca.2011.05.008

[73] Spycher, N. F., Issarangkun, M., Stewart, B. D., Sevinç Şengör, S., Belding, E., Ginn, T. R., Peyton, B. M., & Sani, R. K. (2011b). Biogenic uraninite precipitation and its reoxidation by iron(III) (hydr)oxides: A reaction modeling approach. *Geochimica et Cosmochimica Acta*, *75*(16), 4426–4440. https://doi.org/10.1016/j.gca.2011.05.008

[74] Suzuki, Y., Kelly, S. D., Kemner, K. M., & Banfield, J. F. (2003). Microbial populations stimulated for hexavalent uranium reduction in uranium mine sediment. *Applied and Environmental Microbiology*, *69*(3), 1337–1346. https://doi.org/10.1128/AEM.69.3.1337-1346.2003

[75] Tokunaga, T. K., Wan, J., Kim, Y., Daly, R. A., Brodie, E. L., Hazen, T. C., Herman, D., & Firestone, M. K. (2008). Influences of organic carbon supply rate on uranium bioreduction in initially oxidizing, contaminated sediment. *Environmental Science and Technology*, *42*(23), 8901–8907. https://doi.org/10.1021/es8019947

[76] Tompson, A. F. B., Schafer, A. L., & Smith, R. W. (1996). Impacts of physical and chemical heterogeneity on cocontaminant transport in a sandy porous medium. *Water Resources Research*, *32*(4), 801–818. https://doi.org/10.1029/95WR03733

[77] Uçankuş, T., & Ünlü, K. (2008). The effect of aquifer heterogeneity on natural attenuation rate of BTEX. *Environmental Geology*, *54*(4), 759–776. https://doi.org/10.1007/s00254-007-0861-0

[78] Vrionis, H. A., Anderson, R. T., Ortiz-Bernad, I., O'Neill, K. R., Resch, C. T., Peacock, A. D., Dayvault, R., White, D. C., Long, P. E., & Lovley, D. R. (2005). Microbiological and geochemical heterogeneity in an in situ uranium bioremediation field site. *Applied and Environmental Microbiology*, *71*(10), 6308–6318. https://doi.org/10.1128/AEM.71.10.6308-6318.2005

[79] Wan, J., Tokunaga, T. K., Brodie, E., Wang, Z., Zheng, Z., Herman, D., Hazen, T. C., Firestone, M. K., & Sutton, S. R. (2005). Reoxidation of bioreduced uranium under reducing conditions. *Environmental Science and Technology*, *39*(16), 6162–6169. https://doi.org/10.1021/es048236g

[80] Wang, Z. wei, Chen, H. wei, & Li, F. lin. (2019). Identifying spatial heterogeneity of groundwater and its response to anthropogenic activities.

Environmental Science and Pollution Research, *26*(28), 29435–29448. https://doi.org/10.1007/s11356-019-06121-x

[81] Weber, K. A., Achenbach, L. A., & Coates, J. D. (2006). Microorganisms pumping iron: Anaerobic microbial iron oxidation and reduction. In *Nature Reviews Microbiology* (Vol. 4, Issue 10, pp. 752–764). https://doi.org/10.1038/nrmicro1490

[82] Wilkins, M. J., Livens, F. R., Vaughan, D. J., & Lloyd, J. R. (2006a). The impact of Fe(III)-reducing bacteria on uranium mobility. *Biogeochemistry*, *78*(2), 125–150. https://doi.org/10.1007/s10533-005-3655-z

[83] Williams, K. H., Bargar, J. R., Lloyd, J. R., & Lovley, D. R. (2013). Bioremediation of uranium-contaminated groundwater: A systems approach to subsurface biogeochemistry. In *Current Opinion in Biotechnology* (Vol. 24, Issue 3, pp. 489–497). https://doi.org/10.1016/j.copbio.2012.10.008

[84] Wu, M. Z., Post, V. E. A., Salmon, S. U., Morway, E. D., & Prommer, H. (2016). PHT3D-UZF: A Reactive Transport Model for Variably-Saturated Porous Media. Groundwater, 54(1), 23–34. https://doi.org/10.1111/gwat.12318

[85] Wu, W. M., Carley, J., Fienen, M., Mehlhorn, T., Lowe, K., Nyman, J., Luo, J., Gentile, M. E., Rajan, R., Wagner, D., Hickey, R. F., Gu, B., Watson, D., Cirpka, O. A., Kitanidis, P. K., Jardine, P. M., & Criddle, C. S. (2006). Pilot-scale in situ bioremediation of uranium in a highly contaminated aquifer. 1. Conditioning of a treatment zone. *Environmental Science and Technology*, *40*(12), 3978–3985. https://doi.org/10.1021/es051954y

[86] Wufuer, R., Wei, Y., Lin, Q., Wang, H., Song, W., Liu, W., Zhang, D., Pan, X., & Gadd, G. M. (2017a). xx. *Advances in Applied Microbiology*, *101*, 137–168. https://doi.org/10.1016/bs.aambs.2017.01.003

[87] Yabusaki, S. B., Fang, Y., Long, P. E., Resch, C. T., Peacock, A. D., Komlos, J., Jaffe, P. R., Morrison, S. J., Dayvault, R. D., White, D. C., & Anderson, R. T. (2007). Uranium removal from groundwater via in situ biostimulation: Field-scale modeling of transport and biological processes. *Journal of Contaminant Hydrology*, *93*(1–4), 216–235. https://doi.org/10.1016/j.jconhyd.2007.02.005

[88] Yabusaki, S. B., Şengör, S. S., & Fang, Y. (2015). A uranium bioremediation reactive transport benchmark. *Computational Geosciences*, *19*(3), 551–567. https://doi.org/10.1007/s10596-015-9474-y

[89] Yan, L., Herrmann, M., Kampe, B., Lehmann, R., Totsche, K. U., & Küsel, K. (2020). Environmental selection shapes the formation of near-surface groundwater microbiomes. *Water Research*, *170*. https://doi.org/10.1016/j.watres.2019.115341

[90] You, W., Peng, W., Tian, Z., & Zheng, M. (2021). Uranium bioremediation with U(VI)-reducing bacteria. In *Science of the Total Environment* (Vol. 798). Elsevier B.V. https://doi.org/10.1016/j.scitotenv.2021.149107

[91] Zhang, F., Wu, W. M., Parker, J. C., Mehlhorn, T., Kelly, S. D., Kemner, K. M., Zhang, G., Schadt, C., Brooks, S. C., Criddle, C. S., Watson, D. B., & Jardine, P. M. (2010). Kinetic analysis and modeling of oleate and ethanol stimulated uranium (VI) bio-reduction in contaminated sediments under sulfate reduction conditions. *Journal of Hazardous Materials*, *183*(1–3), 482–489. https://doi.org/10.1016/j.jhazmat.2010.07.049

[92] Zhang, Y., Wu, C., Hu, B. X., Yeh, T. C. J., Hao, Y., & Lv, W. (2019a). Fine characterization of the effects of aquifer heterogeneity on solute transport: A numerical sandbox experiment. *Water (Switzerland)*, *11*(11). https://doi.org/10.3390/w11112295

[93] Zhou, Y., Kellermann, C., & Griebler, C. (2012). Spatio-temporal patterns of microbial communities in a hydrologically dynamic pristine aquifer. *FEMS Microbiology Ecology*, *81*(1), 230–242. https://doi.org/10.1111/j.1574-6941.2012.01371.x